



**Sewer Inspection autonomous robot**

## D28.1 - Detailed Robot Design

SIAR Consortium

IDMind (IDM), PT

Universidad de Sevilla (USE), ES

Universidad Pablo de Olavide (UPO), ES

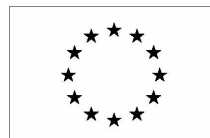


# Table of Contents

- 1. Introduction
  - 2.1. Robot Features and Components
    - 2.1.1. Locomotion Platform Main Features
    - 2.1.2. Sensors
    - 2.1.3. Actuators
  - 2.2. Platform Design and Mechanics
  - 2.3. Robot Architecture
    - 2.3.1. Electronic Power Architecture
    - 2.3.2. Low-level Communication Architecture
    - 2.3.3. High-level Communication Architecture
  - 2.4. Locomotion Platform Electronics
    - 2.4.1. Motor Controller Board
    - 2.4.2. Sensor&Management Board
    - 2.4.3. Wireless Joystick Controller Board
    - 2.4.4. Wireless Power Switch Control Board
    - 2.4.5. Environment Monitor Board
    - 2.4.6. Sampling system board
  - 2.5. Robot Safety
    - 2.5.1. Control Station Remote E-Stop Commands
    - 2.5.2. Radio Remote Controller & E-Stop
    - 2.5.3. Local E-Stop Push Button
    - 2.5.4. Auxiliary Radio Remote Shutdown
- 3. Communications
  - 3.1 Overview
  - 3.2 Solution
    - 3.2.1 Primary link
    - 3.2.2 Backup link
    - 3.2.3 Automatic deployment of repeaters
    - 3.2.4 Antenna considerations
    - 3.2.5 Frequency considerations
  - 3.3 Tests and experiments
    - 3.3.1 Experiments at the UPO basements
    - 3.3.2 Experiments at the Passeig of Sant Joan sewers
- 4. Software Architecture
  - 4.1 SIAR Control Station
  - 4.2 Details on the proposed communication middleware
    - 4.2.1 Standard ROS middleware
    - 4.2.2 Proposed communication middleware
- 5. Localization and Navigation

- 5.1 Enhanced Odometry
  - 5.1.1. Image feature detection
  - 5.1.2. Image feature description
  - 5.1.3. Pairwise Feature Matching and Key-Framing
  - 5.1.4. Attitude Correction
  - 5.1.5. Translation checking with wheel odometry
  - 5.1.6. Experimental results in sewers at Barcelona
- 5.2 Localization
- 5.3 Navigation
- 6. Perception
  - 6.1 Local 3D Mapping
    - 6.1.1 Implementation details
    - 6.1.2 Experimental results at Barcelona
  - 6.2 Map Analysis
    - 6.2.1 Sewer elements location
    - 6.2.2 Sewer serviceability inspection
    - 6.2.3 Structural defects inspection
- 7. Logistics required and operational issues by using the solution
- 8. Economic Viability Study
  - 8.1. Opportunity
    - 8.1.1. Market
    - 8.1.2. Competition
    - 8.1.3. SWOT Analysis
  - 8.2. Marketing
    - 8.2.1. Positioning
    - 8.2.2. Price
    - 8.2.3. Promotion
    - 8.2.4. Distribution
  - 8.3. Financial Projections
    - 8.3.1. Pre-production Costs
    - 8.3.2. Sales
    - 8.3.3. Purchases
    - 8.3.4. Personnel Costs
    - 8.3.5. Equipment Costs
    - 8.3.6. Costs with External Services and Subcontracting
    - 8.3.7. Total Costs
    - 8.3.8. Operating Income
  - 8.4. Implementation and Control
  - 8.5. Sewer Inspection Economical Impact

## References





# 1. Introduction

The SIAR project proposes the development of a fully autonomous ground robot able to navigate and inspect the sewage system with a minimal human intervention, and, when required, with the possibility of manual intervention to control its movements and/or its sensing payload.

The Consortium started their studies and evaluation of the sensors, actuators and processing system, based on the existing IDM's RaposaNG. Partners USE and UPO have been using locally the platform to test the navigation sensors and wireless communication between the robot and the remote control console (see Figure 1.1).



Figure 1.1. Experiments at UPO's premises with IDM's RAPOSA<sup>®</sup> NG remote inspection platform.

After the kick-off meeting and after an evaluation of scenario based on the collected videos and images, it became clear to the team that a tracked solution based on RaposaNG would have many difficulties to adapt to the different sewer configurations encountered in Barcelona. Hence, IDM team started the study of other robotic kinematic configurations that could be more suitable for the proposed sewer scenario. This study took us to a six-wheeled robot configuration, based on six independent motor actuators, depicted in Figure 1.2.

A first prototype was built and used to test the locomotion, communication and teleoperation control in the sewers of Barcelona. Two visits to the sewers of Barcelona allowed the team to have a better understanding of the different issues related with sewer inspection and the requirements of the autonomous system.

A survey of the commercial sensors available on the market was performed and the systems to be used onboard were defined.

The hardware and software architectures were set and the power requirement has been defined. With the definition of the components to be installed in the robot, the team proceeded with the design of the SIAR platform.



Figure 1.2. SIAR prototype.

A new robot will be built based on the acquired know-how, with the following key features beyond the state of the art required to properly address the challenge: a robust IP67 robot frame designed to work in the hardest environmental conditions with increased power autonomy and flexible inspection capabilities; an adaptable robot frame that allows to increase/decrease the width of the platform from 460 mm to 666 mm to accommodate to different sewer dimensions; robust and increased communication capabilities; onboard autonomous navigation and inspection capabilities; usability and cost effectiveness of the developed solution. Figure 1.3 depicts the proposed SIAR solution.

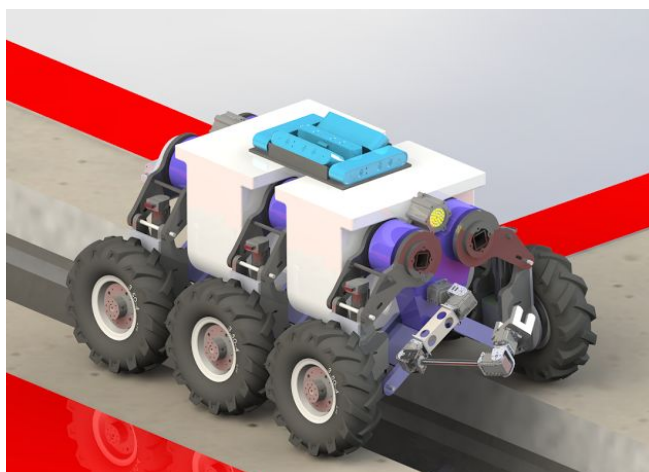


Figure 1.3. SIAR proposed design

This document is as organized as follows. Section 2 presents the SIAR robot platform, its main features, components, mechanical design, electronics and low-level communication architecture, robot safety. Section 3 details the proposed communication system that will provide the SIAR platform with continuous wireless connection with the base station. Section 4 presents the software architecture. Section 5 presents the autonomous localization and navigation methodology. Section 6 details how the robot will perceive and inspect the environment. Section 7 describes the required logistics and operational issues when using the solution. This document ends in section 8 with an economic viability study for the developed solution.

## 2. SIAR Robot Platform

The SIAR robot will be based on a six-wheeled platform configuration with the ability to change its width between the wheels to address the different sections of the sewer network. The robot will be fully equipped to move autonomously for about 5 hours while executing the inspection operation. The following section describes the hardware configuration of the proposed solution.

### 2.1. Robot Features and Components

This subsection introduces the main features and devices that will be present on the SIAR robot.

#### 2.1.1. Locomotion Platform Main Features

The following main specifications are expected for the SIAR robot platform:

- Robot Kinematics: 6 wheeled with 6 independent locomotion motors and 3 linear motors for width control
- Weight: 50Kgs
- Battery autonomy: >5 hours
- Maximum Velocity: 0.75 m/s
- Acceleration: 1 m/s<sup>2</sup>
- Emergency Stop Acceleration: 3,3 m/s<sup>2</sup>
- Size (Height x Width x Length) : 60 x 46-67 x 80 cm (automatic adaptation of platform width)

The SIAR robot system will have two onboard computers and an external Control Center computer:

- The i3 Navigation computer (aka PC-NAV) will be running Linux OS (Ubuntu) and will be responsible for the navigation and system control. It will be also responsible for the sensor acquisition and processing.
- The i7 Perception computer (aka PC-PERCEPT) will be running Linux OS (Ubuntu), all the RGBD cameras will connect to this computer. This computer will be responsible for the scan capturing and management, local 3D mapping and the perception functionalities related to sewer inspection and the localization of the SIAR robot in the environment.
- The Control Center Computer (aka Control Center) is a Laptop and will be responsible for robot monitoring, receiving system alerts, and further sewer monitoring and analyzes functionalities.

Table 2.1 lists the devices that will be present in the SIAR solution.

	Quantity
<b>Robot processing</b>	
navigation i3 computer (AKA PC-NAV)	1
perception i7 computer (AKA PC-PERCEPT)	1
<b>Sensor&amp;Management Board</b>	
main board	1
batteries	2
<b>Motors Board</b>	
main board	1
traction motors + encoders	6
width motor + encoder + potentiometers	3
motor&driver coling fans	3
<b>Wireless deploy device</b>	
robotic arm	1
<b>Sensors&amp;Actuators</b>	
IMU sensor	1
3D (RGB & Depth Sensor) Camera	5
environment sensors	1
wireless repeater	4
Sampling&Measuring system	1
wireless deploy/retrieve system	1
Illumination LED light projector	2
<b>Contol Station</b>	
control station computer	1

Table 2.1. SIAR devices.

## 2.1.2. Sensors

The robot will be equipped with perception, navigation and environmental sensors. For **navigation** the robot uses encoders to control the velocity of the traction motors and encoder plus potentiometer to control the position and velocity of the platform width motor. An inertial sensor gives the orientation of the robot. The depth cameras are able to give an estimation of the obstacles/walls distance to the robot, and are also used to refine the odometry estimates. For **perception** the robot uses the RGBD cameras to analyze the sewer environment and detect any abnormal situation. For the **environment** the robot will use a set of small sensors able to measure different environment parameters, like temperature, humidity or CO2.

### Navigation Sensors

The robot will navigate in the environment while making a fusion of measures provided by different sensors. The robot will be able to use the RGBD cameras, encoders odometry and the IMU sensor to estimate its position and orientation. For obstacle avoidance, mapping and localization it can use the RGBD cameras.

- Inertial sensor IMU: Arduimu v3  
Function: Orientation estimation  
Position on Robot Platform: in the robot's center of rotation

Obtaining a good estimation of the robot's displacement and orientation is crucial not only when generating a 3D map of the environment, but also when performing complex maneuvers in such a challenging scenario as the sewers are. To this end, we have been employing with great results the inexpensive Arduimu version 3 device since the FROG project<sup>1</sup> together with our own IMU filtering, and we will be considering it here.

- 5 x RGBD cameras: 2 Orbbec's Astra RGBD sensor (8 m. range) and 3 Orbbec's Astra S RGBD sensor (6 m range)  
Function: refined odometry, obstacle detection and space geometry analysis  
Position on Robot Platform: top of the robot pointing to front, back, left, right and top (the last three, the short range sensors).

### Perception Sensors

The robot will make use of RGBD cameras for sewer monitoring and analysis. The perception sensors are the following:

- 5x RGBD camera: 2 Orbbec's Astra RGBD sensor (8 m range) and 3 Orbbec's Astra S RGBD sensor (6 m range)  
Function: obstacle detection and space geometry analysis  
Position on Robot Platform: top of the robot pointing to front, back, left, right and top (the last three, the short range sensors).

The SIAR platform should be equipped with sensors in order to sense the scenario where it is navigating. This is essential for localization and mapping purposes and also to fulfill the requirements on sewer scanning and inspection stated in [ECHORD++, 2014]. There are several kind of sensors that can provide a robot with detailed measurements of the environment. These sensors include 2D Laser such as Hokuyo, 2D tilting laser that can obtain 3D measures, LiDAR sensors such as the velodyne HDL-32E<sup>2</sup>, stereo cameras and RGB-D cameras.

When analyzing these options, 2D Laser can obtain precise measures at frequencies ranging on the tens of Hertz, but can only sense distances confined in a determinate 2D plane local to the robot. Therefore, it can be used to sense obstacles in the surroundings, but it would have to be complemented if 3D obstacles like holes in the floor have to be detected, or in order to perform a 3D scan of the environment. On the other hand, tilting laser sensors could be employed to perform hole detection and 3D scans, but they offer the data at a low rate (Hertz). Lidar sensors can provide the robot with a detailed 3D map of its surrounding usually at ten Hertz, but they are quite expensive (thousands of dollars) and heavy (usually more than one kilogram). Stereo cameras would need a good illumination in order to be able to detect matches between the two cameras, and then compute their disparity. This is not the case when inspecting sewers.

Therefore, RGB-D cameras emerge as a very convenient alternative for performing 3D scans of the surroundings of the robot as they offer distance measures at high frequencies (30 Hz) even without the presence of illumination. Also they are inexpensive (around 150€) when compared to the other Radar and LiDAR alternatives.

In the proposed solution we are employing two different RGB-D devices provided by Orbbec Ltd<sup>3</sup>. These are Orbbec Astra and Orbbec Astra S whose main characteristics can be found in Table 2.2.

---

<sup>1</sup> <https://www.frogrobot.eu/wordpress/>

<sup>2</sup> <http://velodynelidar.com/hdl-32e.html>

<sup>3</sup> <https://orbbec3d.com>

Device	FOV	Range (m)	Size (cm)	Resolution	Accuracy	SIAR use
Astra	H 60°, V 49,5°	[0.45,8]	16.5x3x4	640x480	1-3 mm. (below 1 m.) 12.7 mm. (below 3 m.)	Front and rear
Astra S	H 60°, V 49,5°	[0.35,6]	16.5x3x4	640x480	1-3 mm. (below 1 m.) 12.7 mm. (below 3 m.)	Vault and sideways

Table 2.2. Orbbec Astra family characteristics.

As seen in Table 2, the horizontal range of both Astra and Astra S is 60°. Therefore, several Astra sensors have to be equipped in the SIAR in order to have enough information for both navigation and 3D reconstruction goals.

In the final design, we propose to use 5 cameras simultaneously (see Figure 2.1). Each sensor costs 150€, so the total cost of the proposed sensing solution will be of only 750€.

Two long-range RGB-D cameras (up to 8 meters) are located in the front and rear parts. They will be mainly used for navigation and obstacle avoidance, although they also will be used for 3D reconstruction of the ground and the walls. The remaining three sensors have been placed in order to enhance the detection of possible structural defects at the ceiling and in the upper parts of the walls. The vertical disposition of the last three sensors is detailed in Figure 2.2. Note that the FOV of the sensors has been taken into account in order to obtain a continuous point cloud of the environment.

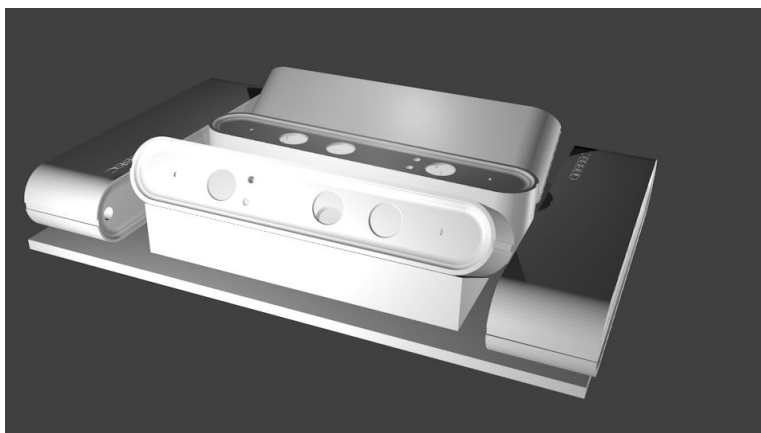


Figure 2.1. Proposed disposition of the sensors. Front view.

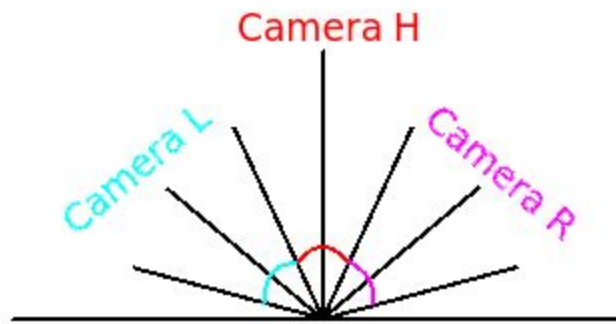


Figure 2.2: Tilting of lateral cameras (R & L) for obtaining continuous measures.

### Environmental Sensors

The environmental sensors will be used to monitor the environment temperature, humidity and gases, determine the variations and alert the operator in case of danger. The included sensors will be able to monitor air and water variables of interest.

### Air Sensors

An Air sensors setup system will be used to perform the air test. There is already a commercial system that allows the measurement of required air parameters. The Libelium Gas PRO board (Figure 2.3) together with the Waspote board fulfil the requirements for the temperature, humidity and calibrated gases measurement.



Figure 2.3. Libelium air sensor system.

The Libelium Gas PRO system will be connected to the Waspote developer board. The Waspote developer board allows the users to process all the information from the sensors and transmit the processed information using different types of wired and wireless communications.

- **Temperature (°C) sensor MCP9700A**
  - MCP9700A Specifications
    - Measurement range: -40°C to 125°C
    - Response time: 1,65s

- **Relative Humidity (%RH) sensor 808H5V5**
  - 808H5V5 Specifications
    - Measurement range: 0 to 100%RH
    - Operating Temperature: -40°C to +85°C
    - Response time: <15s
  
- **Carbon Monoxide (CO) sensor TGS2442**
  - TGS2442 Specifications
    - Gases: CO
    - Measurement range: 30 to 1000ppm
    - Operating temperature: -5 to +50°C
    - Response time: 1s
  
- **Hydrogen sulphide (H<sub>2</sub>S) sensor TGS2602**
  - TGS2602 Specifications
    - Gases: C<sub>6</sub>H<sub>5</sub>CH<sub>3</sub>, H<sub>2</sub>S, CH<sub>3</sub>CH<sub>2</sub>OH, NH<sub>3</sub>, H<sub>2</sub>
    - Measurement range: 1 to 30 ppm
    - Operating Temperature: +10 to +50°C
    - Response time: 30s
  
- **Methane (CH<sub>4</sub>) sensor TGS2611**
  - TGS2611 Specifications
    - Gases: CH<sub>4</sub>, H<sub>2</sub>
    - Measurement Range: 500 to 10000ppm
    - Operating Temperature: -10 to 40°C
    - Response time: 30s
  
- **Oxygen (O<sub>2</sub>) sensor SK-25**
  - SK-25 Specifications
    - Gases: O<sub>2</sub>
    - Measurement range: 0% - 30%



- Operating temperature: +5 to 40°C
  - Response time: 15 s
- **Lower explosive limit (LEL)**
- **Volatile organic carbons (VOCs) sensor MiCS-5524**
  - MiCS-5521 Specifications
    - Gases: CO, Hydrocarbons, Volatile organics Compounds
    - Measurement range: 30 to 400ppm
    - Operating temperature: -30 to +85°C
    - Response time: 30s

### **Water sensors**

A Water sensors setup system will be used to perform the required water test. There is already a commercial system that allows the measurement of required air parameters. The Libelium Smart Water sensor board (Figure 2.4) together with the Wasp mote board fulfil the requirements for the project with the inclusion of the following probes:

- **Temperature (°C) sensor PT1000**
  - PT1000 Specification
    - Measurement range: 0 to 100°C
- **PH sensor PH**
  - Libelium PH sensor Specifications
    - Measurement range: PH 0-14
    - Temperature range: +0 to 80°C
    - Response time: < 60s
- **Conductivity sensor**
  - Measurement range: 0 to 60,000 uS/cm
- **Turbidity Sensor**
  - Libelium Turbidity Sensor Specifications
    - Range: 0 to 4000 NTU
    - Temperature range: -10 to +60°C

The Libelium Smart Water sensor system will be connected to the Waspote developer board. The Waspote developer board allows the users to process all the information from the sensors and transmit the processed information using different types of wired communication.



Figure 2.4. Libelium Smart water system

The system will use a peristaltic pump to take water from the sewer and inject the sewer water into the water sensors assembly. Figure 2.5 shows the D1/PHS SUPERPRO water sample system that allows to control the PH and Temperature. The idea is to create a more complex sampling sensor system using the same principle.

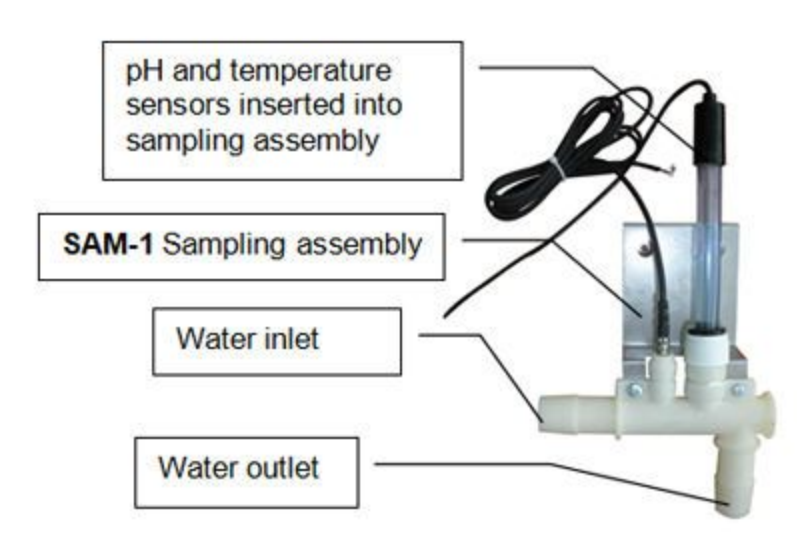


Figure 2.5. Water sensor system.

### 2.1.3. Actuators

The robot will be equipped with actuators for locomotion, for water sampling and for the deploy/collection of the communication repeaters.

### **Locomotion Actuators**

For locomotion the platform uses six motors to drive the 6 wheels and three linear motors to change the width of the robot.

- Six Maxon RE 35 90W 15V motor with a Maxon GP 32 HP 28:1 Gearbox and encoder HEDS 5540 with 500 pulses
  - Function: providing independent locomotion to each wheel of the robot
- Three Linear motors with encoder and potentiometer.
  - Function: changing the width between each pairs of wheels.

### **Sampling Actuators**

The SIAR robot will be able to collect samples from the environment. The robot will carry three different sampling systems:

- Water Sampling. It will transport a system able to collect water from the sewer and store it in 300 ml reservoirs;
- The system will use a Peristaltic pump to collect water from the sewer and using up to 8 water solenoid electric valves redirect the water to small 300 ml reservoirs. Each reservoir will be equipped with a level sensor to determine if the reservoir is full.
- Air Sampling. It will carry commercial air capsules that will be used to collect samples from the air;
- Sediments sampling. It will carry a device able to collect samples from the sediments.

### **Communication repeaters deploy/retrieve system**

One problem inside the sewers are the wireless communications. To increase the range of the communications between the SIAR robot and the Control Console the SIAR robot will be able to deploy wifi repeaters along its path. For this purpose, the SIAR robot will be equipped with a robotic arm which will deploy and collect these repeaters.

### **Illumination LED light projectors**

In normal operation the SIAR robot will run in non-illuminated areas. The operators camera requires a minimum of illumination which will be provided by two LED 6W MR16 GU5.3 lamp 6000K projectors, in the front and rear of the robot.

## **2.2. Platform Design and Mechanics**

The SIAR robot will be based in a six-wheeled configuration. Each wheel will be powered by an independent motor and mechanic suspension. Figure 2.6 depicts the concept.



Figure 2.6. Siar prototype Mechanic Suspension.

The front and back wheels are a little bit elevated relatively to middle ones (see Figure 2.7), so that the middle ones have more traction. This eases the rotation of the robot, reducing in this way the current consumption during the rotation.

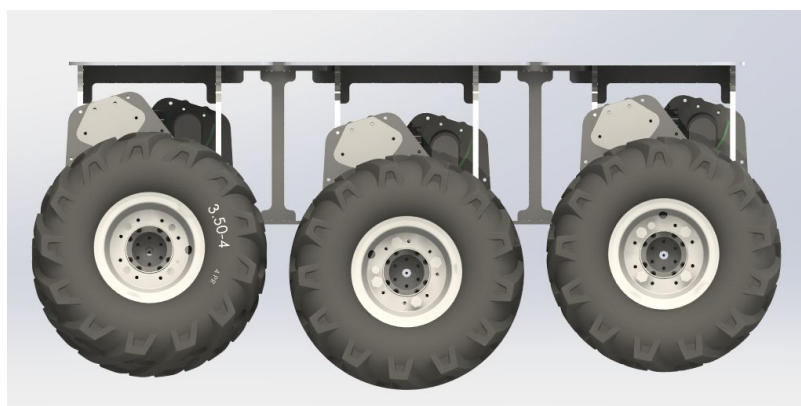


Figure 2.7. Siar prototype lateral view.

To evaluate the adopted solution in the sewers two prototypes were designed and created. A first solution was developed to validate the six wheels solution (with independent motors + suspension) over offroad rough terrain. The developed solution, depicted in Figures 2.8 to 2.11, allowed to test the type of wheels, type of suspension and motor demultiplication.

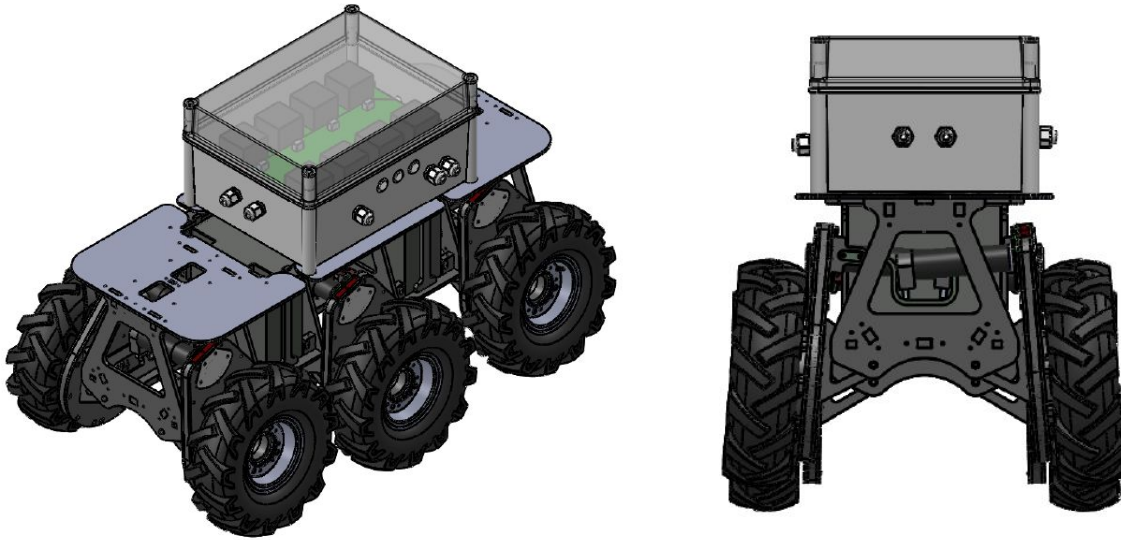


Figure 2.8. Siar first prototype design

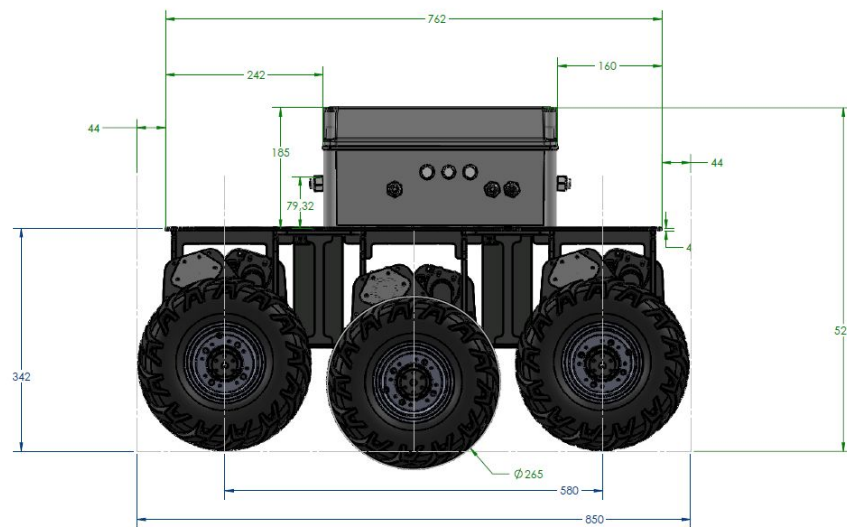


Figure 2.9. Siar first prototype measurements lateral view.

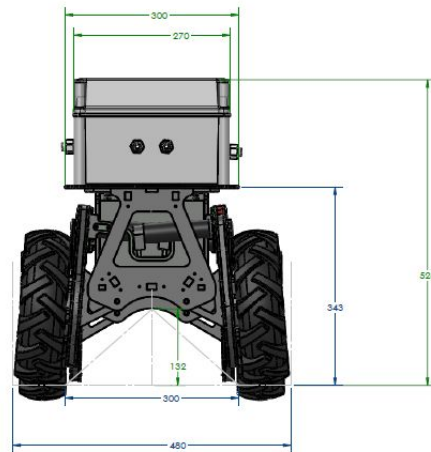


Figure 2.10. SIAR first prototype measurements front view.



Figure 2.11. SIAR first prototype skills.

After tuning the different parameters, the robot was tested in the real sewers. The test performed in Barcelona was the opportunity study the robot mobility in the sewer system (see Figure 2.12).



Figure 2.12. SIAR first prototype sewer testing.



The performed study allowed to understand some of the difficulties that the robot will face in the sewers.

To improve the performance of the robot in the sewers, the team redesigned the prototype increasing its width from 480 mm to 560 mm. And went again to Barcelona to test the new approach. This experiments allowed to:

- safely teleoperate the robot in the the sewers where the sewer gully is around 400 mm,
- cross a perpendicular sewer gully;
- with some maneuvers, cross a perpendicular sewer gully, rotate and align the front of the robot with the sewer gully.
- in Passeig de Sant Joan main sewer, drive inside the 70 cm sewer gully and in all sections where the pedestrian floor is wider than 54cm.

After the second period of tests it was verified that the robot must be able to automatically change its width to be able to safely maneuver inside the different sections of the sewer system. The robot platform was redesigned according to this new feature, Figures 2.13 and 2.14 depict the dimensions of the final prototype of the platform. Three linear motors were introduced in the robot design which will allow to increase/decrease the width of the platform from 460 mm to 666 mm ( see Figure 2.13).

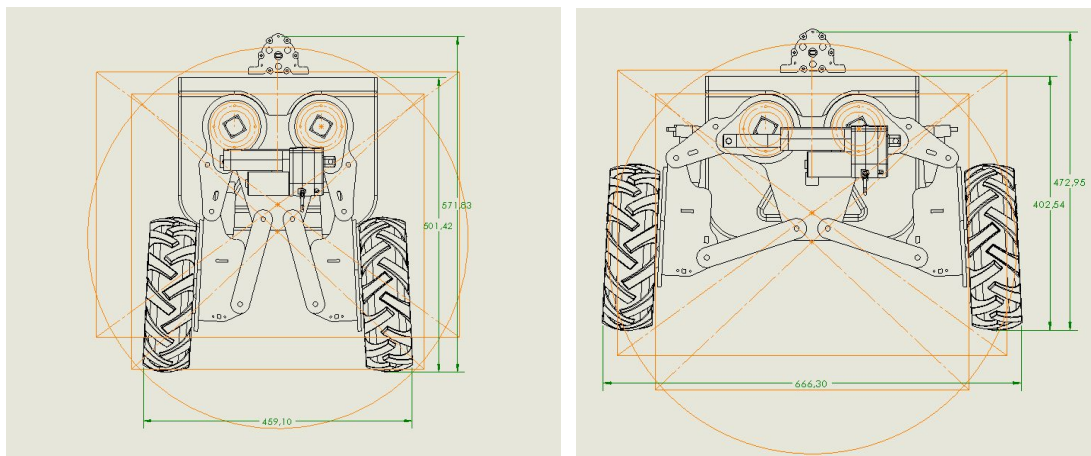


Figure 2.13. SIAR robot 460 and 666 mm width configurations.

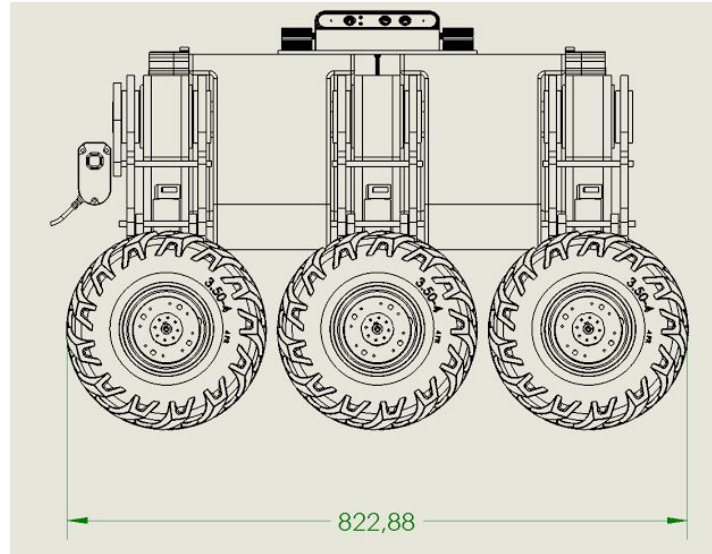


Figure 2.14. SIAR robot 823 mm length.

The SIAR robot final prototype design includes 6 dc motors to drive the wheels, three dc linear motors to change the width of the robot and a robotic arm that will be used to deploy the wireless repeaters. Figure 2.15 illustrates the final design.

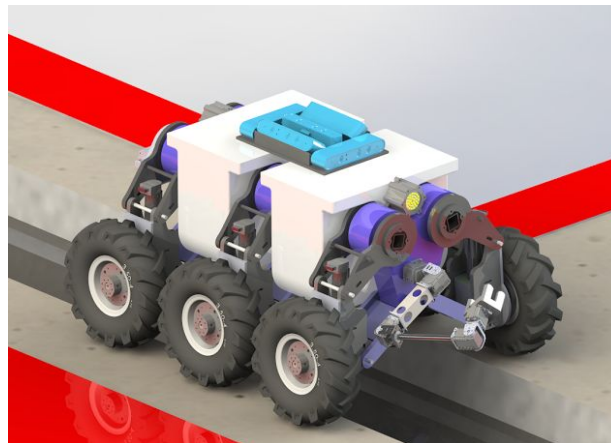


Figure 2.15. SIAR robot final prototype design.

The design will allow the robot to dynamically change its width configuration during the operation for a better adaption to the different sewer sections. Figures 2.16 to 2.18 depict this concept.



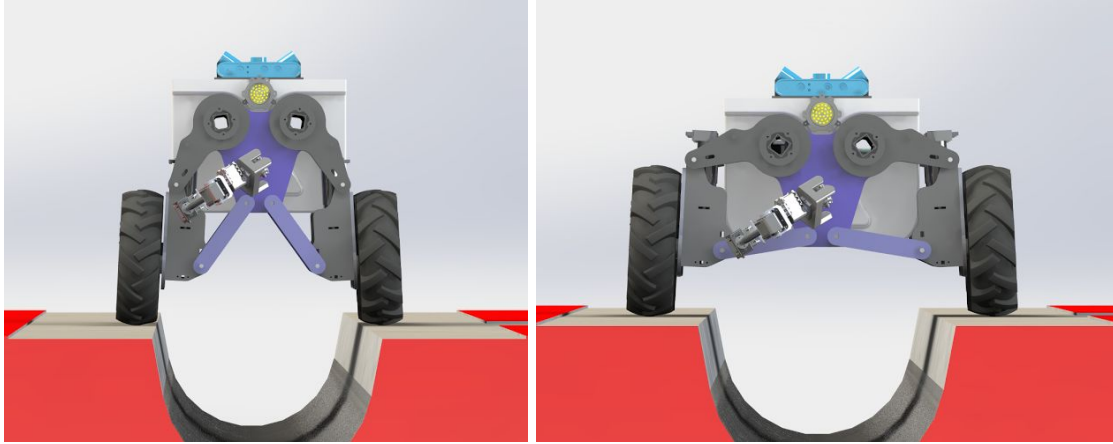


Figure 2.16. SIAR over different sewer gullys.

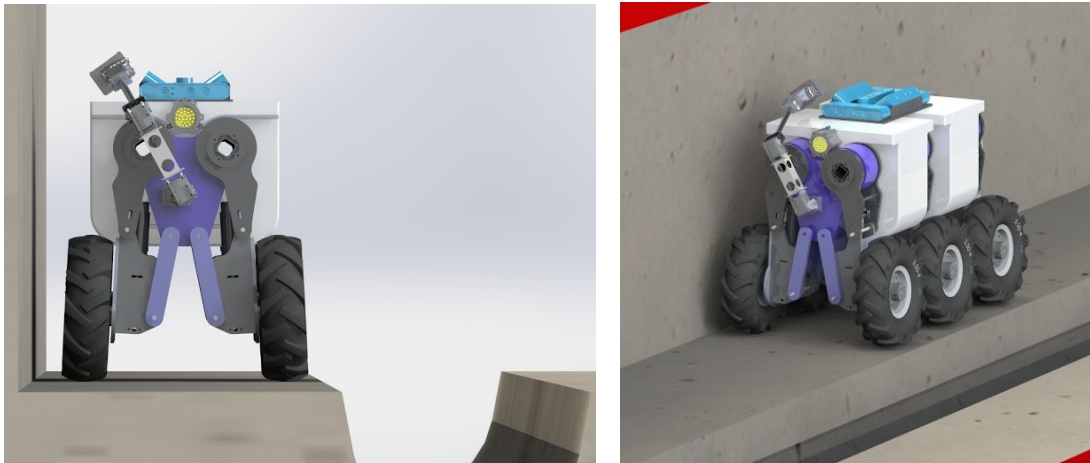


Figure 2.17. Reducing the width of the robot to drive in pedestrian surfaces.

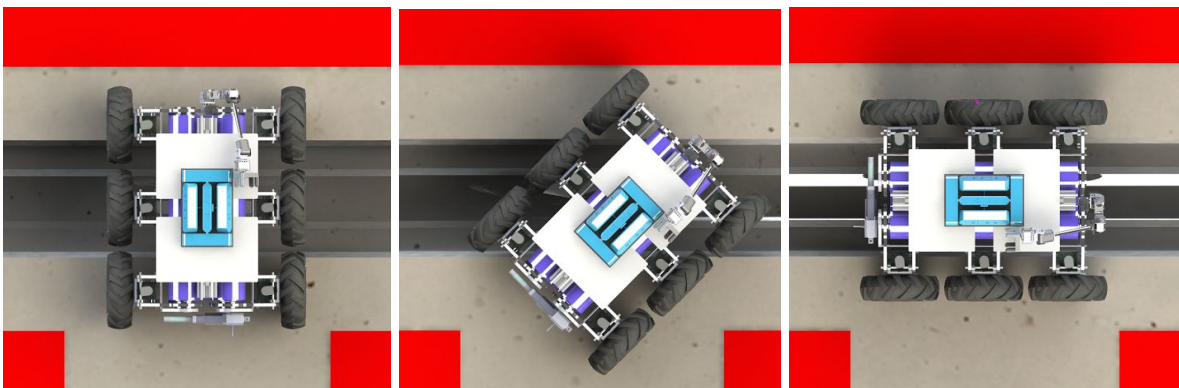


Figure 2.18. Increasing the width to rotate over the sewer gully.

## 2.3. Robot Architecture

The following sub-section describe the power, low-level and high-level communication architectures between all the low level electronic devices.

### 2.3.1. Electronic Power Architecture

The robot platform is powered by two LiFePO<sub>4</sub> 12V 20AH battery packs. One battery pack delivers power to the motor drivers and the other provides energy to all other electronics (e.g. computer, electronics and sensors). Each of these packs, depicted in Figure 2.19, has the following specifications:

- Voltage: 12 V (12.8 V nominal)
- Capacity: 20 AH
- Charging Voltage: 14.6 V
- Charging Current: < 3 A
- Max Continuous Discharging Amperage: 20 A
- Maximum Discharging Current: 34 A
- Lifecycle of the whole pack: >85% capacity after 1000 cycles.
- Lifecycle of single cell: >85% capacity after 1500 cycles, >70% capacity after 3000 cycles. (<1C discharge rate and <1C charge rate).
- Low voltage (minimal): 9.5V
- Includes an embedded battery management system (BMS) circuit.

There will be a total of approximately 0,25 KWh of installed power which will provide an expected autonomy of 5 hours of operation. Additionally a power charger will be able to charge the battery system in less than 3 hours. This Power Charger will be able also to power the robot electronics while it is in the charge mode. The batteries will be installed in a way that they can be easily accessed and replaced by another charged pack to continue with the operation.



Figure 2.19. 12V 20AH LiFePO<sub>4</sub> battery pack

Two external batteries chargers and an external power supply will connect to the robot allowing to power all robot components while charging both SIAR batteries. The batteries and the power in the robot will be managed by the Sensor&Management Board that measures the battery levels, battery charge, and also controls the units (motors, sensors and actuators) powered by the batteries. Figure 2.20 depicts the onboard power architecture.

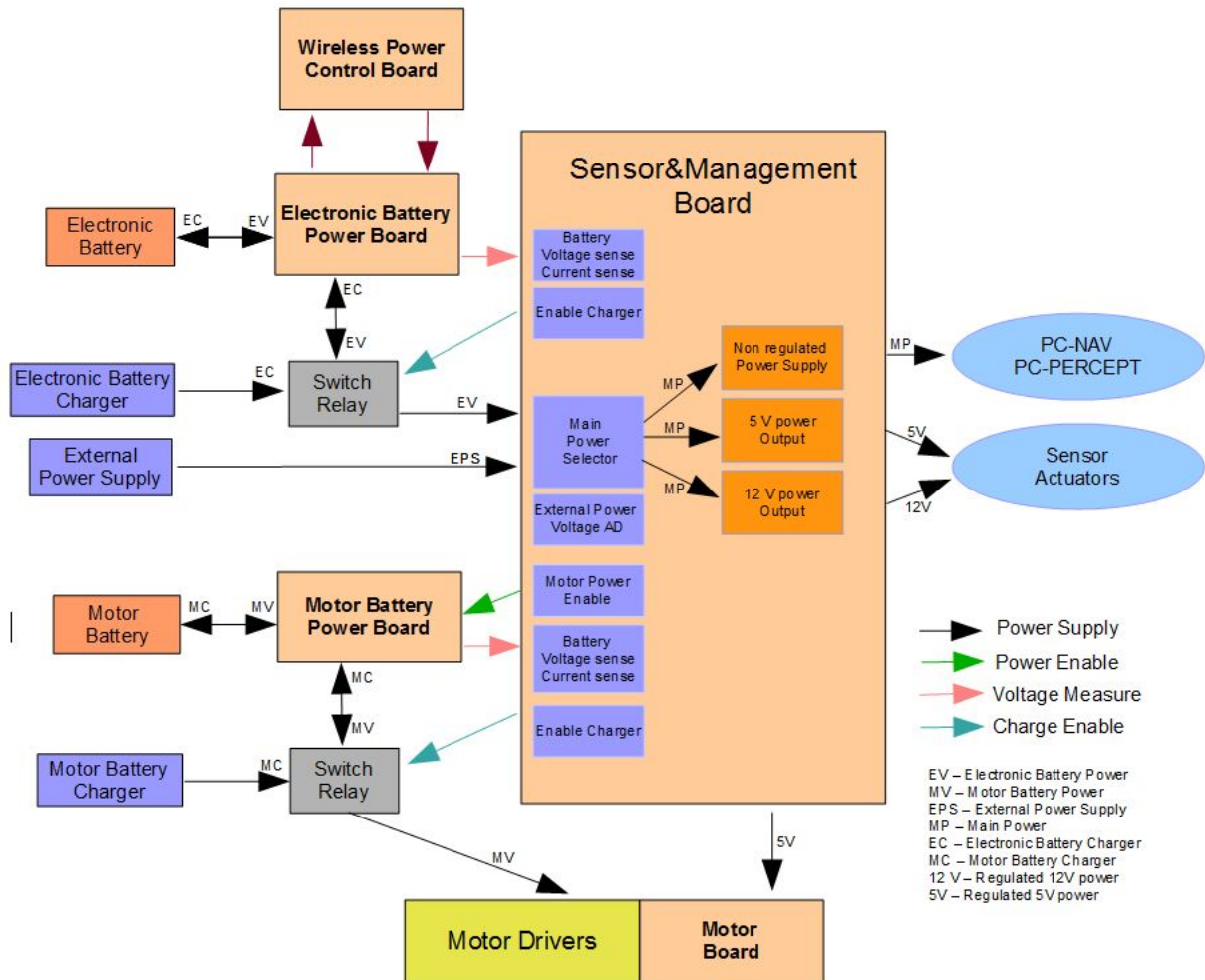


Figure 2.20. Sensor&Management Board architecture

The Sensor&Management Board controls the Enable/Disable and the Charge of each battery, while measuring their voltage levels. To accomplish this task, two additional boards and two relays were introduced.

The Electronics battery will connect to the Electronics Battery Power Board, which uses a set of two high-power P-Type Mosfets to switch ON/OFF the electronics power. The switch ON/OFF is controlled by Wireless Power Control board, then a Start push button is used to energize the Electronic Battery Power Board. To cut the power on the robot there are two possible ways: through a Stop push button installed in the robot body; or through external wireless shutdown device. They will both drive down the power of the Electronic Battery

Power Board. The wireless shutdown device is able to shut down the power of the robot from a distance up to 100m in line of sight.

The Electronics Battery Power Board will also provide all the needed electronics to allow the Sensor&Management Board to read the voltage level and consumed current level of this battery. Finally a high-power relay will be used to switch to and from the charge mode. The relay will be controlled by the Sensor&Management Board.

When the relay is not on charging mode, the output of the Electronics battery will go inside the Sensor&Management Board. Using two high-power diodes this high-power voltage is compared with the power from the external power supply, and the higher one will power all the main electronic components.

In the case of the Motor battery, a Motor Battery Power Board was created, using four high-power P-Type Mosfets to switch ON/OFF the motor drivers' power. The switch is controlled directly by the Sensor&Management Board, and it will be able to control the enable/disable of the motor drivers' power. The Motor Battery Power Board will provide all the needed electronics to allow the Sensor&Management Board to read the voltage level and consumed current of this battery. A high-power relay will be used to switch to and from the charge mode. The relay will be controlled by the Sensor&Management Board. When the relay is not on charging mode, the output of the Motors battery will go directly to the motor drivers. In charging mode the motors drivers will be unpowered.

Tables 2.3 and 2.4 shows the equipment that is connected to batteries and their predicted maximum current and power consumption.

Battery Name	Powered item	Nominal Current (Ah)	Power (Wh)
Motor (2,8Ah)			
12V 20Ah	Traction wheels motors	2,5	30
240W	Linear width change motor	0,3	3,6
<b>Total</b>		<b>2,8</b>	<b>33,6</b>

Table 2.3: SIAR motor battery and maximum power usage

Battery Name	Powered item	Nominal Current (Ah)	Power (Wh)
Electronics (3,8Ah)	PC-NAV and PC-PERCEPT	1,5	18
12V 20Ah	Sensor&Management board	0,2	2,4
240W	Motors board	0,15	1,8
	4x Asus Xtion Camera	1	12
	PTZ HD Camera	0,25	3
	TOF Sensors	0,05	0,6
	Inertial sensor (by the Computer USB port)	0,05	0,6
	Environment Sensors	0,25	3
	Water sampling system	0,1	1,2
	Wireless Deploy/Retrieve system	0,05	0,6
	Led light projector	0,2	5
<b>Total</b>		<b>3,8</b>	<b>48,2</b>

Table 2.4: SIAR Electronic battery and maximum power usage

### Energy consumption measuring calculations

Each of the SIAR batteries will be monitored using the actual voltage and the overtime integrated current. With this information and using the discharge curves for the LiFePO4 batteries, it will be possible to estimate the remaining time of operation for each battery. Because the robot uses two batteries, the remaining

operation time will be given by the battery that has a lower value. The Sensor&Management board will calculate all the data for each battery.

The Sensor&Management board is used to measure the actual voltage and the instantaneous current of each battery. This current measurement is performed by the use of a “shunt” resistor of 0.025 Ohms that connects between the (-) of the battery and the GND of all the onboard electronics. Because the expected current that is flowing through the “shunt” resistor is less than 20A, the maximum voltage drop on the resistor will be around 0.5V. The current flowing through the resistor will be proportional to the voltage drop in that resistor. The microcontroller inside the Sensor&Management Board will measure that voltage and calculate the instantaneous current. Then it will integrate all the instantaneous current over time and will use the integrated current to calculate the discharge level.

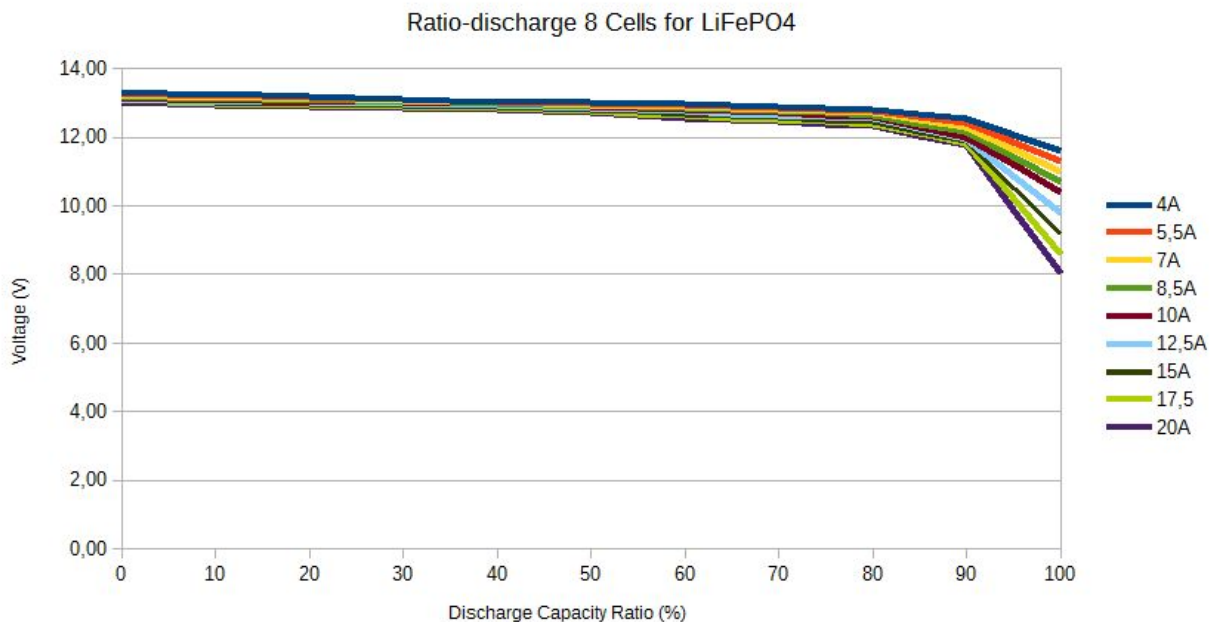


Figure 2.21. LiFePO4 discharge curves.

Each curve in Figure 2.21 represents an integrated current overtime vs actual voltage to determine the discharge level of the battery. LiFePO4 batteries, as it can be seen in the graphics, for a constant current will drop almost linear until they reach 80% of discharge, then it will start to drop faster. The voltage between two consecutive curves will have small changes, this fact allow to limit the number of curves that the microcontrollers has to process.

The curves are then represented in nine lookup tables, each one for a specific current. The 4A curve is used to calculate the level of discharge for the integrated curves between 0A and 4A.

Each lookup table, for a constant current, will represent the actual voltage for a specific discharge percentage, in 5% steps.

The integrated current is used to determine the current curve lookup table and the actual voltage will give the position on the lookup table from where we can derive the discharge percentage of the battery.

Given the discharge percentage of each battery, it is possible to calculate the remaining time of operation (RTO), using the battery capacity (BC), the level of discharge (L) and the integrated current over time (C). The following equation is being used:

$$RTO = (BC/C) \times 60(\text{minutes}) \times (100-L) / 100$$

### 2.3.2. Low-level Communication Architecture

The onboard navigation computer (PC-NAV) communicates with the Sensor&Management Board and the Motor Board using 2 USB ports.

The Motors Board will be able to communicate with the motor drivers controllers using I2C communication and it will have a wireless serial link to an external Joystick Controller. The Sensor&Management Board will communicate with the Sample and Measure systems by the use of the I2C communication. Figure 2.22 shows the adopted low-Level communication architecture.

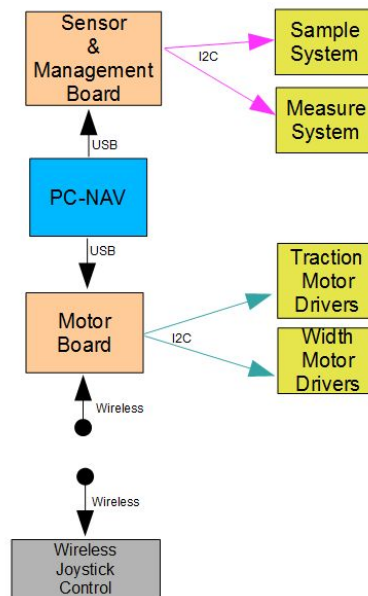


Figure 2.22. Low-level Communication Architecture.

### 2.3.3. High-level Communication Architecture

The PC-NAV will be connected to the navigation sensors and to the platform board controllers using USB and Ethernet ports.

The high-level communication architecture is depicted in Figure 2.23.



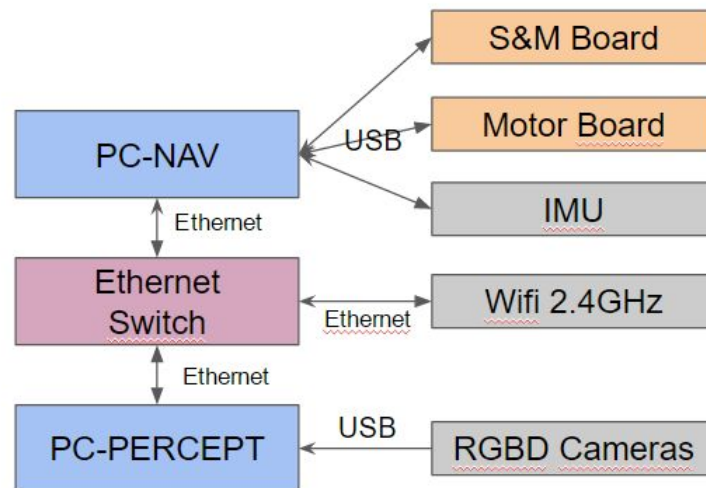


Figure 2.23. High-level Communication Architecture.

## 2.4. Locomotion Platform Electronics

Several electronic boards will be designed for SIAR which will be described in the following subsections.

SIAR platform includes the following electronic systems:

- **Motor Controller Board** – connects to the PC-NAV computer and allows manual control of the robot using an external wireless joystick controller.
- **Sensor&Management Board** - communicates with the PC-NAV, manages onboard power while connecting, disconnecting, measuring and charging the onboard batteries, connects and controls external actuators and sensors.
- **Wireless Joystick Controller** – allows direct manual control through the use of an external wireless joystick controller, to actuate the locomotion motors, platform width motors, Enable/Disable the motors, actuate the QuickStop or send a command that will cut the robot power.
- **Wireless Power Control Board** – controls the power on the robot. Allows the user to power/unpower the robot by the use of a start and stop buttons (on the robot body) and to cut the power using the wireless shutdown controller.
- **Electronic Power Board** – it can switch ON/OFF the electronics power, sample the voltage level and consumed instantaneous current.
- **Motors Power Board** – it can switch ON/OFF the motors power, sample the voltage level and consumed instantaneous current.
- **Bar-LED Voltage displays** – displays the electronics and motors remaining battery power using a 10 colored LED bar. This system will connect to the Sensor&Management Board.

- **Environment monitor board** – allows the robot to monitor several air and water parameters. This system will connect to the Sensor&Management Board.
- **Sampling system board** – controls the collection of water and sediments samples from the environment and placement in 300 ml reservoirs. Controls also the collection of air samples using air capsules. This system will connect to the Sensor&Management Board.

### 2.4.1. Motor Controller Board

The Motor Controller Board manages the robot locomotion. The Master Motor Controller uses a PIC18F6527 microcontroller to control and manage all the communication between the high-level robot PC-NAV, the **Wireless Joystick Controller** and the **Slave Motor Driver Controllers**. The **Slave Controllers Motor Driver Controllers** use a PIC18F2431 microcontroller to provide all the necessary control signals to the motor drivers. The overall architecture of the Motor Controller Board is depicted in Figure 2.24.

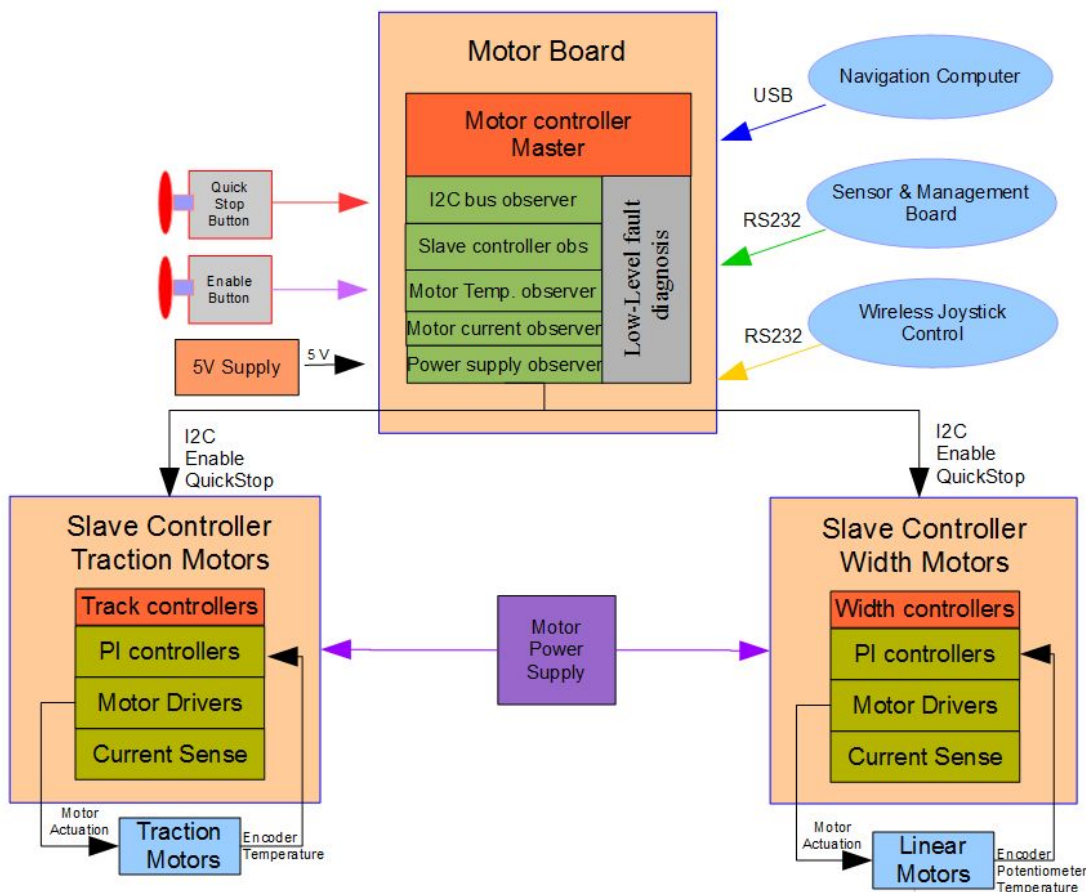


Figure 2.24. Motor Board architecture

The Master Motor Controller will:

- run low-level control loops to check for critical changes in the motor system that can affect the robot operation.



- provide an I2C bus Observer that checks the information received from the I2C Slave devices to understand faults in the communication and/or on the devices.
- check the proper operation of each Slave Controller through exchange of status information.
- monitor the electronics, motors and the drivers' power supply.
- exchange information with the PC-NAV computer.
- receive information from the Wireless Joystick Controller.
- enable/disable the motor drivers.
- enable/disable the QuickStop control of the motor drivers.
- exchange information with the Sensor&Management board using a RS232 communication link.
- read the temperature of each motor.

The Slaves PI Traction Motor Controllers will:

- receive velocity references from the Master Motor Controller;
- periodically read the encoder pulses;
- send the read encoder pulses to the Master Motor Controller;
- calculate the error between the reference velocity and the read velocity;
- implement a PI controller to calculate the motor actuation;
- implement an anti-windup error limit;
- implement a reference velocity acceleration/deceleration profile;
- remove the dead zone of the motor;
- limit the maximum velocity of the motors.
- measure the motors' current.

The Slaves PI Platform Width Motor Controllers will:

- receive width and velocity references from the Master Motor Controller;
- periodically read the encoder pulses and linear potentiometer values;
- send actual width to the Master Motor Controller;
- calculate the error between the reference velocity and the read velocity;
- implement a PI controller to calculate the motor actuation;

- implement an anti-windup error limit;
- implement a reference position and velocity acceleration/deceleration profile;
- remove the dead zone of the motor;
- limit the maximum velocity of the motors.
- measure the motors' current.

The Master Motor Controller receives velocity and width commands from the computer and returns the encoder pulses and the width values. The Controller connects to traction and width PI microcontrollers that generate the control actuation to follow velocity and width references. Each traction microcontroller connects to the motors using a power H-bridge, and provides the pulses measured by encoders. Each width microcontroller connects to the motors using a power H-bridge, and provides the width measured by encoders and potentiometers.

Each microcontroller is optically isolated from the motor driver using a high-speed optocoupler for the control actuation signals and an optical amplifier for the current measurements. It is also optically isolated from the computer communication port, again using a high-speed bidirectional optocoupler. Several low-level fault diagnostics have been implemented to detect problems in the normal working of each component or lack of communication.

The **Motor Board** controller is able to communicate with the PC-NAV using a USB-to-RS232 converter and with the **Sensor&Management Board** using a RS232 communication link.

#### 2.4.2. Sensor&Management Board

The Sensor&Management Board is responsible for the power management and also low-level sensor acquisition. It receives orders from the onboard robot PC-NAV and returns information about the batteries, sensors and actuators. The Sensor&Management Board Architecture is depicted in Fig. 2.25.

The Sensor&Management Controller uses a PIC18F6527 microcontroller to manage all the communication with the high-level robot PC-NAV and control all the actuators and sensors devices connected to the Sensor&Management Board.

The Sensor&Management Board is responsible for managing all the power system, including:

- measuring the energy level in each battery;
- connecting/disconnecting the power of the devices;
- managing the connection to the Charge Station;
- exchange information with the motors board;
- controlling the charge of each battery;

This board is also responsible for connecting a set of sensors and actuators that will be used in the project. Several low-level fault diagnostics will be implemented to detect problems in the normal work of each component and communication. The Sensor&Management Controller will analyze the information gathered from the sensors and will run low-level control loops that will check for critical changes in the environment or system that can affect the robot operation.

The Sensor&Management Board controller is able to communicate with the PC-NAV using a USB-to-RS232 converter and with the Motors Board using a RS232 communication link.

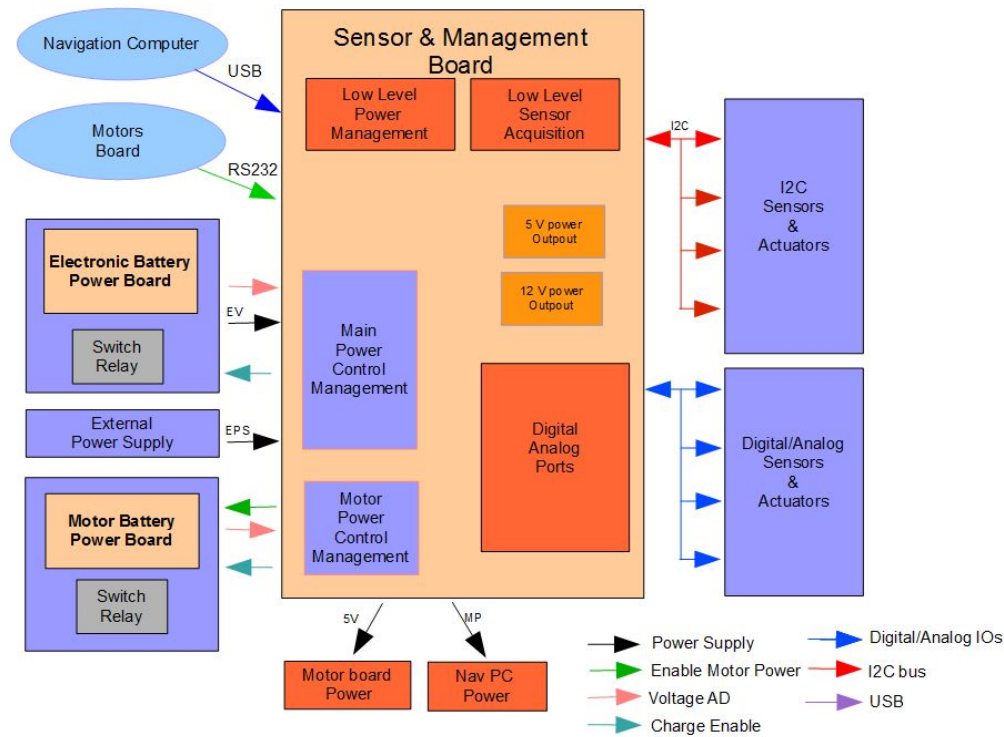


Figure 2.25. Sensor&Management Board architecture.

### 2.4.3. Wireless Joystick Controller Board

The Wireless Joystick Controller Board is an external wireless controller of the SIAR robot that can be used to take control the robot. This controller allows the user to take control of the SIAR platform, move the robot from one place to another, change the width of the robot and send a QuickStop command. It has also the ability to completely shut off the robot power.

The Wireless Joystick Controller has a “take” control button that when pressed will send motor control data to the Motors Board. When this button is pressed all the data sent by the PC-NAV to the Motors Board will be ignored. When the “take” control button is not pressed and the PC-NAV is controlling the movement, all the commands from the Joystick will be ignored, by the Motors Board, but Quickstop button will be always enable and can be actuated in case of need.

The “shut off” button will be also enabled to be actuated in case of need. The Motors Board will not use the information provided by this command but Wireless Power Control Board will. If pressed it will disconnect the batteries from the powered electronics.

The Wireless Joystick Controller Board Architecture is depicted in Figure 2.26.

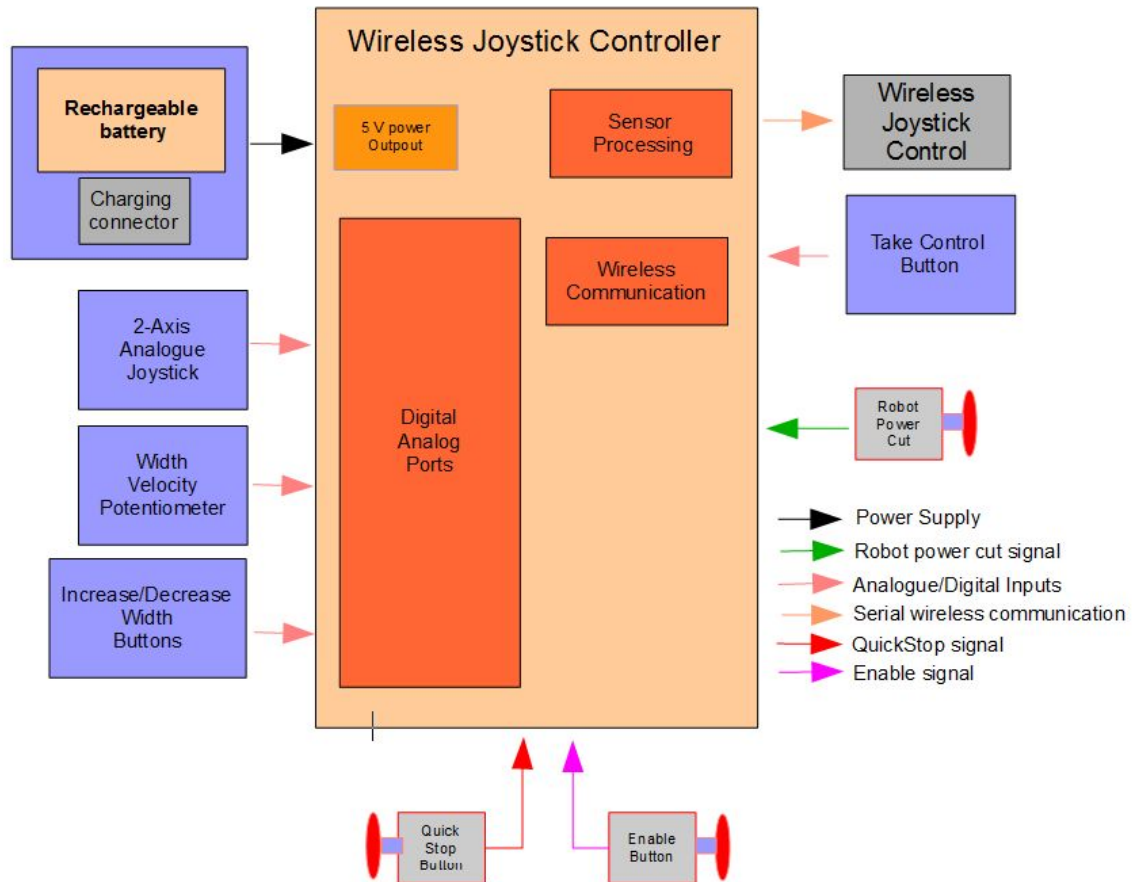


Figure 2.26. Wireless Joystick Controller Board architecture

The wireless Joystick Controller Board will be responsible for:

- Reading the 2-Axis Joystick analogue inputs.
- Reading the width controller.
- Read the take control button.
- Read the Shutdown button.
- Reading the Enable and QuickStop buttons.
- Sending processed information through the 868MHz wireless connection.

## 2.4.4. Wireless Power Switch Control Board

The Wireless Power Switch Control Board is used to control the connection and disconnection of the robot power. It uses a two stage power up system. A rotary switch is used to enable the power of the Wireless Power Switch Control Board and a Start push button is used to energize the board and close the power relay. A Stop push button is used to open the power relay and unpower all the devices on the SIAR Robot. The Start and Stop push buttons are connected to discrete logic gates allowing a fast power up/down of the robot.

The Wireless Power Control Board uses a PIC18F2431 microcontroller that is used to receive a shutdown command through a wireless 868MHz serial module from the external shutdown device. The microcontroller output connects to a AND gate that is able to open the power relay disconnecting all the devices on the SIAR Robot.

The Wireless Power Switch Control architecture is depicted in Figure 2.27.

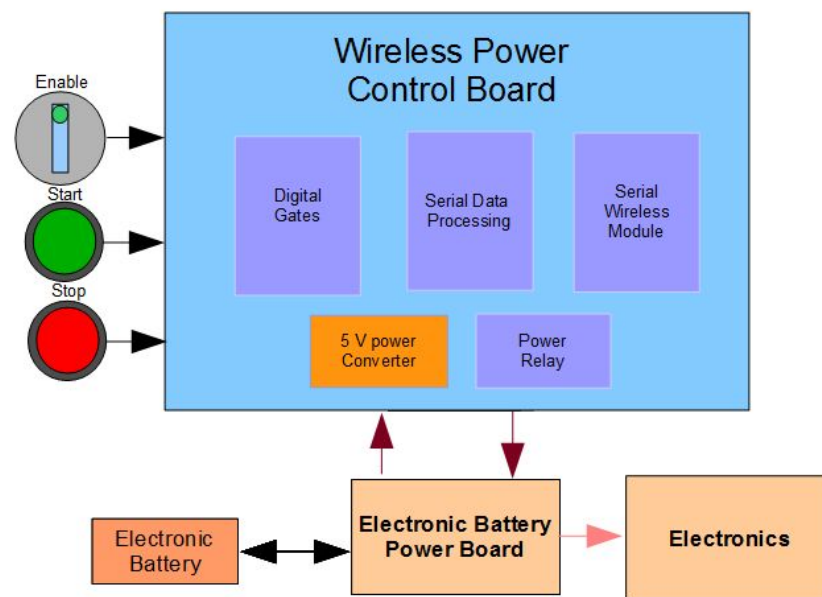


Figure 2.27. Wireless Wireless Power Control Board architecture

## 2.4.5. Environment Monitor Board

The environment monitor board is used to measure air and water variables parameters. The board receives orders from the Sensor&Management board and sends sensor data back. The environment monitor board connects to two boards: Air Sensors and Water Sensors.

The Air Sensors will be connected to the sensors that monitor the Air. The included sensors are: Temperature; Relative Humidity; Carbon Monoxide; Hydrogen sulphide; Methane; Oxygen; Lower explosive limit and Volatile organic carbons.

The Water Sensors will be connected to the sensors that monitor the Water. The included sensors are: Temperature, PH, Conductivity and turbidity.

The environment monitor board will have all the needed hardware to drive/actuate/read the individual sensors. Providing the necessary voltages, signals and AD converters.

The environment monitor board is an I2C Slave board of the Sensor&Management board. Its architecture is depicted in Figure 2.28.

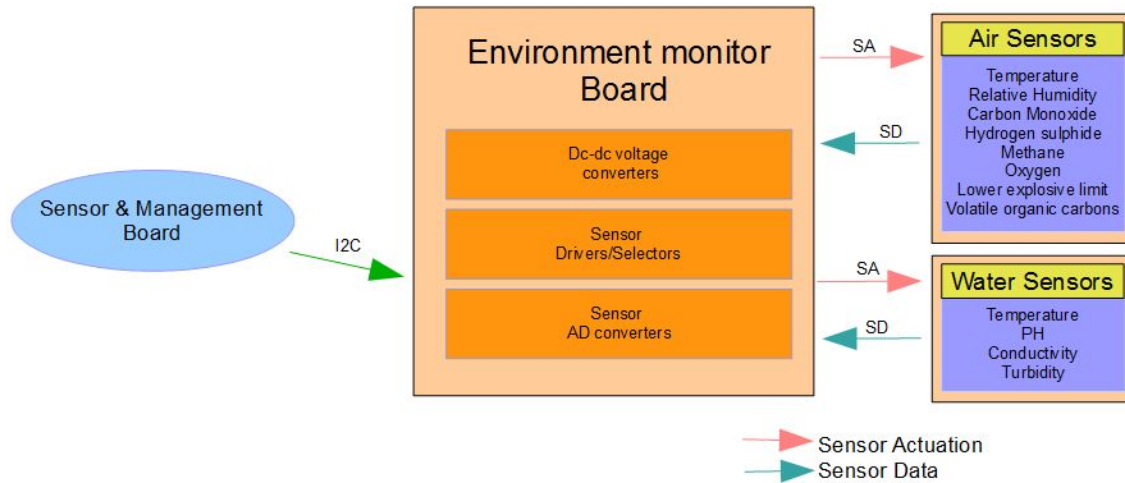


Figure 2.28. Environment Monitor Board architecture

#### 2.4.6. Sampling system board

The sampling system board is used to collect air, water and sediment samples from the environment. The board receives collecting orders from the Sensor&Management board. The sampling system board connects to three sampling systems: Air sampling system; water sampling system; and the sediment sediment sampling system.

The sampling system board will have all the hardware to drive/actuate/read the individual sampling systems. Providing the necessary voltages, signals and AD converters.

The sampling system board is an I2C Slave board of the Sensor&Management board. Its architecture is depicted in Figure 2.29.

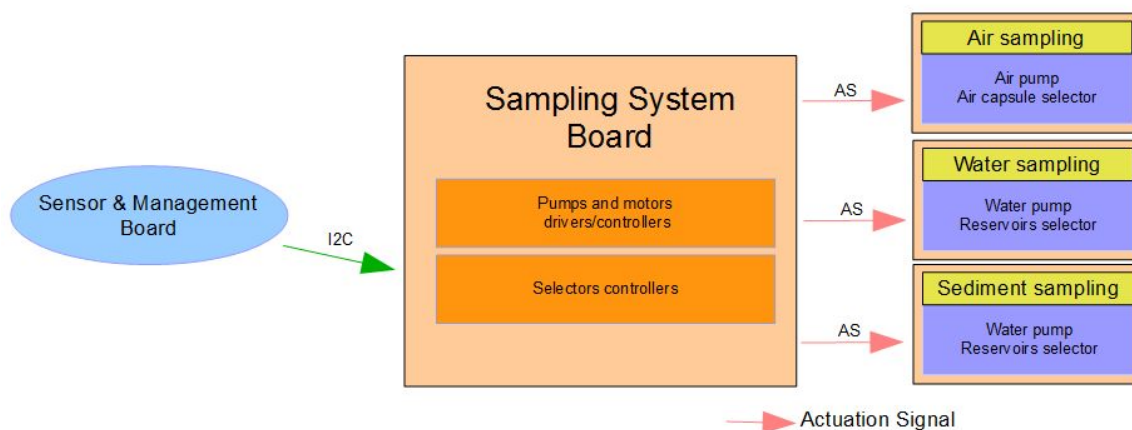


Figure 2.29. Sampling System Board architecture

## 2.5. Robot Safety

Figure 2.30 depicts all the safety triggers to be included in the SIAR robot.

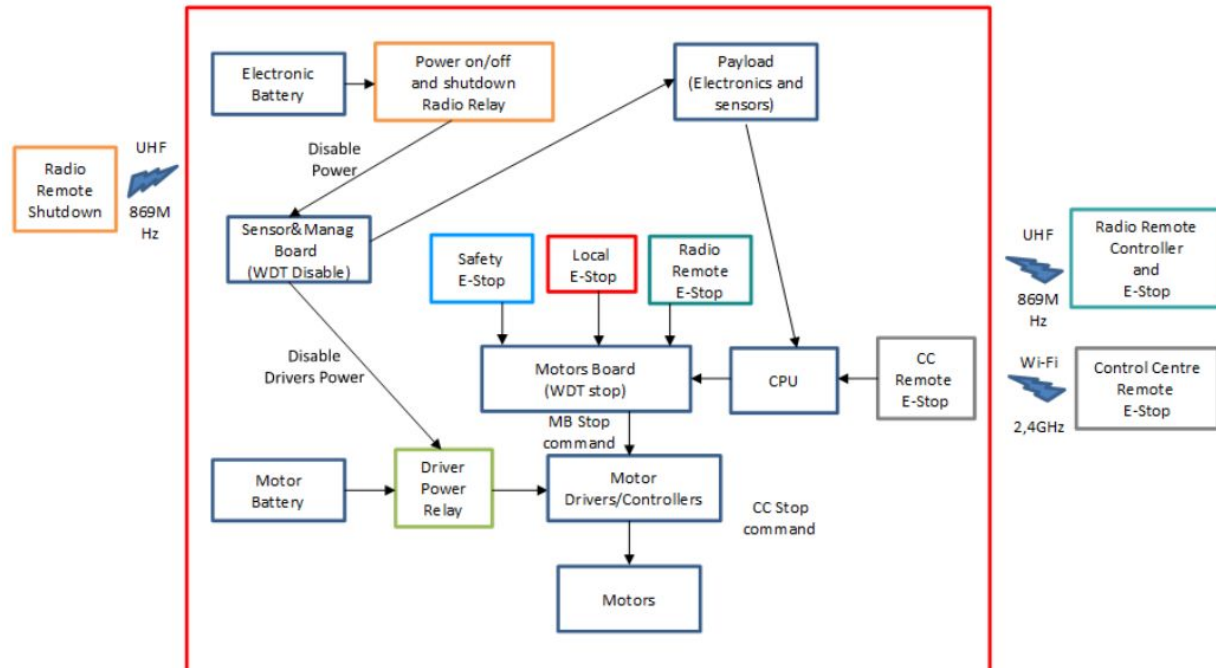


Figure 2.30. SIAR Safety diagram

The following elements will be included in the robot chassis, allowing a local operator to have some control over the robotic platform:

- **Enable Power Button** - Allows the power connection of the robot;
- **Power Start button** - Connects the batteries to the electronics and motors drivers;
- **Power Stop button** - Disconnects the batteries from the electronics and motors drivers;
- **Enable Motors button** - Enables/Disables the motor power signals. When disconnected the driving motors of the robot will become free and a human operator will be able to push and easily move the robot;
- **Emergency Stop button** - Send a quick stop command that sends a stop signal to all the motor drivers. The motors will stop with a high acceleration. In this mode the motors will not become free, being impossible to push the robot;
- **Voltage level LED/Bar** - Shows the estimated operation time of each battery by the use of a LED bar.

### 2.5.1. Control Station Remote E-Stop Commands

The PC-NAV receives a wireless remote stop command from the Control Station and sends an E-Stop command to the Motors board. The Motors board activates the QuickStop pins of the motor drivers which will immediately stop the motors. If the Control Station sends a start command to the navigation computer, then the navigation computer will send a start command to the Motors board and it will then clear the QuickStop pins of the motor driver. Otherwise the Motors board will keep the QuickStop pins activated.

### 2.5.2. Radio Remote Controller & E-Stop

This is a low-level 868 MHz based remote controller that can be used to control the robot when the PC-NAV is not controlling the robot. This controller allows the user to move the robot from one place to another, change the width of the robot, enable the drivers and send an E-Stop command.

When the PC-NAV is controlling the movement, commands of movement from this controller will be ignored by the robot, but the E-Stop will be enabled and can be actuated in case of need.

With the Radio Remote Controller powered, if the operator presses the E-Stop button on the remote controller, the remote controller sends an E-stop command to the Motors board, using the 868Mhz transceiver that is present on the Motors board and in the radio remote controller. The Motors board activates the QuickStop pins of the motor drivers which will immediately stop the motors. If the operator releases the E-Stop button, the Radio Remote Controller will start to send control commands to the Motors board and it will then clear the QuickStop pins of the motor drivers. Otherwise the Motors board will keep the QuickStop pins active.

### 2.5.3. Local E-Stop Push Button

The local on-board E-Stop push button is directly connected to the Motors board. When this button is pressed, the Motors board activates the QuickStop pins of the motor drivers which will then immediately stop the motors. If the operator releases the E-Stop button, the Motors board deactivates the QuickStop pins of the motor drivers, allowing the PC or the Joystick to regain control of the SIAR motors. Otherwise the Motors board will keep the QuickStop pins active.

### 2.5.4. Auxiliary Radio Remote Shutdown

The Auxiliary Radio Remote Shutdown will be installed on the Radio Remote Controller. This uses the same low-level 868 MHz communication channel of the Radio Controller to remotely cut the power of all the on-board electronics. This remote controller is able to cut the power of the robot to a distance of 100 m (line of sight).

If the operator presses the “ShutOff” button on the remote controller, the remote controller sends a ShutOff command to the Wireless Power Control Board, using the 868 MHz transceiver that is present on the Wireless Power Switch Control Board.

After receiving the ShutOff command, the microcontroller on the Wireless Power Control Board deactivates the electronic power switch of the electronic power board, disconnecting the batteries’ power supply from the system. Figure 2.31 shows the schematics of the electronic power switch.



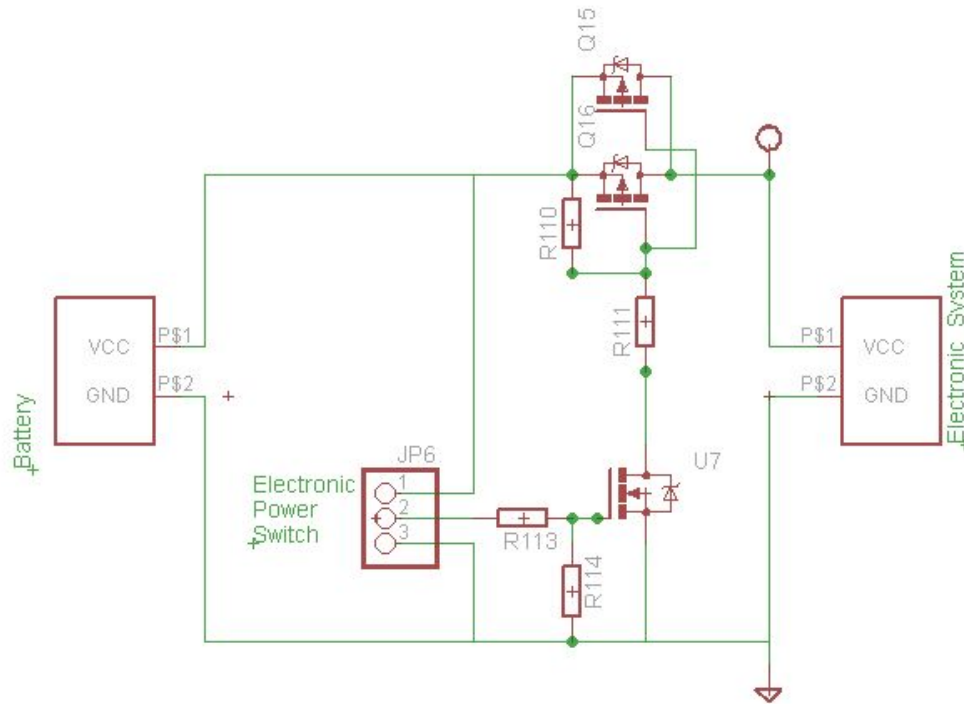


Figure 2.31. Electronic power switch..

The electronic power switch is connected to the Mosfet gates. When the switch is turned OFF, the P-type Mosfets block the current flow from the battery to the Electronics. When ON, it allows the current to flow from the battery to the Electronics. This switch can cut up to 148A, which is a very high current when compared with the maximum current that flows in the robot.

For safety a two stage power up system was created with two different ways to cut the power of the robot. This is explained on the following section.

### Onboard Wireless Power Switch Control Board Receiver

The Wireless Power Switch Control Board Receiver is used to control the connection and disconnection of the robot power. It uses a two stage power up system. A rotary switch is used to enable the power of the Wireless Power Switch Control Board and a Start push button is used to energize the board and close the power-ON relay. A Stop push button is used to open the power-ON relay disconnecting all the devices on the SIAR robot. The Start and Stop push buttons are connected to discrete logic gates allowing a fast power-up and power-down of the robot.

The Wireless Power Switch Control Board Receiver uses a PIC18F2431 microcontroller that is used to receive a shutdown command through a wireless 868 MHz serial module from the auxiliary radio remote shutdown Emitter. The microcontroller output connects to an AND gate that is able to open the power-ON relay disconnecting all the devices on the SIAR robot.

The Wireless Power Switch Control is depicted in Figure 2.32.

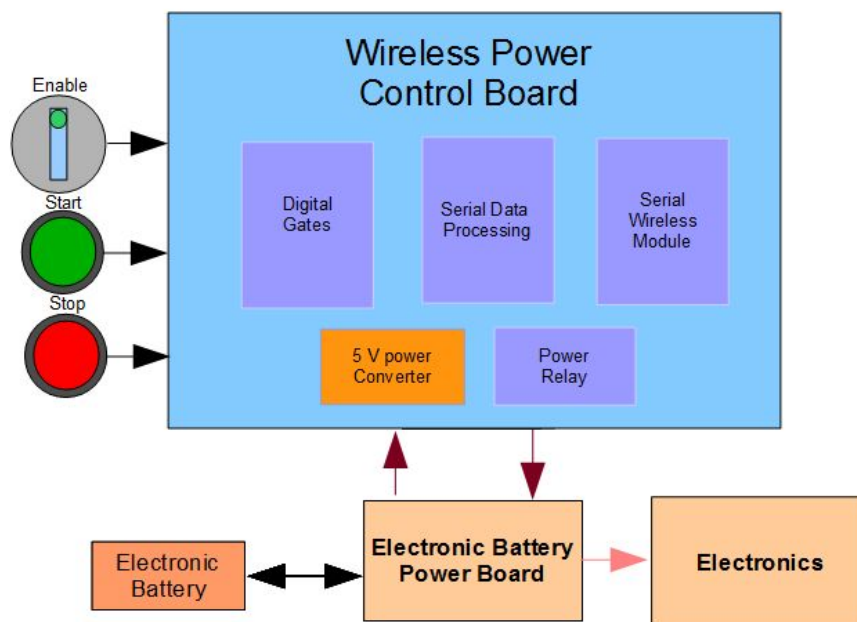


Figure 2.32. Wireless Power Switch Control Board receiver architecture

Figure 2.33 depicts the power switch control schematics. JP6 in Figure 2.31 connects to JP6 in Figure 2.33 (Electronic power switch connector). The top connector pin will have the battery voltage (IN), the next pin (OUT) will have 0V if the system is OFF or the battery voltage if the system is ON and the bottom pin will connect to the ground of the battery.

The IN pin connects to the Rotary Switch that is Enabling/Disabling the possibility to power ON the system.

To turn ON the system, the switch connected to JP9 (“Press to Switch ON”) must be pressed. When pressed, the K2 relay is energized and  $V_p$  is connected to the  $V_{out}$ . In this moment the microcontroller that is on the Receiver board will put the RC2 pin to High. Consequently the K8 relay will be energized, closing the connection made by the JP9 (Press to Switch ON) switch.

To turn OFF the system, the JP10 (“Press to Switch OFF”) switch must be pressed or the RC2 PIN of the microcontroller must be taken to LOW. If one of these conditions is true, the K8 relay will be released and by doing so the K2 is also released, cutting the current between  $V_p$  and  $V_{out}$ .

The microcontroller will only put the RC2 pin to LOW if it receives a wireless shutdown command from the Wireless Power Switch Control Board Emitter.

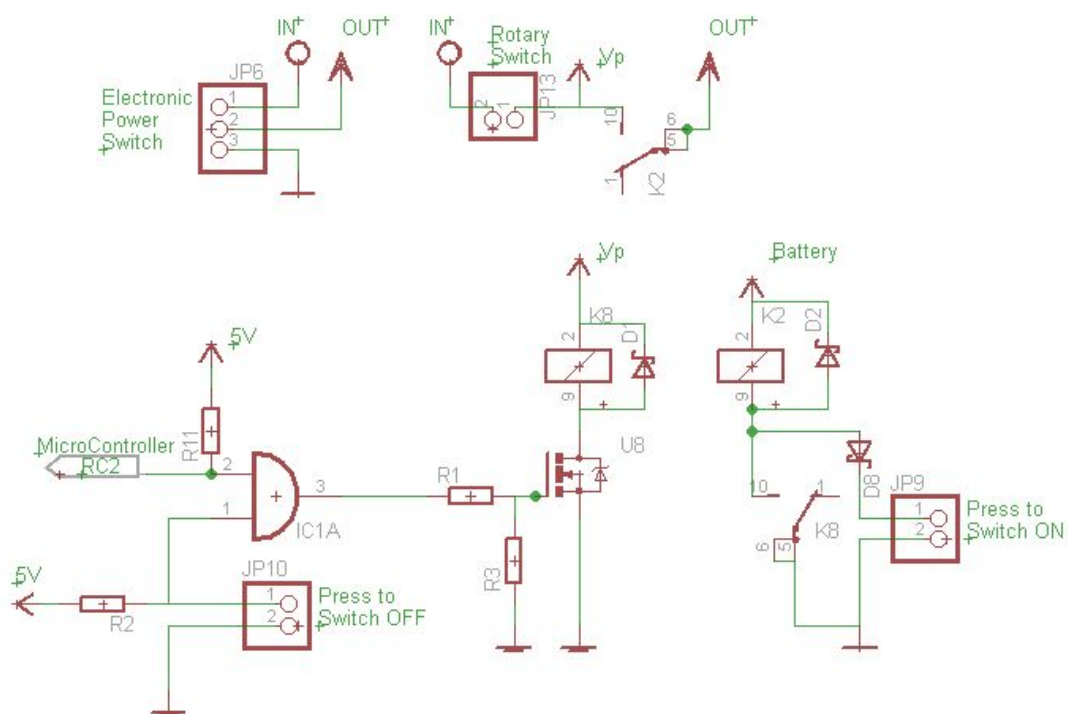


Figure 2.33. Power Switch control schematics

## 3. Communications

One of the requirements of the robot is the capability of receiving commands from the operator, who, at the same time, should receive images and other data from the robot [ECHORD++, 2014]. This section details the proposed communication system that will provide the SIAR platform with continuous wireless connection with the base station even without direct line of sight (LoS) and with a long distance between the robot and the base station (hundreds of meters or even kilometers). Initial field experiments with the proposed equipment are presented in order to prove the validity of the solution.

### 3.1 Overview

Wireless communications in the sewage system is an open issue that would simplify the robot setup when available thanks to the elimination of tethers and cables, used by most of current solutions, and that limit the lengths that the robot can explore. Our solution aims to solve this problem by means of autonomous deploying self-powered wireless repeaters when they are needed.

The design of a wireless communication system inside the sewer system involves a great challenge due to the harsh environmental conditions and its architecture. In fact, it is common to find 100% humidity condition. Another major issue is the presence of obstacles, such as walls, pipes or garbage which would not allow LoS transmission between the robot and the base.

In these circumstances, it is well known that signals with lower frequency would have better penetration properties than the ones with higher frequency. Therefore, it can be convenient the use of a standard 2.4GHz wireless connection for data intensive communications and a sub-1GHz link for more reliable communications. In this way, we ensure that a communication link is available, if the 2.4 link is broken. Moreover, the deployment of repeaters of both links whenever the LOS is expected to be lost and therefore the quality of the links would begin to degrade is proposed.

### 3.2 Solution

In this section the technical details of the proposed solution in which the robot can communicate with the base station by two independent data links. These are:

1. **Primary link:** the robot and base station will be equipped with a long range WiFi router Microhard nVIP-2400 in order to provide the different computers onboard of the robot and the comms package with a high baudrate (up to 54 Mbps) WiFi connectivity.
2. **Backup link:** the robot and base station will also be equipped with Microhard 900 MHz serial equipments. This link is able to connect two devices separated up to 50-100 Km with a data rate of 236 Kbps in outdoor environments with LoS. However, a range drop to less than 1 Km is expected in indoors. This range could be extended by the use of a directional antenna in one of the sides.

This link will be used for reliable image transmission at low rates and reliable command transmission.

In order to extend the LoS when performing the experiments, one or more repeaters of the communication package (including WiFi and the radio modem at 400-900 MHz) can be deployed from the SIAR platform. In this way, we can always obtain wireless connectivity with the base station even in the presence of turns.

### 3.2.1 Primary link

The communication block will be equipped with a long range WiFi router Microhard nVIP-2400, with an expected range of 50 Km, that will likely drop to less than 1 Km in indoors environments. This link will provide the robot with a high bandwidth connection that could be used for video streaming and sending additional data information such as the generated point clouds of the environment.

Additionally, a Ethernet Switch with more than three RJ-45 will be installed in order to connect the main computers to the WiFi network and thus with the base station. This will give the two computers wired connectivity for data-intensive communications, such as the RGB-D sensors video links.

### 3.2.2 Backup link

Three different devices with interesting characteristics have been found that could be useful in that 900 MHz range:

- Ubiquiti NanoStation Loco M900. This station can transmit WiFi over the 900 MHz band with up to 150 Mbps of throughput. Offers a range (with LoS) of 10 Km.
- MicroHard Nano IPn920. This device can be acquired with an IP67 certified enclosure. Its main advantage can be its size (57 x 98 x 98 mm) and range (50km+@1.2Mbps). It can be used with repeaters. It offers optional 869 MHz spectrum to meet the European restrictions on RF transmission.
- MicroHard Pico P900. This device offers a serial link, with the possibility of installing mid-term repeaters, in Point-to-Point or Point-Multipoint configurations at the bands of 900 MHz. Its expected range could reach 100km@236Kbps.

For the initial prototype we have selected the Microhard Nano-series P900 devices as they offer the longest communication range of the three and an appropriate baud rate for a backup link. They can be used in Point-to-Point or Point-Multipoint communication topologies, which could be of interest if a multi-robot system is deployed.

The main characteristics of the selected devices in the family are listed in Table 3.1.

Model	Size (mm)	Weight (g)	Pow. cons.	Baudrate	Temp (°C)	Humidity
P900	46 x 66 x 25	120	5 W (3.3V 1.5A)	Up to 236 Kbits/s	-55 to 85 °C	5-95% non cond.
nVIP2400	57 x 98 x 38	200	5.5 W	Up to 54 Mbits/s	-40 to 85 °C	5-95% non cond.

Table 3.1. Main characteristics of the proposed communication equipment

### 3.2.3 Automatic deployment of repeaters

The deployment of repeaters of both links whenever the LoS is expected to be lost, and therefore the quality of the links could begin to degrade, is proposed. This will extend the operational range of the robot in more than 300m for each repeater.

To this end, the robotic platform will be equipped with a 3DoF manipulator which will automatically pick-up one of the available communication repeaters and deploy it on the back side of the robot (see Figure 3.1). This manipulator will also be used in order to retrieve the already deployed repeaters, which will be tagged with AR tags.



Figure 3.1. SIAR Robot deploying one wifi communication repeater

### 3.2.4 Antenna considerations

The P900 comes with 2dBi antennas, which offer an omnidirectional pattern, which are connected externally. In the base station, it could be a good idea to install a sectorial antenna which can extend the range in the exploration direction.

Additionally this antenna could be installed in a pan&tilt platform to make the base station able to point the antenna to the places where the signal is stronger. There are OTS products that could provide the robot with this type of abilities<sup>4</sup>.

### 3.2.5 Frequency considerations

<sup>4</sup> [https://www.servocity.com/html/fpv\\_antenna\\_tracker\\_setup\\_-\\_se.html](https://www.servocity.com/html/fpv_antenna_tracker_setup_-_se.html)

As stated before, the selection of 900 MHz band could be useful as a backup link because of the enhanced penetration properties of a radio signal which emits at a lower frequency. However, the use of equipment at this signal range presents some drawbacks:

- The antennas that are used to emit at these frequencies are much larger than their equivalents at 2 and 5 GHz. A directional antenna with interesting properties can be found in this link <http://www.gowifi.co.nz/antennas/900-mhz/directional/arc-902-928mhz-12.5dbi-antenna.html> but it has a weight of 1 kg.
- The devices found emit at the USA ISM (non-commercial) band (902-928 MHz), which does not englobe same frequencies as the European ISM band (862-868). On the other hand, the ISM frequencies have been established worldwide at the 2 and 5 GHz frequencies. This does not apply to the 400 MHz which is also standardized worldwide. However, this is not expected to become an issue when using the SIAR inside the sewer systems, as only a neglectable fraction of the signal would be emitted to the outside of the sewers. At the same time, similar devices on the 868MHz band will be analyzed.

### 3.3 Tests and experiments

Several communication experiments with the proposed NVIP2400 equipments have been carried out in two different scenarios to validate the communication using several repeaters. First, several tests were carried out at the basements of the University Pablo de Olavide (UPO) in similar conditions, although with less humidity, as the sewers. The equipments have been also partially tested in the sewers located at the test environment.

#### 3.3.1 Experiments at the UPO basements

Two experiments have been carried out in the basements of the University Pablo de Olavide, Seville for testing the proposed communication system. Figure 3.2 represents the disposition of the communication equipment in the experiments. Note that these experiments were carried out to test the primary link, i. e. the NVIP2400 WiFi connections. A short description of each experiment can be found below.

- **Long range experiment.** The main goal of this experiment is to test the maximum range of the aforementioned equipments with LoS and in an indoor environment. Then from that location, a repeater was deployed for extending the communication range. The trajectory of the robot is represented in a red line in Figure 3.2.
- **Experiment with two corners.** The goal of the experiment is to test the communication devices in conditions as close as possible as the test to be performed in Barcelona on July 7th. Therefore an experiment with two turns and 300m of total distance has been carried out. The trajectory of the robot is represented in a green line in Figure 3.2.



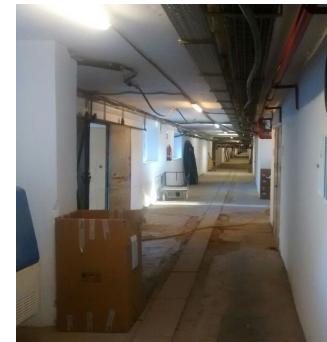


Figure 3.2. Location of the communication equipment and trajectories of the robot in the experiments at the UPO basement. Red: experiment with one repeater; the first leg is 330 m long, while the second is 120 m. Green: experiment with two repeaters; each leg is approximately 100 m long. The circles represent the position of the ground station.

### Long range experiment

As stated above, the main purpose of this experiment is to characterize the performance of the NVIP2400 without repeaters. Therefore, the robot was directly teleoperated as far as possible, until the performance of the link started to decrease. Then, a repeater was deployed and the robot was commanded to inspect a gallery on the left until its very end.

Figure 3.3 represents the mean value of the measured bandwidth with respect to the traveled distance by the robot. These measures were obtained by executing the iperf3 multiplatform network benchmark tool<sup>5</sup>. Note the first valley on the bandwidth that can be produced by transmitting at an excessive power when taking into account the separation between nodes. Then, the bandwidth starts to increase. This can also be produced by a slight elevation of the terrain, that could improve the visibility between antennas. At the end of the corridor, the measure bandwidth starts to fall noticeably due to signal degradation. The final three measures were obtained thanks to the deployment of one repeater, as no LoS transmission could be obtained between the robot and the base station (see Figure 3.2). In these circumstances, the available bandwidth seems to be halved with respect to the measures with distances 275 and 290 meters. Note that the bandwidth obtained in the furthest measure is noticeably lower than the other two: this is produced due to signal degradation in the link between the robot and the repeater, there was no direct LoS in this link. Figure 3.4 represents the Received Signal Strength Indication (RSSI) perceived by the receiver on the robot as a function of the distance to the base station in direct communication (without the presence of repeaters). Note that the communication floor of the equipments in the configuration was -96 DBm.

<sup>5</sup> <https://iperf.fr>



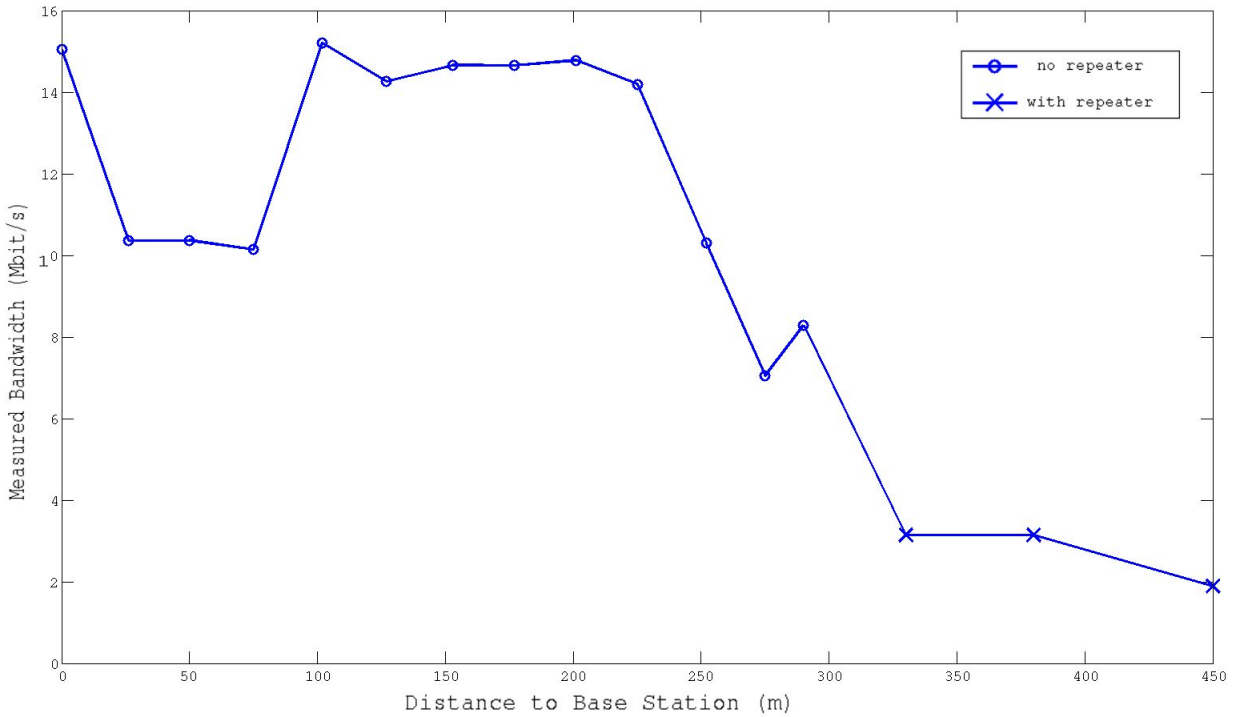


Figure 3.3. Measured bandwidth of the communication in the range experiments.

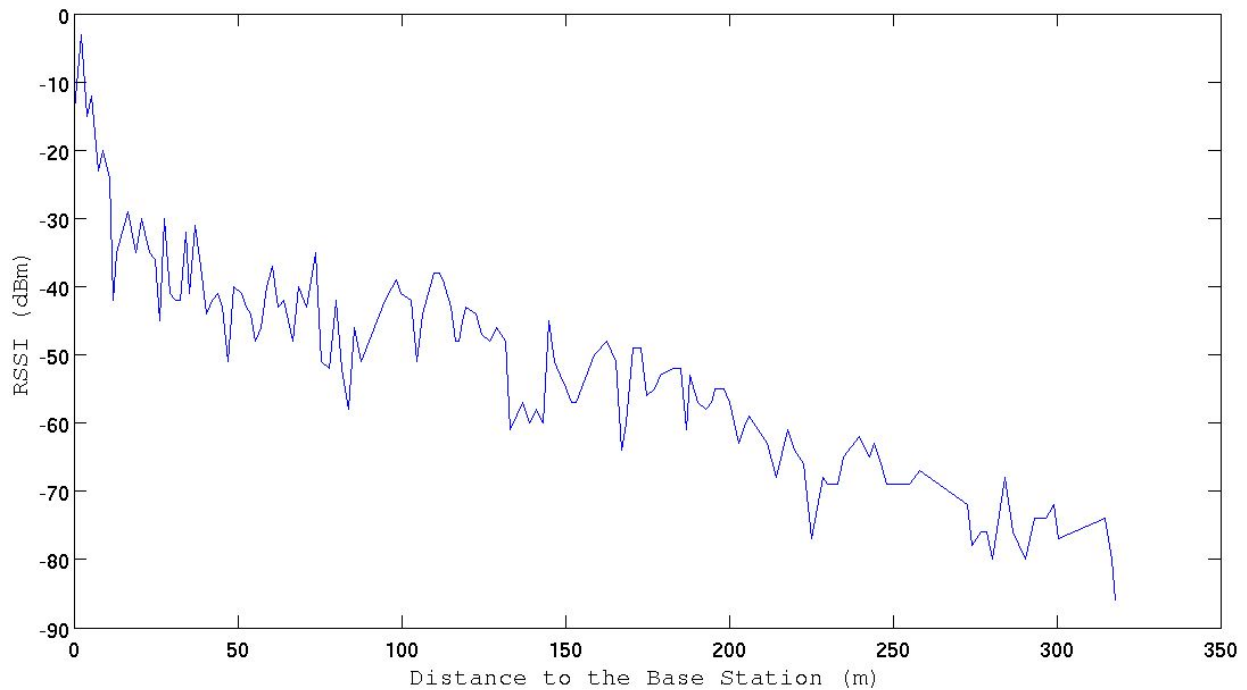


Figure 3.4. RSSI with respect to the distance to the base station.

Figure 3.5 shows the evolution of the wireless communication delay obtained with the tool provided by the consortium (UPC). The first part was obtained without the presence of repeaters in the network. In this case, the obtained measurements are in the surroundings of 1 millisecond (average delay), while the highest delay

was produced at a distance of 290 m with a value of 5 milliseconds. Then, the distribution of the delays raises when a repeater is connected. In the first two cases (330 and 380 meters), the average delay was 1.6 and 2.0 milliseconds, respectively. Finally, the last distribution of delays (450 m) was significantly different to the other two. As the performance of the two links was not ideal, the results presented more diversity and also the median value (in red) raised to 4 milliseconds, while the 97% of the measures were below 0.05 seconds. Even though this is a significant raise, it is still a very satisfactory result for teleoperation purposes, as will be proven in the next experiment.

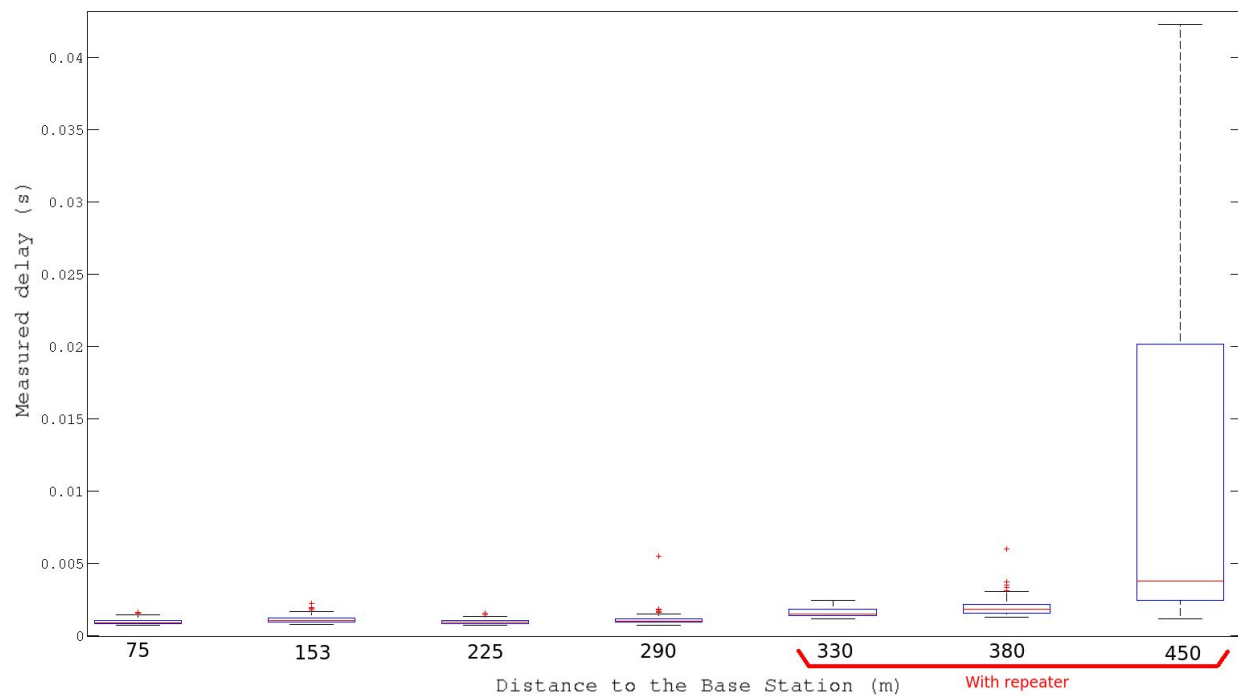


Figure 3.5. Box plot of the delay measures obtained in the long range experiment.

### Experiment with two corners

This experiment was designed to present two corners and thus to have the necessity of including two repeaters in order to have direct LoS visibility in all links, although the total distance between the robot and the base station (300 m) is shorter than the previous experiment. In this experiment, the bandwidth and delays measures were obtained just before placing the corresponding repeater.

The experiment was divided in two stages. In the first stage, the base station was located at the main corridor of the UPO (see Figure 3.2 in a green circle) and the robot was directly operated towards its final location, marked in the same figure with a star. The first repeater was placed in order to ensure LOS transmission between robot and base station.

In the second stage, the base station was moved into a second location (see Figure 3.2) and a second repeater was deployed to ensure connectivity. In this stage, the measures with two repeaters were obtained and then, the robot was teleoperated back to the base station.

Figure 3.6 shows the bandwidth measures obtained with different number of repeaters in the network. Notice that the bandwidth decreases with the number of repeaters as just a single channel is available. On the other hand, Figure 3.7 represents the measured delay obtained with different number of repeaters in the

system. In this case, even though there is a raise in the median value of the delay, which is 1, 1.4 and 2.8 milliseconds with 0, 1 and 2 repeaters, respectively, the amount of delay would not be noticeable by an operator in the base station and thus, the system will be able to provide the operator with real-time images in spite of the number of deployed repeaters.

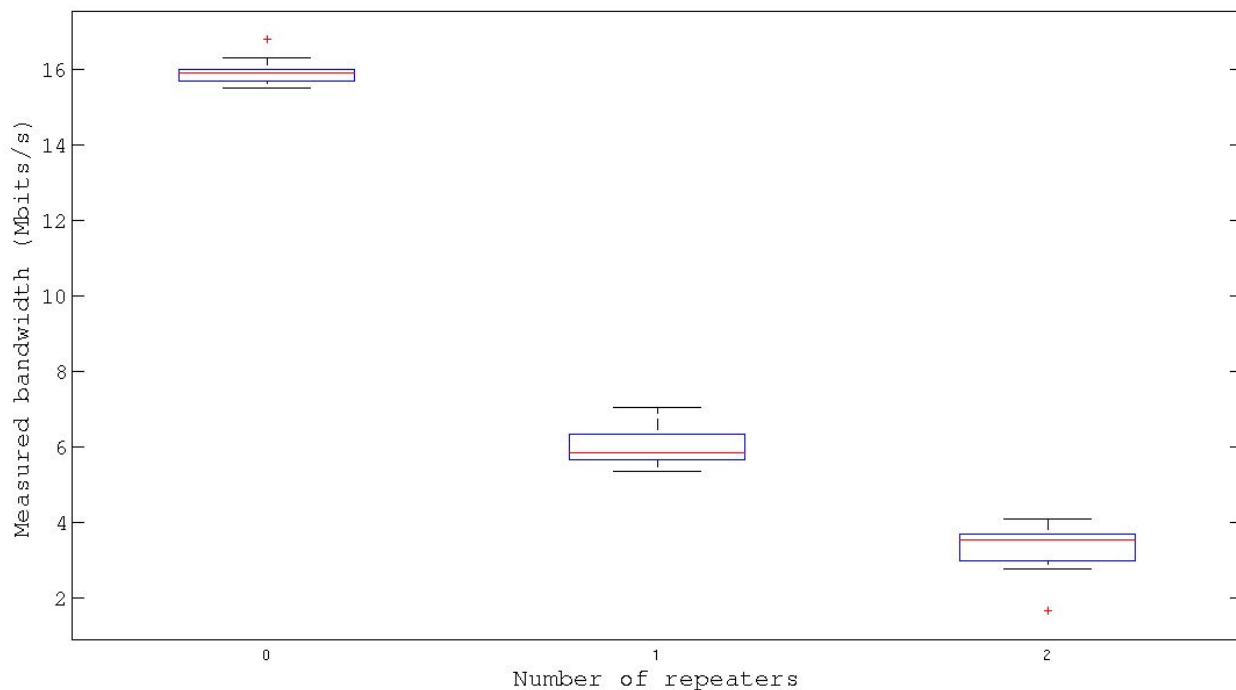


Figure 3.6. Bandwidth of the experiment with two corners as a function of the number of repeaters in the system.

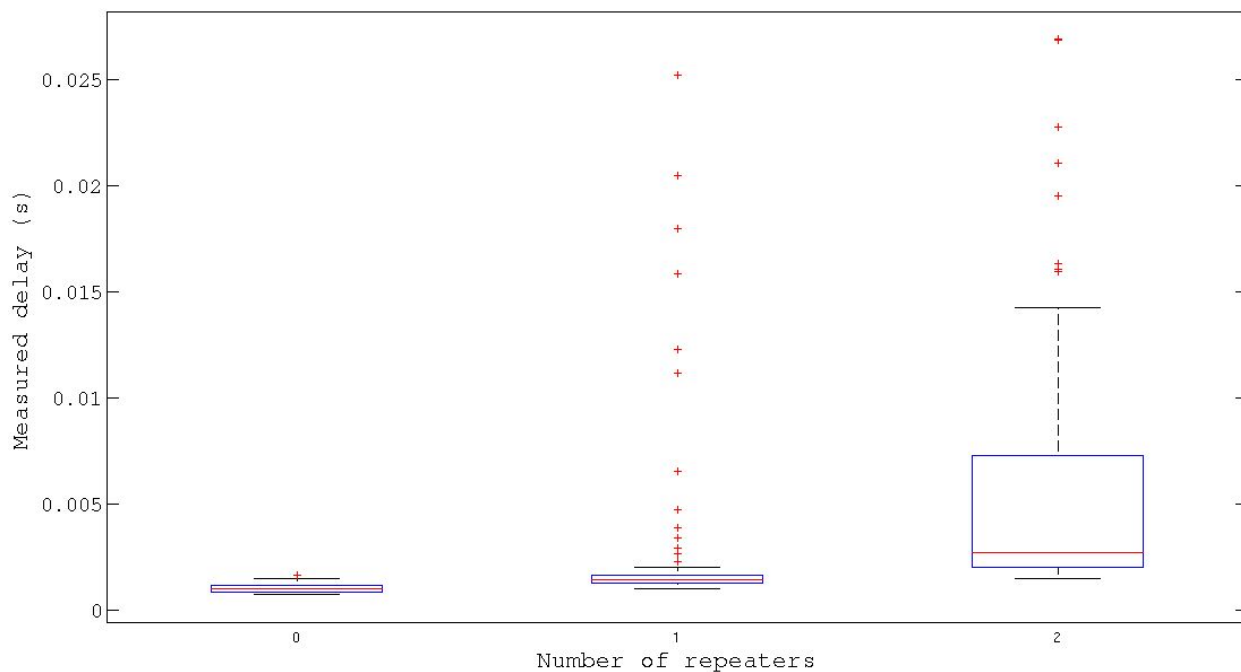


Figure 3.7. Dependence of the delay with the number of repeaters in the system.

Finally, in the last part of the experiment the robot was teleoperated back to the the base station. Each time a repeater was reached, two bandwidth and delay measures were obtained at the same point before and after disconnecting the repeater. This was carried out in order to further test the dependency of the network with the number of repeaters. Table 3.2 represents the mean and standard deviations of both measured delay and bandwidth before and after the disconnections. Note that the bandwidth estimations are lower than before, because the link was also used for sending images and other messages in real-time for teleoperation purposes.

	Location of repeater 1		Location of repeater 2	
	2 repeaters	1 repeater	1 repeater	0 repeaters
<b>Bandwidth (Mbit/s)</b>	1.0244+/-0.63	6.1+/-0.57	5.7+/-0.7	13.1+/-0.97
<b>Delay (s)</b>	0.0118+/-0.017	0.007+/-0.013	0.008+/-0.010	0.0015+/- 0.0023

Table 3.2. Results of the communication tests during the teleoperation tests at the basement of the UPO.

### 3.3.2 Experiments at the Passeig of Sant Joan sewers

Additionally, the communication devices were also tested at the location of the final experiments. Two different tests have been performed. In the first test, the robotic platform was used and the communication devices were active to test the reliability of the video link and to perform some teleoperation tasks. In the second test, only the communication devices were tested. They were deployed at the locations specified in the final communication tests and the tools provided by the consortium were used to estimate the quality of the link.

#### **Autonomy, mobility and teleoperation tests**

The first experiment was carried out on June 7th and 8th with the SIAR platform. The communication system was tested as the teleoperation base station was active during the whole experiment and real-time images from the front and rear cameras of the robot were obtained consistently in all moments.

Figure 3.8 represents the path followed by the SIAR platform in the extended mobility test. As stated before, video images from the front and rear cameras were obtained in real-time. To this end, a repeater was deployed in the corner of streets Valencia and Bailén, as indicated in the figure.

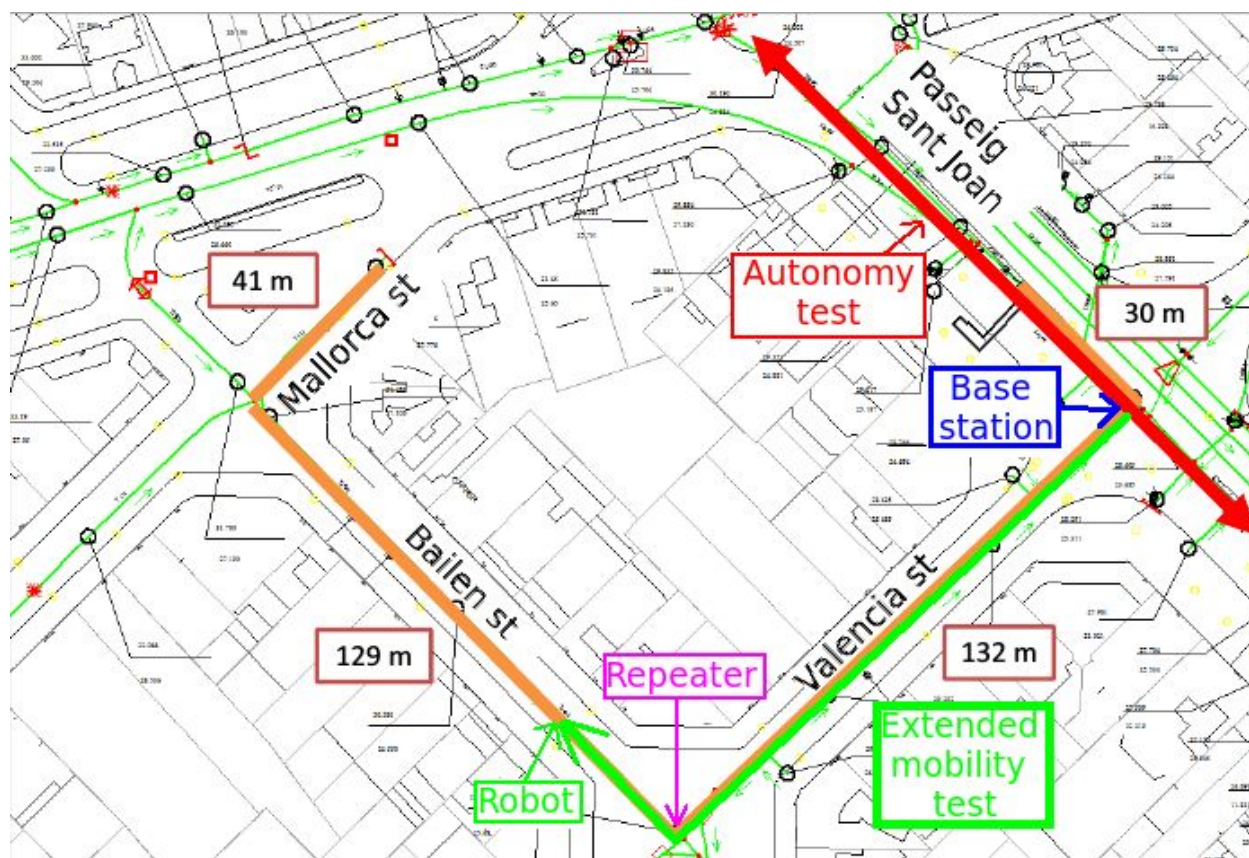


Figure 3.8: Path followed by the robot in the extended mobility tests and in the autonomy test.

The experiments also included a teleoperation test over the Valencia street. In this test, the robot was able to reach half of the street without external intervention.

An autonomy test was also performed afterwards. In this test, the robot was commanded to travel the sewer at the Passeig of Sant Joan for a one-way distance that exceeded 200 m. The SIAR platform was able to perform more than four travels, thus covering almost 1 km of total traveled distance. The test was carried out partly teleoperated from the base station (one of the travels) and the rest of the time was directly operated.

Therefore, these tests demonstrate the suitability of the proposed communication systems, as they were able to transmit real-time images without noticeable lag during all the three tests and an operator was able to tele-operate the platform from a base station in both Valencia street and Passeig of Sant Joan.

### Communication tests

A visit to the sewers for further test the communication devices was carried out on June 21st. In this case two laptops were connected to the initial and final communication devices and the tools provided by the consortium were used to evaluate the quality of the links. Figure 3.9 shows the location of the base station on a brown circle and the different locations where the transmission has to be tested on red circles. The results in these locations of the different tests are listed in Table 3.3.



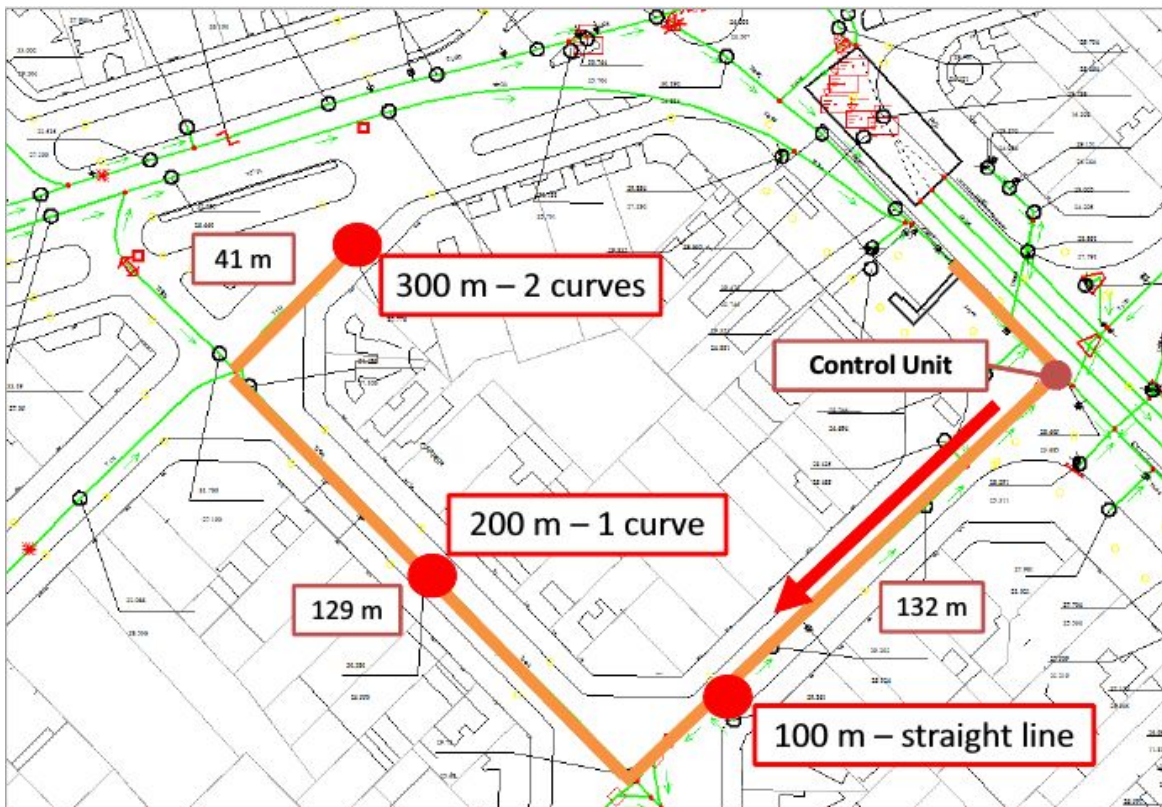


Figure 3.9: Location of the control unit (on brown circle) and successive locations of the end of the link. The tests were performed in the first and second red spots.

	Location 1 (100m)	Location 2 (200m)	Location 3 (300m)
<b>Bandwidth (Mbit/s)</b>	4.45	N/A	N/A
<b>Delay (s) (median)</b>	0.0014+/-0.17	0.0012+/-0.28	0.023+/-0.48
<b>Error rate (%)</b>	0	0.1	0.1

Table 3.3. Results of the communication tests at the sewers of Passeig of Sant Joan.

The bandwidth estimated by the software provided by the consortium in that time turned out not to be reliable when compared to other tools such as the one used in Section 3.3.1 (iperf). In fact, in locations 2 and 3, the program exited before obtaining response, so it could not estimate the bandwidth. These issues with the tool have been reported to the consortium so the bandwidth would be better estimated in the final tests on July. The other estimations (delay and error rate) are very satisfactory, as delays in the order of milliseconds were usually obtained and less than 0.1% of package losses were obtained in all places. Note that the median of the delay result is presented to avoid the presence of some outliers in the estimation produced by sewer workers blocking the LoS.

## 4. Software Architecture

The SIAR software architecture is a set of modules that make use of the robot platform, sensors and communications described in the previous sections to develop the required functionalities (self-localization, navigation, inspections, etc). This architecture is implemented under the Robotic Operating System<sup>6</sup> (ROS) framework, using the ros-indigo distribution under Ubuntu 14.04.

The software modules reflect the functionalities required for the sewer inspection, as established in [ECHORD++, 2014]. Figure 4.1 shows the main modules that are envisaged for the architecture of the final system.

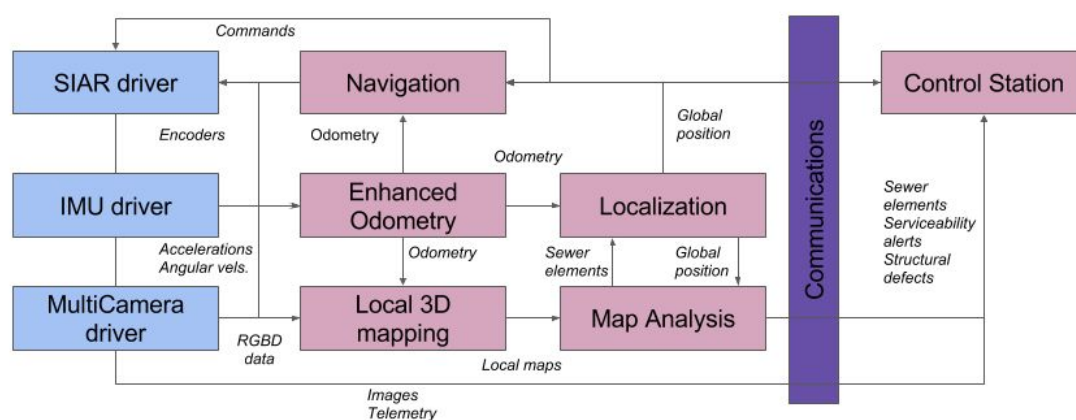


Figure 4.1. Software Architecture

These modules are the following:

- SIAR driver. Software that interfaces with the hardware board of the robot described in Section 2, and offers a standard ROS commands and services for easy integration of the robot with the rest of the system.
- IMU driver. This package filters the raw data produced by the inexpensive IMU sensor Arduimu v3.
- Multi-camera driver. This package extends the functionality of the `openni2_camera`<sup>7</sup> and `openni2_launch`<sup>8</sup> ROS packages. It provides the user with a utility for generating launch files that sequentially activate each camera. Each camera can be configured with its own setup, i.e. changing the image rate, its resolution and many other parameters.
- Enhanced Odometry (Section 5.1). This package provides enhanced odometry estimates by fusing IMU and encoders measures with visual odometry estimates. In this way, the SIAR platform is able

<sup>6</sup> <http://ros.org>

<sup>7</sup> [http://wiki.ros.org/openni2\\_camera](http://wiki.ros.org/openni2_camera)

<sup>8</sup> [http://wiki.ros.org/openni2\\_launch](http://wiki.ros.org/openni2_launch)

to precisely and robustly estimate a 6-DOF odometry. A good odometry estimation is necessary for obtaining precise 3D maps of the environment.

- Localization (Section 5.2). The precise odometry estimations are used by this module in order to estimate the global position of the platform. This block uses prior information of the sewer systems (localization of manholes, inlets, to name a few), and the detection of such elements provided by the map analysis module, in order to correct the drift which is accumulated in the odometry estimation and to provide the location of the robot within the sewer network.
- Navigation (Section 5.3). The SIAR robot will be commanded in three different operating modes. This module will also allow the operator to command actions to the SIAR which are not directly related to navigation, such as taking air or water measures and deploying repeaters.
- Local 3D mapping (Section 6.1). This package gets the enhanced odometry outputs and uses them to integrate the measurements from the different RGB-D sensors disposed over the SIAR robot. This would allow the operator to have a precise 3D local reconstructions of the sewer. With the localization outputs, these local maps can be referred to the global sewer network.
- Map Analysis (Section 6.2). This module provides the high level information required for sewer inspection. It receives the local 3D maps and analyzes them to extract sewer elements, estimate the serviceability and inspect critical defects.
- Control Station (Section 4.1): This module will send an alert to the operator when critical conditions occur. These conditions can include automatic detection of structural defects, bad state of the radio links, low battery indicator, the robot has lost traction and should be recovered, among others. It will also display the localization of the robot and the images from the onboard cameras in real-time.
- Communication block (Section 4.2): even though ROS offers a middleware for inter-process communication, we experienced that it was not very optimized for real-time transmissions where the delay should be as low as possible. Therefore, we opted to bring up two independent ROS cores in both the robot and the base station and to design and implement new ROS modules that would act as bridge between the different ROS cores in the system.

## 4.1 SIAR Control Station

A preliminary base station, based on the `rqt`<sup>9</sup> and `rviz`<sup>10</sup> ROS tools, has been designed in order to allow the operator to remotely operate the SIAR platform in real-time using a joystick. Figure 4.2 represents a snapshot of the base station when performing an experiment at the IDM facilities in Lisbon. It counts with the following features:

- Real-time RGB-D video-link with frontal or rear cameras. Optionally, it can be configured to transmit both video-links or to select another camera of interest.
- Switch for operating backwards. This switch will affect not only the joystick commands, but also will change the camera used as source for the video-link. In this way, the rear camera is being transmitted when operating backwards so the operator can easily change the exploration direction.

---

<sup>9</sup> <http://wiki.ros.org/rqt>

<sup>10</sup> <http://wiki.ros.org/rviz>



- RSSI indicators and battery level indicators in real time. A plot with the historic data is represented at the bottom of the Figure 4.2.
- A 3D-model of the platform is represented in order to inform the operator about the size of the real platform. In this way, the robot can be safely tele-operated into narrow corridors. Figure 4.2 presents a snapshot where the SIAR platform was about to cross a narrow door. The 3D model was used as a guide to tele-operate the robot from the base station.
- The quality and rate of the video-links can be on-line modified to adapt to the status of the communication link.

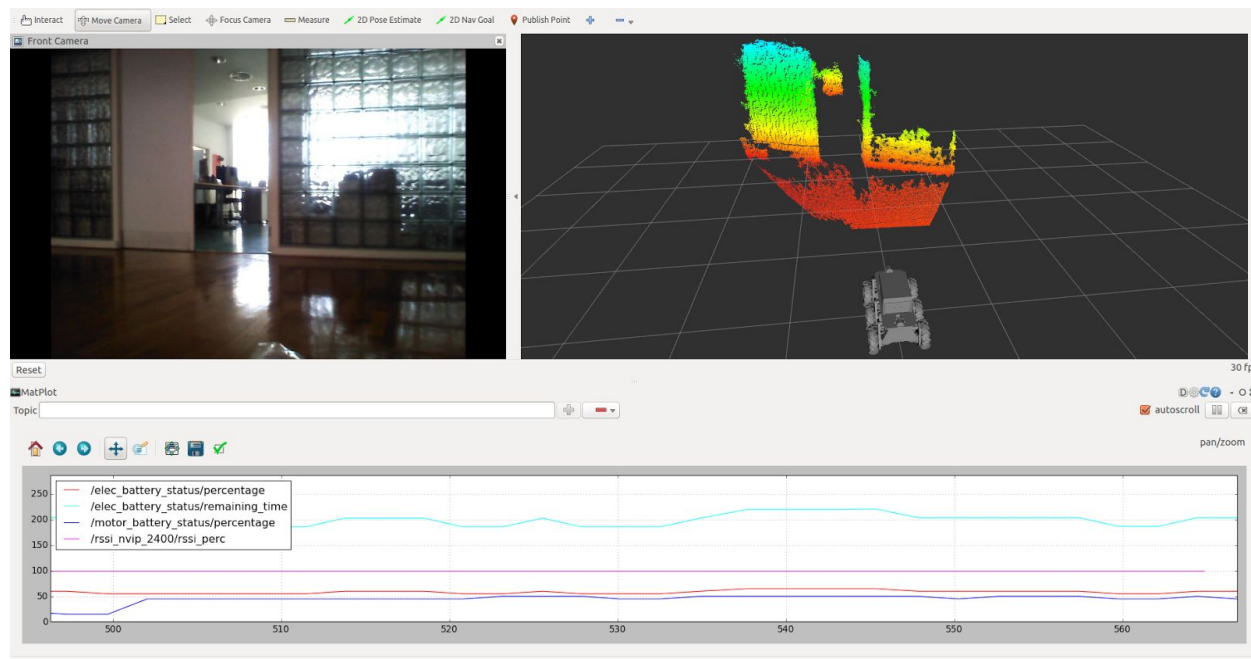


Figure 4.2. Snapshot of the current design of the control base station. On the left side, the RGB images from the front (or rear) cameras are shown. On the right side, the depth information provided by the sensor is represented with a 3D model of the robot. The plot at the bottom shows the status of the batteries on the robot and RSSI level measured by the device onboard the robot.

## 4.2 Details on the proposed communication middleware

As presented in Section 3, the communication system of the SIAR platform consists on two wireless links: the primary link, which operates following the WiFi 802.3b,g standards over the 2.4 GHz band a high baud-rate and the backup link, which connects the robot and the base station with a wireless serial link over the 900MHz band, has extended range at the expense of offering a lower baud-rate (up to 236 Kbits/sec).

### 4.2.1 Standard ROS middleware

ROS provides the user with a middleware that could be used for connecting different machines. The main characteristics of the middleware are listed below.

- Great versatility of types of communication:

- *data-centric* communication, in which publisher and subscribers of different data topics can be created.
  - *service-centric* communication, in which servers can provide clients with services.
  - *action-oriented* services<sup>11</sup>.
- The transmission is carried out only through TCP when processes from different computers are connected.
  - Acts as a nameserver, which is used to generate TCP connections. Once the different modules are connected, the communication does not need to pass through the nameserver node.
  - Multiplatform. It can be used in all platforms where ROS can be installed.
  - Provides a distributed parameter system for configuring the ROS nodes.

Therefore the ROS middleware tool is a well-known and reliable tool that could be used for communicating the robot and the base station. However, we opted not to use it for this purpose for the following reasons:

- It cannot be used over a serial connection. Therefore, it can be difficult to include the backup link while using the ROS middleware. There exists a ROS tool that could be used for this purpose, ROSserial<sup>12</sup>, but it is more oriented for connecting a ROS machine with low-resources computers such as Arduinos and the likes.
- It only uses TCP for connecting the different computers. This turned out to be a critical issue when real-time data should be transmitted, as the reliability comes at the expense of retransmitting lost packages. Therefore, the delay of the obtained data cannot be controlled.

## 4.2.2 Proposed communication middleware

Figure 4.3 shows the block diagram of the proposed middleware solution. In this solution, ROS middleware is employed for connecting the internal nodes on the two computers onboard the robots and for connecting the internal nodes on the base station.

Then, two specific ROS packages have been designed and implemented in order to transmit the topic of interest between the robot and the base station through the communication links. These packages are `serial_bridge` and `udp_bridge`. Each package provides two different nodes: the server node should be executed in the robot computer and the client node should be executed at the computer of the base station. These nodes can be configured to transmit the desired topics of interest at different rates at the request of the operator.

Finally, it is important to mention the modules that are being used to transmit real-time RGBD images to the operator in real-time. As mentioned in section 2.1.2, five RGBD cameras are being used together to gather the information of the environment. However, the proposed communication link would not be able to transmit the information of all cameras at the same time. Therefore, a camera switch module has been designed. It allows the operator to select the camera or cameras of interest to be transmitted, to configure the quality of

---

<sup>11</sup> <http://wiki.ros.org/actionlib>

<sup>12</sup> <http://wiki.ros.org/rosserial>

the images and to enable or disable the transmission of the depth images in real time. It is also responsible of downsampling the images so that a low-quality version can be transmitted over the backup link.

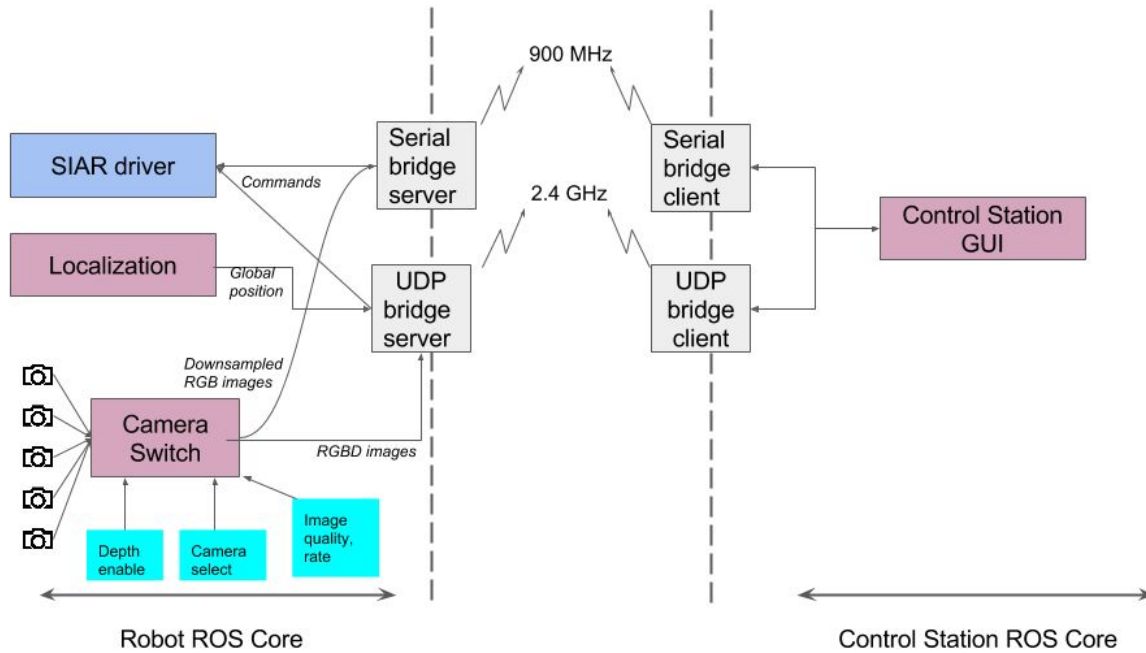


Figure 4.3. Proposed architecture of the middleware of the SIAR solution.

## 5. Localization and Navigation

The added value of a robot with respect to current systems is its capability of performing autonomously the inspection tasks. The basic functionalities required are localization and navigation. Localization is required to register the results of the inspection into the sewer network maps. It is also a requisite of the navigation module, which will allow the robot to move autonomously through the sewer in case it is needed. The following sections describe the designed modules, and, in some cases, preliminary results obtained.

### 5.1 Enhanced Odometry

Robot odometry is one of the main elements into the localization architecture. The more robust and accurate the odometry is, the better is the robot localization in general. Ground robots use to rely on wheel encoders and inertial units to estimate its odometry. While this is a good sensor combination with proven good results in many scenarios, the environmental constraints of sewers navigation forces us to include more sensing modalities in order to have an accurate robot odometry. Thus, humidity, water and waste significantly decrease the wheel grip, distorting the computed linear and angular velocities based on wheel encoders. Last, but not least, the robot will need to navigate into a full 3D environment, so the robot localization will also need full 3D odometry for 3D environment mapping and navigation.

The main sensors used by the SIAR odometry system are the RGB-D cameras mounted in the front and the rear of the robot, the 3D Inertial Measurement Unit (IMU) installed in the robot chassis and the wheel encoders. The main processing modules are presented in Figure 5.1. The RGB-D camera is used to extract the robot rotation and translation between frames, and the IMU is used to stabilize the robot roll and pitch that are fully observable from the IMU accelerometer. In addition, the estimation is double-checked with the velocity provided by the wheel encoders so that the system can face wrong estimations provided by the vision system.

Next paragraphs provides some details of the different stages in the odometry computation.

#### 5.1.1. Image feature detection

With every camera frame, a set of interest points is found in the color image. These interest points are visual features extracted using the Features from Accelerated Segment Test (FAST) algorithm [Rosten and Drummond, 2006], which is a method for corner detection with a strong computational efficiency. The identified interest points contain local information that ideally make them repeatable across consecutive frames.

Smooth and reliable visual odometry needs interest points equally distributed through the image for a better numerical stability of the rotation and translation computation. However, sometimes features are grouped in a specific strong-detailed region in the image. To overcome such situations, a minimum number of features are required to be extracted from equally divided regions of the images, commonly known as buckets. On the other hand, a maximum number of features is defined in order to select from each bucket only the most powerful ones, according to the FAST detector definition. The combination of both parameters allows an homogeneous distribution of the strongest selected features in both images. Our approach is based on subdividing the image into six buckets (two rows and three columns).

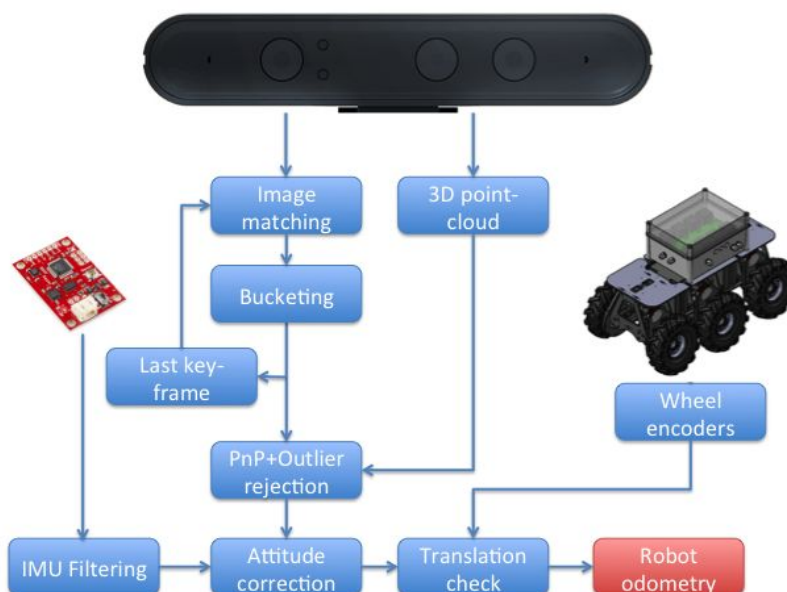


Figure 5.1: SIAR Robot odometry system

### 5.1.2. Image feature description

The next step involves finding correspondences between the current image and previous one. A feature point description is needed in order to compare and find similarities between each pair, and for that the general-purpose Binary Robust Independent Elementary Features (BRIEF) descriptor [Calonder et al, 2012] is used. This descriptor is very efficient since it is based on simple intensity difference tests, and the similarity evaluation is done using the Hamming distance. Together with the computational efficiency, BRIEF descriptors are especially interesting for feature tracking under small visual perturbations, a very usual situation in visual odometry. Other descriptors that include rotation into their formulation have been tested (ORB, BRISK and FREAK), but no significant improvements have been detected for local matching while they increase the computational time, hence the one with smallest computational impact is finally used in this approach, BRIEF.

### 5.1.3. Pairwise Feature Matching and Key-Framing

Once a set of robust features has been found between consecutive frames. If enough matches are found between the features from the previous and the current images, this new set of matches is used to solve a Perspective-n-Point problem (PnP), i.e. the pose estimation from  $n$  3D-to-2D point correspondences (see Fig. 5.2). This algorithm allows to estimate the camera rotation and translation that minimizes the re-projection error of the 3D points of previous frame into the 3D points of the current frame. This is a non-linear optimization that can estimate the camera transform very accurately at a reasonable computational cost.

The 3D points are the coordinates of the surviving features from the last image, while the 2D points are the pixel coordinates of the matched features from the current image. In particular, the EPnP algorithm [Lepetit et al, 2008] has been used, which provides an efficient implementation of the pose change estimation between both images.

Finally, a key-framing approach has been adopted in order to partially mitigate the effect cumulative errors in odometry. Thus, new key-frames are produced only when the feature tracking flow exceeds a given threshold. At that moment, the current image descriptors, their 3D estimated position and the robot position/orientation are stored. Subsequent frames will compute the odometry with respect to the last key-frame (and its pose) instead of the immediately preceding image, so that errors are only accumulated with the introduction of new key-frames.

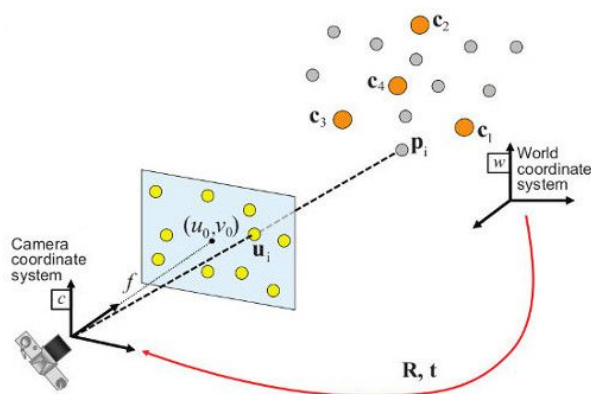


Figure 5.2: PnP algorithm for relative rotation and translation computation

#### 5.1.4. Attitude Correction

The robot has an onboard IMU which provides stabilized roll and pitch estimation and yaw rate that can be fused with the computed pose updates. In particular, the odometry system estimates the camera roll and pitch angles based on accelerometers and gyroscopes and integrates them with the purely visual estimation in a loose-coupling manner. This way, cumulative error will not affect the robot roll and pitch, extending the estimation and making it more coherent through time.

#### 5.1.5. Translation checking with wheel odometry

Although the estimation provided by the wheel encoders is not very accurate, it can be used to remove eventual outliers in the estimation provided by the visual odometry system. Thus, the robot velocity is used as a model-based test of the estimation given by the visual odometry algorithm. In case a spurious wrong estimation is detected, the wheel encoder translation is used instead the visual odometry so that the estimation is continuous.

This test is launched with every new key-frame and it is positive in most cases (more than 95%). It consist on computing the module of the visual odometry translation and comparing it with the wheel odometry; if the absolute difference is below a given threshold the test is positive and the measurement is accepted.

#### 5.1.6. Experimental results in sewers at Barcelona

The visual odometry system have been intensively tested in many different experiments in the laboratory, in the basement of UPO and also real sewers at Barcelona. In this section some results obtained in the sewers are presented.

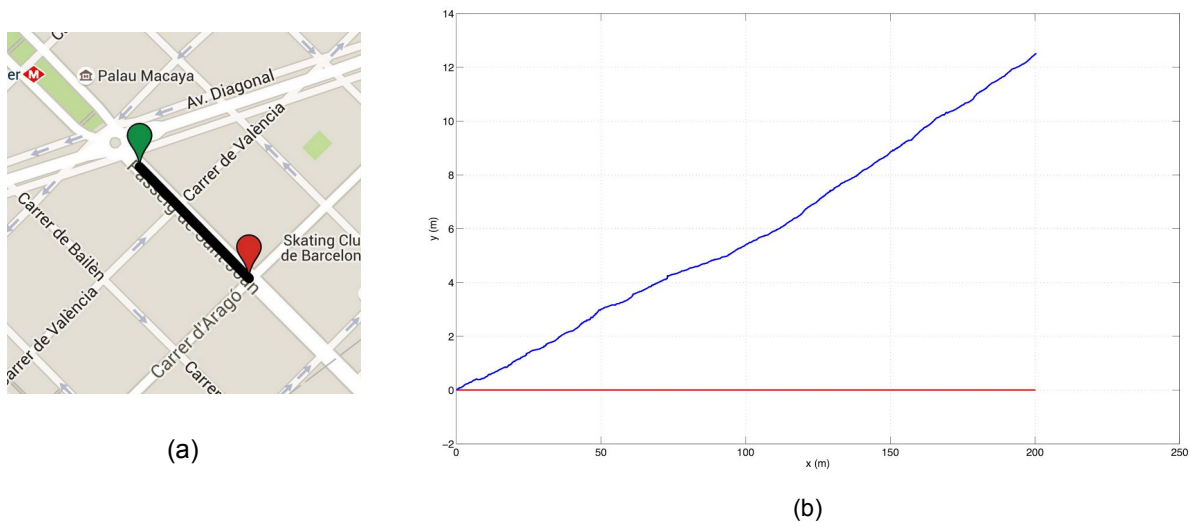


Figure 5.3: Evaluation of the odometry system in Sant Joan sewer, Barcelona.

A good estimate of the accuracy of odometric systems is the relative translation error. It accounts for the relative increase in the error as the robot moves. This can be tested in the laboratory with ground truth but the environment is significantly different and the estimation will be benefited by a better illumination conditions.

In order to perform a fair estimation of the relative translation error an experiment in Barcelona sewers was conceived. The robot was driven in a straight line for a 200-meter long trajectory. The length of the sewer was manually measured in advance, the trajectory started at the beginning of the Sant Joan sewer (green point in Fig. 5.3a) and finished 200 meters down the sewer (red point in Fig. 5.3a).

The resulted estimated trajectory in this experiment is shown in Fig. 5.3b. It can be seen how the odometry system slowly diverges through time and an error of 12.5 meters is accumulated in the robot position after 200 meter of navigation. This global error is translated into a relative translation error of  $\text{error} = 12.5 \cdot 100 / 200 = 6.25\%$ . This means that the odometry system diverges 6.25cm for every single meter the robot traverses. Although the state of the art reports relative translational errors around 2%, it is worth to mention that our estimation is obtained online in a very poor environment.

Finally, different experiments have been performed in order to estimate the computational overhead of the proposed algorithm. The total time required for odometry estimation is 33ms in average, considering that images are acquired at 10 Hz, we are far from the maximum allowed delay (100ms in our case). The experiments have been performed in the navigation computer, an i7 with two cores.

Further results related to the odometry can be seen in Section 6.1, as the local maps generated by the map system are strongly dependant on the local alignment of the odometry system.



## 5.2 Localization

According to the requirements on [ECHORD++, 2014], one of the main functionalities required from SIAR is the registration of the monitored elements on the sewer network. This requires a localization system able to estimate the robot's position with respect to the previously existing map of the sewer system. Current solutions typically provide only odometric readings for robot localization because they do not include enough computational capabilities onboard. Refined position can be later computed based on the sensor data gathered by the robot.

SIAR will thus include a map-based localization system, able to relate the pose of the robot to the sewer network online. It will not require a detailed map of the environment a topological map with metric distance information and sewer connections will be enough.

The robot localization system will be composed by a relative front-end framework able to accurately compute the robot motion based on improved odometry and a global back-end framework in charge of keeping the robot position estimation globally consistent and aligned with the sewer map. This relative front-end is the visual odometry presented in Section 5.1.

The global back-end framework will be based on the sewage system map available to BCASA, and the automatic detection of sewer elements based on 3D information (as described in Section 6.2). This information will be used in a Monte Carlo localization approach [Pérez-Lara et al, 2015] together with the improved robot odometry to build a reliable position estimation.

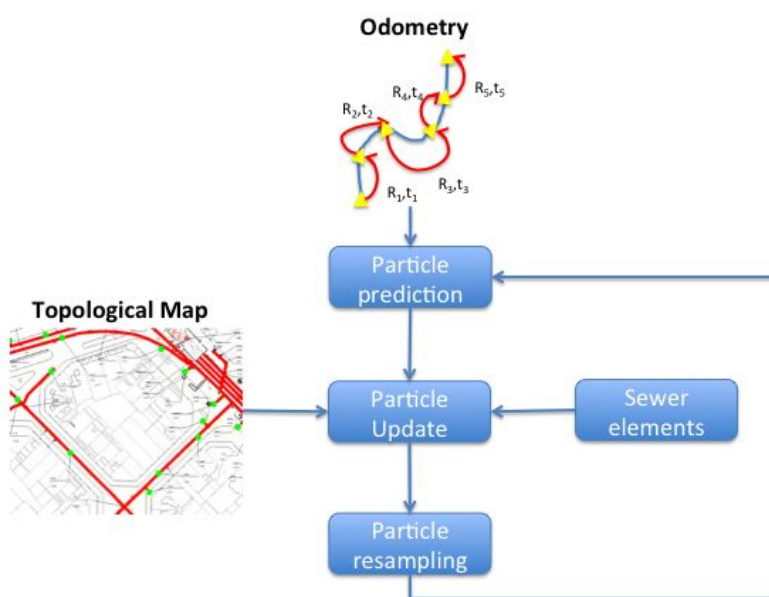


Figure 5.4: Topological map based localization approach. The detected sewer elements, like manholes, and a map of the sewer network including such elements are used to provide a global localization tracking within this map.

The approach for localization in SIAR project is depicted in Fig. 5.4. As previously introduced, the approach is based on Monte Carlo Localization and makes use of a particle filter to represent the robot localization



belief. In this filter, each particle represents a position hypothesis into the map and the hypotheses are validated (weighted) with measurements of the environment taken by the robot.

The position hypotheses (particles) are predicted based on the robot odometry, the algorithm presented in Section 5.1 in our case. The filter also needs a method to validate that particles are in the right position. To this end, the perception system will make use of the 3D maps to search for sewer elements like manholes in the ceiling (Fig. 6.5 in Section 6.2 shows an example with real sewer in Barcelona). These manholes are georeferenced and marked in the topological map.

Finally, once particles have been weighted according to the eventual detection of a manhole in the vicinity of the robot, particles are re-distributed around the most likely areas in the map. This stage is called resampling.

## 5.3 Navigation

The navigation module is in charge of the motion and decision making of SIAR. The module offers the capability to be controlled by the operator at all times through the communication system. However, some sections of the sewer system can be very difficult to navigate by an operator. Thus, this module provides also semi and fully autonomous navigation capabilities through the sewage system if needed.

We envisage three main navigation modes that will be offered by the navigation module:

- **Teleoperation:** in this mode, the robot can be purely teleoperated from the base station, where the operator controls the degrees of freedom of the robot. This mode has been already implemented and tested for the initial version of the robot.
- **Assisted teleoperation:** this method will be developed in order to make the robot automatically navigate through the center of the sewer, avoiding falling into holes, etc, while the operator commands the velocity of the inspection. To this end, this module has to get a partial 3D reconstruction of the environment from the mapping module, in order to detect the safe navigation areas where the robot can go through.
- **Finally, a fully autonomous operating mode will be implemented.** This operating mode will further reduce the operator's workload, as complete inspection plans could be loaded to the platform, that will execute it automatically. Moreover, it would be crucial in case where the communication was lost. In this way, the platform can safely perform an automatic return home procedure.

The (semi-)autonomous navigation task is a complex task considering the narrow spaces in which the robot will navigate and the presence of obstacles such as garbage, pipes or other objects. These constraints can only be solved if full 3D navigation and perception of the environment are considered. The robot orientation could be critical in particular areas like stairs, slopes or holes, and the motion planner must consider this.



Figure 5.5: The envisaged final platform.

Furthermore, the navigation strategies are directly linked to the final robot platform and its kinematics (Fig. 5.5). The platform is designed in such a way that the main strategy considered is navigating over the sewer section gully, with the wheels on the curbs at both sides, except in cases in which the robot fits in one of the curbs. The robot needs to avoid obstacles, and while the platform can negotiate certain situations, it is very important to consider the restrictions to avoid that the platform get stuck or bend over. Also, the robot will have to manoeuvre to deal with intersections, as shown in Section 2.2

Thus, accurate planning taking into account kinematic and dynamic restrictions [Karaman and Frazzoli, 2010; Teniente and Andrade-Cetto, 2013] will be implemented in order to have an optimal while time responsive approach for robot motion planning. The mapping data provided by the perception modules (Section 6.1) will be used to detect both positive and negative obstacle in order to properly plan robot motions.

The navigation module action space includes not only the wheels speed, but also the actuators to modify the width of the robot, as explained in Section 2.2. It will also consider motion planning for getting samples for sewer monitoring and for the recovery of repeaters.

## 6. Perception

According to the Challenge document [ECHORD++, 2014], a set of perception functionalities are required related to the monitoring of sewers:

- Providing 3D scanning data
- Sewer map building
- Sewer elements localization
- Sewer serviceability inspection
- Structural defects inspection

The developed sensor payload using RGBD sensors (Section 2.1.2) is able to provide the scanning data. At full resolution, it can provide point clouds of more than 800.000 points per scan. Not having mobile parts, it is able to produce these scans without requiring the robot to stop. And while the robot carries illumination devices, it could even provide these data without illumination.

Several additional modules are considered in the architecture to provide the rest of functionalities. A mapping module able to integrate scans in time to produce local 3D maps with the adequate resolutions to support the rest of functionalities, which are considered by the map analysis module. They are described below.

### 6.1 Local 3D Mapping

Building 3D maps of the robot environment is an important task with many applications in autonomous navigation, teleoperation and automatic environment inspection. The 3D map will be used by the navigation functionalities in order to plan actions and control the position of the robot within the sewer. This is very important because the robot will move in a full 3D environment with small obstacles and holes, so actions must be planned considering these constraints, even if the robot moves in 2D most of the time.

The 3D map is also very important in order to provide environment awareness to the teleoperator. The operator has a first-person perspective of the environment thanks to the cameras onboard the robot, but sometimes is also needed the third-person perspective in order to fully understand the robot with respect the scene. Figure 6.1 shows a snapshot of the information presented to the operator, we can see that images are good to detect possible defects or to understand the operation, but the third-person perspective provides a global view of the robot position that contributes to understand how the robot interacts with the scene.

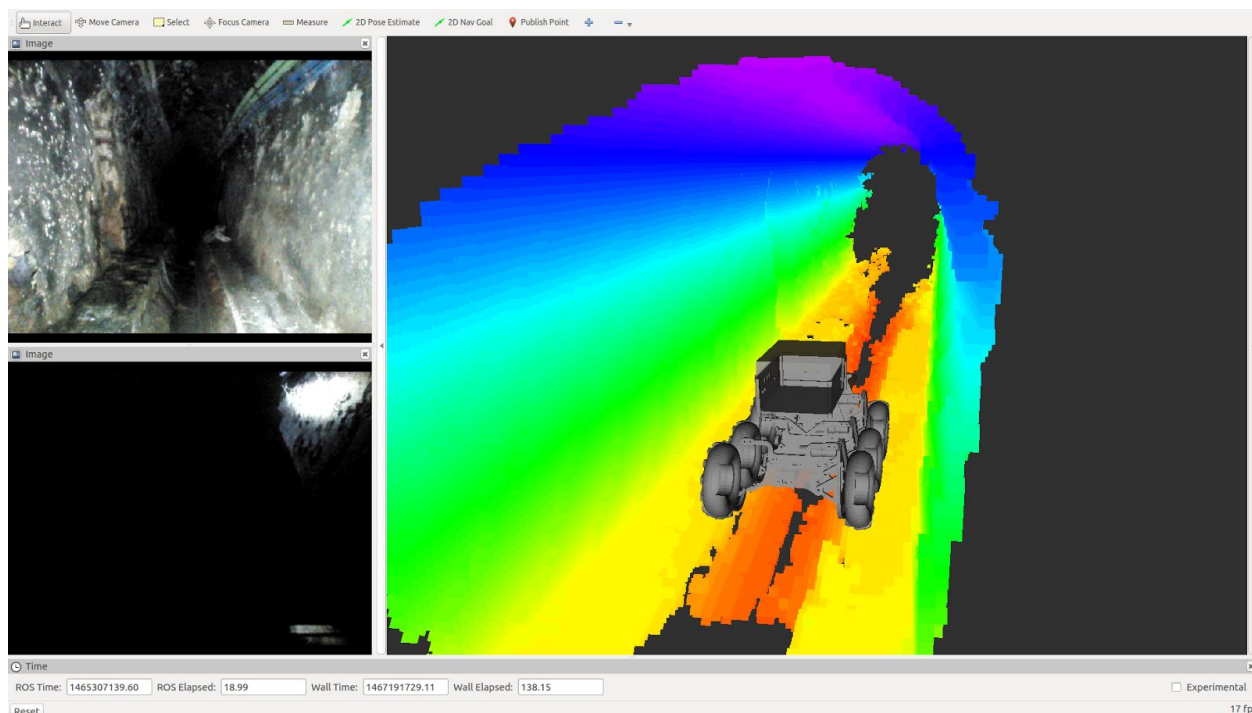


Figure 6.1. Different views of the operator while command the SIAR platform.  
Left: First-person perspective (front and rear cameras). Right: Third-person perspective.

Finally, the 3D map will be used as the basis for automatic inspection of the sewer. The metric representation of the environment allows taking real measurement of the sewer and even compare the 3D reconstruction with pre-computed 3D models of the gallery in order to detect possible defects. This will be elaborated in Section 6.2.

Finally, these maps, combined with the localization outputs (Section 5.2), can be georeferenced into the sewer network.

Next paragraphs will provide some details about the 3D mapping process together with some initial experiments carried out in Barcelona to validate the approach.

### 6.1.1 Implementation details

The main purpose of the 3D mapping module is to provide a locally coherent 3D map of the robot environment. For this purpose two elements will be used as inputs: 3D point-clouds provided by RGB-D cameras mounted in the robot and an accurate robot odometry for the integration of the point-cloud information through time.

Figure 6.2 shows the different stages of the local 3D mapping process. As previously introduced, the main inputs of the system are a single point-cloud provided by the RGB-D sensors and the estimated translation since last map update given by the visual odometry system detailed in Section 5.1. With this information the point-cloud is aligned with the current map so that it can be merged with it.

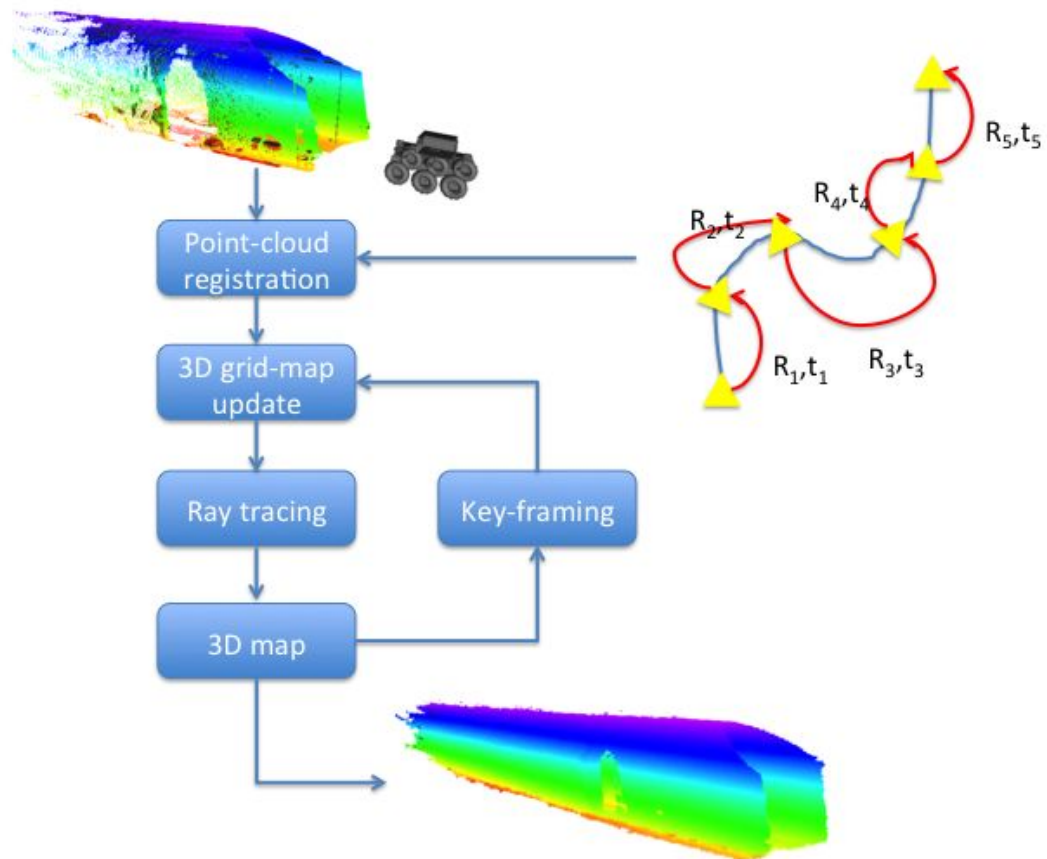


Figure 6.2. Overview of the local 3D mapping technique developed in SIAR.

The local map is represented as a 3D occupancy grid that stores the probability of cell of having an obstacle. This 3D occupancy grid has a predefined resolution of 25mm and a fixed size around the robot that can be adjusted depending on the requirements. The occupancy grid is implemented as an octomap [Hornung et al, 2013] in order to make a very efficient use of the computer memory.

The occupancy grid can be updated with different probabilistic models depending on the sensor used to obtain the 3D point-cloud. This way, the map can account for different noise modalities and easily fuse information from different sensors. A ray is traced between the robot position and each 3D point in the cloud. This allow to remove measurement outliers or misalignment transparently at reasonable computation cost.

Finally, the motion of the robot is checked in order to detect a new key-frame position. If the robot moves more than a given threshold, a new key-frame is added and all the map points are translated to the reference of the new key-frame. This method allows reducing the computational requirements for map building and map representation.

## 6.1.2 Experimental results at Barcelona

The mapping system was firstly tested at the laboratory with data gathered by RaposaNG. However, as with the visual odometry, the sewer environment is very harsh so we also tested intensively the 3D local mapping system with sensor data gathered in the sewers at Barcelona.

For these experiments, the map was unbounded in order to have a very large map for visualization purposes. Figure 6.3 shows the 3D reconstruction of the sewer under Sant Joan street; the robot was manually controlled for 40 meters approximately. It can be seen how the structure of the sewer is perfectly visible and how the map is locally coherent and, in addition, diverges very slowly thanks to visual odometry.

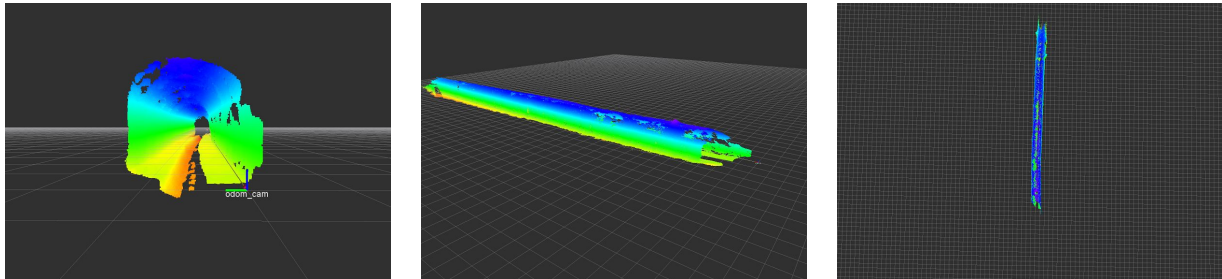


Figure 6.3. 3D map reconstruction of a 40 meters long section of Sant Joan sewer.

The 3D reconstruction of Valencia Street is also shown in Fig. 6.4. The map shown is only 50 meters of the total 130 traversed with robot during mobility test in Barcelona. It can be seen how the structure is also very clear locally and how the map diverges slowly.

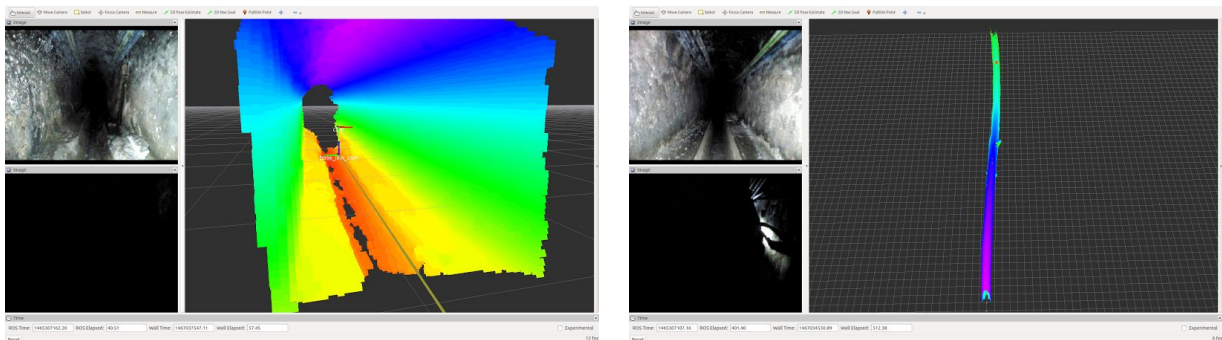


Figure 6.4. 3D map reconstruction of a 50 meters long section of Valencia sewer.

All the 3D reconstruction were computed offline using experimental logs, but using the computer onboard the robot (Intel i7 with two cores). All the computation works on real time: point-cloud computation, visual odometry and 3D mapping.

## 6.2 Map Analysis

Given the local maps obtained following the approach described above, it is possible to analyze the resultant point clouds to detect and localize sewer elements and for serviceability and structural defects inspection, as required according to [ECHORD++, 2014].



## 6.2.1 Sewer elements location

It is of interest to be able to locate sewer elements like manholes, inlets, crossings and others.

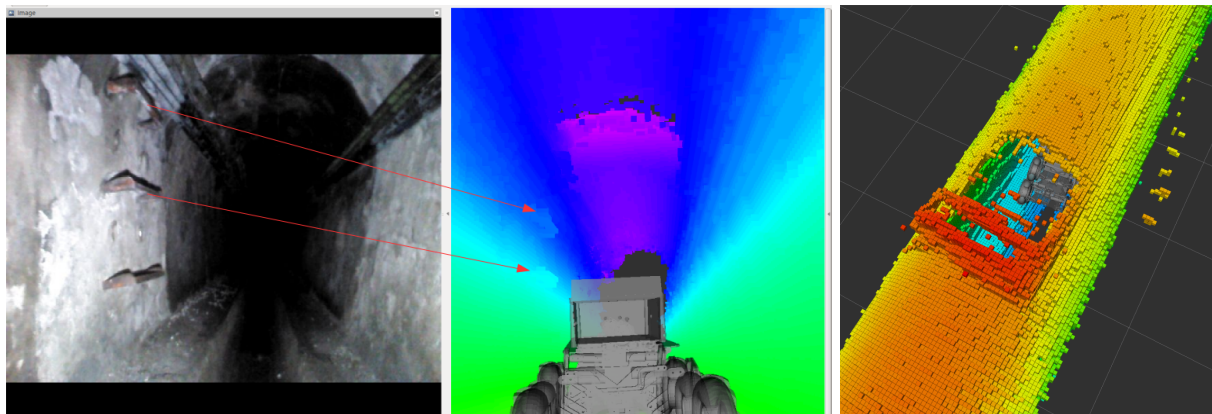


Figure 6.5: A manhole as seen in the local maps created. Left and centre: the stairs and the manhole can be observed in the 3D map. On the right, a 3D view of the robot from the “outside” of the sewer through the manhole.

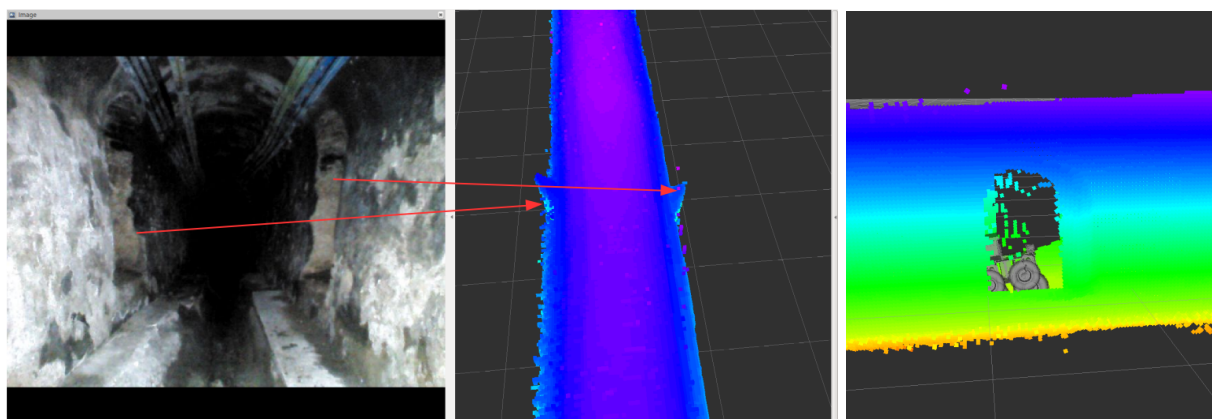


Figure 6.6: Inlets as seen in the local maps created. Left and centre: the two inlets can be observed in the 3D map. On the right, a 3D view of the robot from the “outside” of the sewer through the right inlet.

The map analysis module will provide these elements by analyzing the scans combined into the local maps. An initial analysis can be seen in Figs. 6.5 and 6.6, where some of these elements can be identified in maps gathered in the sewers.

These elements will be also fed back to the localization module, as they will be used as landmarks to perform localization on the sewer network.

## 6.2.2 Sewer serviceability inspection

The system should be also able to determine if the serviceability of the sewer has been reduced, raising alarms in case this occurs.



This requires, according to [ECHORD++, 2014] to distinguish waste on the sewers, of different sizes. Figure 6.7 shows the 3D data and how a 5-cm. tall rock can be identified visually in the 3D cloud.

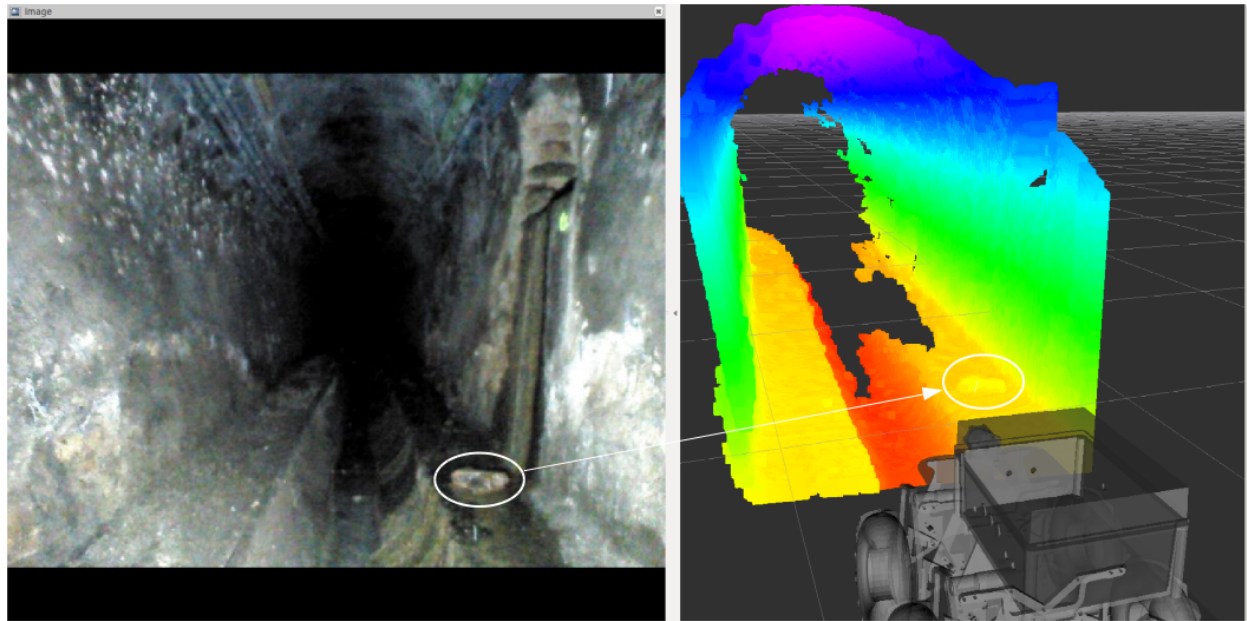


Figure 6.7: Left: a rock can be seen in the curb of the sewer. Right: 3D reconstruction. The rock is around 5 cm. tall.

The module Map Analysis will employ techniques for 3D point cloud segmentation and recognition in order to automatically detect serviceability reduction situations.

At this design stage, only preliminary tests have been carried out to evaluate the capacity of performing point cloud operations in real-time. Knowing the geometry of the sewer it is possible to detect potential degraded zones in it, by comparing the expected situation and the data. Figure 6.8 shows some preliminary results using the data from one of the visits to the sewer. In this case, the main plane at floor level is extracted (actually, composed of two planes at the sides of the channel), and the differences are used to segment potentially degraded zones. This, together with the modules of enhanced odometry and local map making can run in real-time, at more than 10Hz.

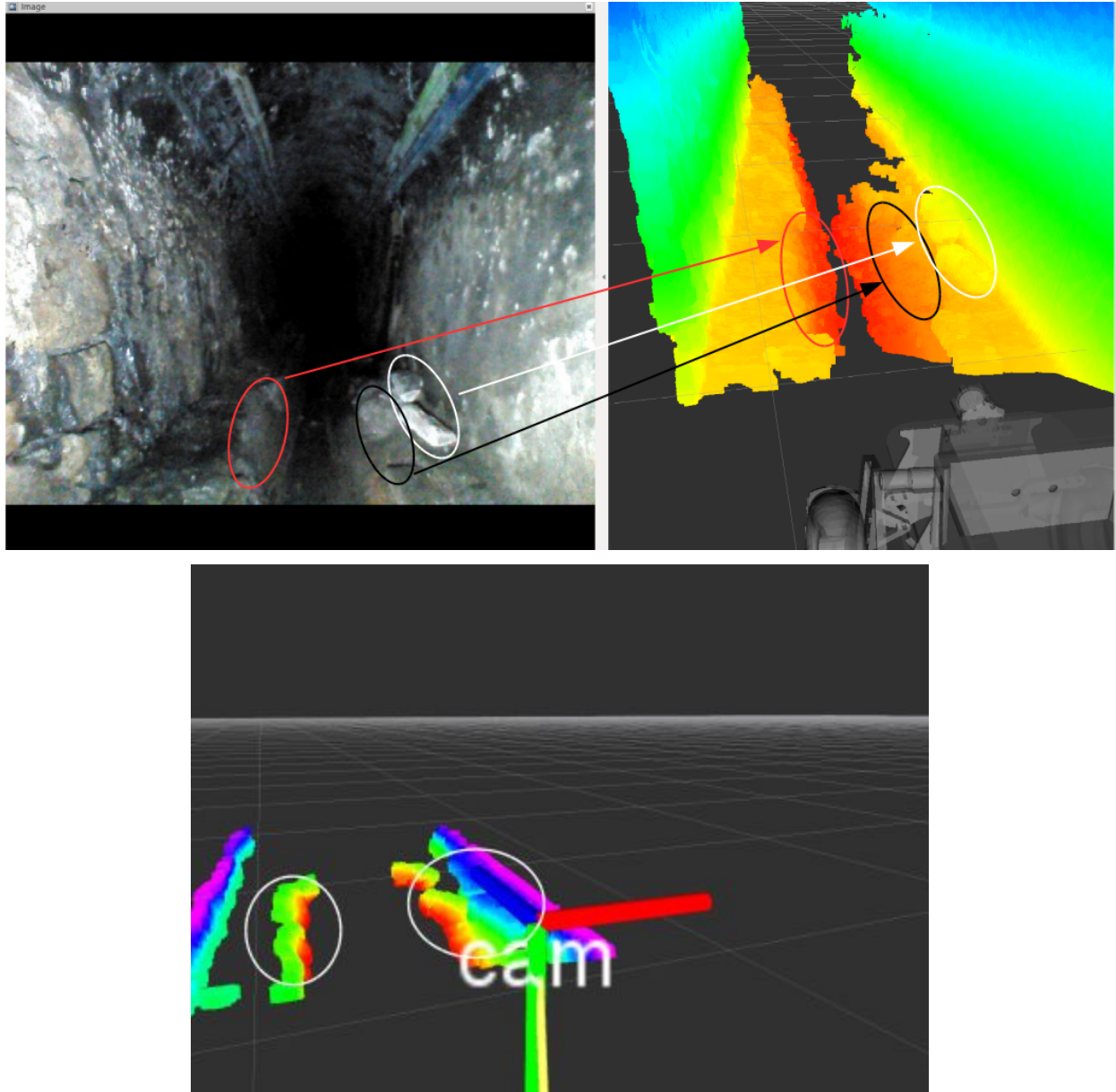


Figure 6.8: Top: The reconstructed 3D cloud. Some rocks (white) and break with losses on the curbs (red and black) can be noticed in the image in the top left, and in the cloud on the right. Bottom: automatic extraction of the breaks with geometric reasoning filters.

### 6.2.3 Structural defects inspection

The map analysis module will deal with the inspection of structural defects. According to [ECHORD++, 2014], different critical defects have to be detected, from cracks and fractures to collapses.

The module will automatically analyze the 3D information to search for such defects, to alert the operator, who can then confirm the defect. From the local sensors on the robot, it is possible to determine if the defect is located in the vault, the walls or the floor. The information from the localization module will be used to provide the distance to the closest manhole of the defect.

For the automatic detection of defects, the same principle as above will be considered here, by using the known geometry of sewers. Figure 6.8 shows a break with loss on the curb of the sewer by applying geometric reasoning. In the next phases, new methods will be developed for inspection, in order to provide in real time further information. If needed, in some situations the gathered information could be processed offline at the central station, where more computationally demanding algorithms can be also considered.

## 7. Logistics required and operational issues by using the solution

With an autonomous robot, the composition of a brigade can be redefined. Only one skilled operator and a pawn should be enough for a mission.

The logistics required to operate the robot are:

- Van - to transport the robot and control console;
- Electric winch - to lower the robot into the sewer;
- Spare batteries - expected power autonomy is of 5h which should be enough for a working day. Nevertheless a spare power pack should be included to increase the operation time in case of need;
- Battery charger - To charge the batteries in case of need;
- Wifi repeaters - To increase the communication distance (they will be transported by the robot)

## 8. Economic Viability Study

The Consortium proposes the development of an innovative sewer inspection solution that will result in a close to market prototype. The launch of this product is predicted to happen 18 months after the project completion. These 18 months will be used to prepare the developed prototype for the market as an off-the-shelf product, composed of a hardware robot platform, sensing payload and software packages.

The developed prototype will result from the joint work of all the partners and they will all define their participation on the future commercial exploitation of it (IP exploitation agreements). IDM, as a SME, will lead the exploitation process.

In contrast to current approaches, SIAR focuses on achieving high dependability, usefulness and affordability through technological innovation, but also the provision of a convincing market approach to launch an off-the-shelf product version onto the market 18 months after the project end and through a Business to Business (B2B) model, where the target clients will be organizations (private or public) providing sewer inspection services. IDM will be providing the technological solution while these organizations will provide locally the service. IDM will provide technical support and maintenance (advanced) of the robots. IDM will provide also expertise for the customization of the solution in some specific cases.

This project will have an important impact in the turnover of IDM as well it will open a door for a market with a strong potential of growth and which is simultaneous eager to new (more autonomous) solutions.

This document presents the business opportunity and a preliminary exploitation plan based on financial projections. The economic advantage that the solution will bring to their users is also presented.

## 8.1. Opportunity

### 8.1.1. Market

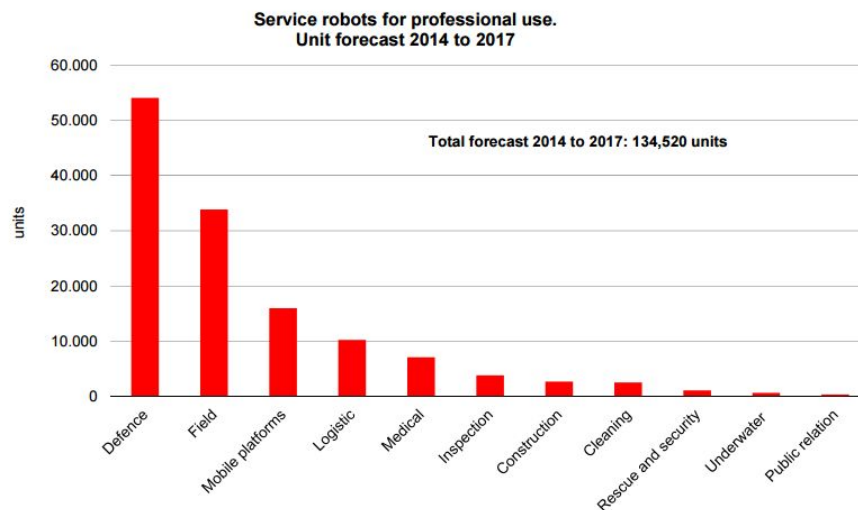
The interest in autonomous robotic solutions for inspection and maintenance is growing rapidly throughout different industries. As indicated in the Multi Annual Roadmap of EU Robotics<sup>13</sup>:

*“The application of robotics technology to the Civil domain is still at an early stage and it is therefore difficult to estimate eventual market size. Key Market drivers are:*

- *Growing interest in UAS not only by US and European countries but also by emerging countries.*
- *Potential for improved coverage of large areas for environmental monitoring.*
- *Increase in quality of monitoring data and regularity of monitoring due to lower cost per task.*
- *Reduction of total operational costs with respect to existing manned systems.*
- *Increasing acceptance of robotics technology.”*

This market is broadly characterised by Business to Government (B2G) business models. Typical purchasers/operators of civil robots are likely to include: civil authorities running or contracting services that can be augmented by robotics technology; private companies operating under contract within the Civil domain.

Based on current trends of robot sales for remote inspection, according to IFR 4,000 robots for inspection and maintenance will be sold during the period between 2015-2018<sup>14</sup>.



Source: IFR World Robotics 2014

<sup>13</sup> Robotics 2020 Multi-Annual Roadmap - MAR 2016 (ICT-25 & ICT-26)

<sup>14</sup> World Robotics 2015 Service Robots

### 8.1.2. Competition

Current sewer inspection scene can be divided in two fields: pipe inspection performed by small robots which can fit inside pipes; and sewer inspection performed by medium to big sized robots which move inside galleries. Pipe inspection can be purely remote controlled, e.g., Alligator, Minigator, Multigator and Flexigator wheeled robots from IBAK<sup>15</sup> or Geolyn's<sup>16</sup> tracked robots, but it can be also autonomous, e.g., Solo tracked robots from REDZone<sup>17</sup> or Makro's<sup>18</sup> wheeled worm type robot. In sewer inspection is also possible to find teleoperated solutions, e.g., PureRobotics' Pipeline Inspection tracked robot<sup>19</sup>, and autonomous solutions, e.g., ServiceRoboter wheeled solution from Fraunhofer IFF<sup>20</sup>. The proposed solution aims the sewer gallery inspection, with the use of a kinematic system that can be adapted to the sewer gallery characteristics.

The SIAR system will go beyond existing solutions through the inclusion of some innovative features: robust configurable locomotion system; reliable autonomous navigation system; modular inspection system with inclusion of devices for air/waste sampling which is currently not available in the commercial inspection robots.

### 8.1.3. SWOT Analysis



#### Strengths

<sup>15</sup> [http://www.ibak.de/en/produkte/ibak\\_show/frontendshow/category/sanierung/](http://www.ibak.de/en/produkte/ibak_show/frontendshow/category/sanierung/)

<sup>16</sup> <http://www.geolyn.ca/>

<sup>17</sup> <http://www.redzone.com/products/solo-robots/>

<sup>18</sup> [http://www.inspector-systems.com/makro\\_plus.html](http://www.inspector-systems.com/makro_plus.html)

<sup>19</sup> <http://www.puretechltd.com/services/robotics/>

<sup>20</sup> <http://www.iff.fraunhofer.de/de/geschaeftsbereiche/robotersysteme/forschung/serviceroboter-inspektion-reinigung-wartung.html>



- The availability of a **high tech product, innovative and unique** will have a great impact on the market.
- The product marketing will focus its **usability and autonomy**.
- One of the major concerns of the Consortium is the development of an **affordable solution** through the minimization of the onboard technology costs.
- The curriculum of the partners certifies their **knowledge and experience** in the various aspects of the project.

### Weaknesses

- The **investment** inherent to the **industrialization process** will be supported through the establishment of partnerships with external entities, both in terms of production or in the capital raising shed.
- The need to establish **partnerships for the exploitation** process (e.g. service providers) can increase the business risks. There has to be a good control of established partnerships.

### Opportunities

- **Current trends in robotics** and the increasing interest in robotic solutions is a key enabler for the entry of new products.
- Despite the existence of a varied range of sewer inspection solutions in the market, the **absence of products with the same capabilities** is an important factor for the success of the project.
- **Global market** for product placement.

### Threats

- With time and by the success of the project, it is expected the emergence of **similar products**. A focus on quality of products and a continuous drive to create new differentiating features will be decisive against possible competitors. The community will have SIAR as the reference.
- The **global economic crisis** effect in robot development/commercialization is twofold. While it negatively impacts the investments that are made in the development of new (more risky) technology, it positively impacts the request for solutions to optimize the costs associated with the execution of specific tasks/services.

## 8.2. Marketing

### 8.2.1. Positioning

The product will be positioned as follows: high dependability, usefulness and affordability. It is intended for clients who are looking for a reliable solution, that can be easily used by current work forces of sewer inspection services and, last but not the least, will contribute for an effective reduction of costs related with the sewer network inspection and maintenance.

The marketing strategy will be based mainly on the technological and reliable nature of the product. In contact with potential customers this will be the differentiating factor transmitted. It is very important that the customer feels that the acquisition of the equipment will improve its service quality.

The marketing will have to convey a sense of quality and high tech character in each image, each campaign and each publication associated with the product. Marketing campaigns will be strengthened by demonstrations which will be recorded and disseminated through the internet social channels.

### 8.2.2. Price

The added value supported by technological product differentiation allows us to offer the customer the state of the art of sewer inspection. The client will value the innovative features of the product and its effectiveness compared to competing offers. This will allow to define the price of the product based on existing top solutions. Price strategy will be to offer more for the same price range of top ranked competitors.

**Preliminary cost estimation.** Considering the prototype that has been developed on this 1st phase of the project and the technological solution that the Consortium is now proposing, the cost of the SIAR solution, when considering the costs of included raw materials and equipment, should be less than 16k€ (see Table 8.1).

Item	Unit Price	Qty	total
<b>Locomotion Platform</b>			
Motors Locomotion	450	6	2700
Linear motors	300	3	900
Low-level electronics	1000	1	1000
Raw materials	1000	1	1000
Batteries	200	2	400
<b>Payload</b>			
Robotic Arm	2000	1	2000
Cameras	140	5	700
Communications	450	5	2250
Batteries for repeaters	50	4	200
Environmental Sensors	1000	1	1000

PC-NAV	500	1	500
PC-PERCEPT	400	1	400
Low-cost IMU	50	1	50
<b>External Equipment</b>			
Laptop	1500	1	1500
Transport case	300	1	300
Communications	450	1	450
		<b>Total</b>	15,350.00€

Table 8.1. SIAR raw materials and equipment costs

IDM estimates a **target price of about 50,000.00€** for the complete SIAR solution at the beginning of its commercialization. This price is based on the costs presented in Table 8.1 (30% of the commercial price), combined with the costs related with the production and commercialization of the solution (presented in section 8.3), and considering a profit of 30% for each sold unit.

### 8.2.3. Promotion

An important vehicle for the promotion will be the publication of the offer in speciality magazines whose target audience are professionals linked to civil infrastructures, urban organization, engineering, etc. In order to better reach these professionals will be sent catalogues for engineering firms and entities with intervention in the public space (city councils, foundations, etc.).

Another important form of promotion will be the participation in fairs related to the sewer inspection sector.

Finally, an important vehicle to promote a global scale is WEB2.0. Apart from maintaining a website with videos depicting the products, social networks and mailing lists will be used in an effective way.

### 8.2.4. Distribution

In order to maximize the profit, the distribution chain should be reduced to a minimum. Given that the product aims to reach international markets, partnerships will be established with local companies to facilitate the entry in these markets and to provide local support.

IDM will privilege a business to business (B2B) model, where the target clients will be organizations (private or public) providing sewer inspection services. IDM will be providing the technological solution while these organizations will provide locally the service. IDM will provide technical support and maintenance (advanced) of the robots. IDM will provide also expertise for the customization of the solution in some specific cases.

## 8.3. Financial Projections

IDM will consider the possibility of creating an internal department or a spin-off company for this specific new business area, which will allow a better definition of the business strategy as well a better control of its execution.

For the financial projections IDM is only considering the part of the business which is related with the production and sales of the SIAR robot. As mentioned in the previous section, IDM will be also providing advanced support and maintenance, as well engineering services for customized solutions, these activities will bring additional income for the company, but because the turnover related with these extra activities is not so easy to account, it will not be included in the financial projections.

### 8.3.1. Pre-production Costs

In contrast to current approaches, SIAR focuses on achieving high dependability, usefulness and affordability through technological innovation but also the provision of a convincing market approach to launch an off-the-shelf product version onto the market 18 months after the project end. Table 8.2 reflects the costs related with the development of SIAR robot in the scope of the ECHORD++ PDTI scheme and the following 18 months to prepare the product for market launch.

Item	2016	2017	2018	2019	Total
Customization	0.00	0.00	25,000.00	60,000.00	85,000.00
R&D	100,000.00	125,000.00	65,000.00	0.00	290,000.00
Registry trademark/patents		0.00	0.00	10,000.00	10,000.00
CE Certification		0.00	0.00	10,000.00	10,000.00
<b>Cumulative Costs</b>	<b>100,000.00</b>	<b>225,000.00</b>	<b>315,000.00</b>	<b>395,000.00</b>	<b>395,000.00</b>

Table 8.2. Pre-production costs.

### 8.3.2. Sales

The targeted price is about 50,000.00€ for the complete SIAR solution. Based on sales forecast for this market, IDM expects to make 5 supplies in the first year of commercialization and 20 in the second year. While the solution is distributed over a larger number of customers it is expected an increase in its popularity and 50 supplies are expected for the third year. These numbers will certainly be overcome in the years to come. Table 8.3 shows the expected number of units sold along 5 years after the product launch in the market. Table 8.4 shows the equivalent gross sales.

Year	Sold Units
2020	5
2021	20
2022	50
2023	70
2024	80

Table 8.3. Expected sales

Product	2020	2021	2022	2023	2024	Total
SIAR Robot	250,000.00	1,000,000.00	2,500,000.00	3,500,000.00	4,000,000.00	11,250,000.00
<b>Gross Sales</b>	<b>250,000.00</b>	<b>1,000,000.00</b>	<b>2,500,000.00</b>	<b>3,500,000.00</b>	<b>4,000,000.00</b>	<b>11,250,000.00</b>

Table 8.4. Gross sales.

### 8.3.3. Purchases

The values presented in Table 8.5 are based on an estimated cost of 16,000.00€ for all the materials and equipment included in each sold unit.

Materials and Equipment	2020	2021	2022	2023	2024	Total
Electronics, mechanics and raw materials	80,000.00	320,000.00	800,000.00	1,120,000.00	1,280,000.00	3,600,000.00
<b>Cost of Materials and Equipment</b>	<b>80,000.00</b>	<b>320,000.00</b>	<b>800,000.00</b>	<b>1,120,000.00</b>	<b>1,280,000.00</b>	<b>3,600,000.00</b>

Table 8.5. Costs of materials and equipment.

### 8.3.4. Personnel Costs

Table 8.6 presents the costs related with the personnel.

Item	2020	2021	2023	2024	2025	Total
Salaries	146,580.00	210,980.00	237,779.50	243,723.99	249,817.09	1,088,880.57
Social Security	34,812.75	50,107.75	56,472.63	57,884.45	59,331.56	258,609.14
Other duties	822.50	1,120.00	1,148.00	1,176.70	1,206.10	5,473.30
Training	500.00	500.00	750.00	750.00	1,000.00	3,500.00
<b>Total Personnel</b>	<b>182,715.25</b>	<b>262,707.75</b>	<b>296,150.13</b>	<b>303,535.13</b>	<b>311,354.75</b>	<b>1,356,463.01</b>

Table 8.6. Personnel costs.

### 8.3.5. Equipment Costs

Table 8.7 presents the costs related with the equipment that supports the activity of the company.

Item	2020	2021	2022	2023	2024	Total
PCs and Laptops	3,000.00	3,000.00	1,500.00	1,500.00	1,500.00	10,500.00
Software licenses	8,500.00	3,500.00	1,400.00	1,400.00	1,400.00	16,200.00
Production Equipment	5,000.00	5,000.00	3,000.00	2,000.00	2,000.00	17,000.00
Reg. trademark/patents/design	5,000.00	5,000.00	5,000.00			15,000.00
<b>Total</b>	<b>21,500.00</b>	<b>16,500.00</b>	<b>10,900.00</b>	<b>4,900.00</b>	<b>4,900.00</b>	<b>58,700.00</b>

Table 8.7. Equipment Costs.

### 8.3.6. Costs with External Services and Subcontracting

Table 8.8 presents the costs related with the external services and outsourcing that support the activity of the company. Of special relevance is the cost related with subcontracting the assembly of some robot parts. An estimation of 3,000.00€ per sold robot was considered for this assembly service.

Item	2020	2021	2022	2023	2024	Total
Premises	16,800.00	17,304.00	17,823.12	18,357.81	18,908.55	89,193.48
Electricity	1,080.00	1,112.40	1,145.77	1,180.15	1,215.55	5,733.87
Communications	1,200.00	1,236.00	1,273.08	1,311.27	1,350.61	6,370.96
Consumables	600.00	600.00	700.00	700.00	700.00	3,300.00
Advertising	5,000.00	20,000.00	25,000.00	40,000.00	40,000.00	130,000.00
Assembly	15,000.00	60,000.00	150,000.00	210,000.00	240,000.00	675,000.00

subcontracting						
Representation expenses	5,000.00	16,000.00	32,000.00	30,000.00	30,000.00	113,000.00
Legal services	3,000.00	3,000.00	3,000.00	3,000.00	3,000.00	15,000.00
External account	2,800.00	2,884.00	2,884.00	2,970.00	2,970.00	14,508.00
<b>Total</b>	<b>50,480.00</b>	<b>122,136.40</b>	<b>233,825.97</b>	<b>307,519.23</b>	<b>338,144.71</b>	<b>1,052,106.31</b>

Table 8.8. Costs with External Services and Subcontracting.

### 8.3.7. Total Costs

The total costs are presented in Table 8.9 and depicted in Figure 8.1.

Costs	2020	2021	2022	2023	2024	Total
Fixed	254,695.25	401,344.15	540,876.10	615,954.37	654,399.45	2,467,269.32
Variable	80,000.00	320,000.00	800,000.00	1,120,000.00	1,280,000.00	3,600,000.00
Pre-production	395,000.00	0.00	0.00	0.00	0.00	395,000.00
<b>Total</b>	<b>729,695.25</b>	<b>721,344.15</b>	<b>1,340,876.10</b>	<b>1,735,954.37</b>	<b>1,934,399.45</b>	<b>6,462,269.32</b>

Table 8.9. Total Costs.

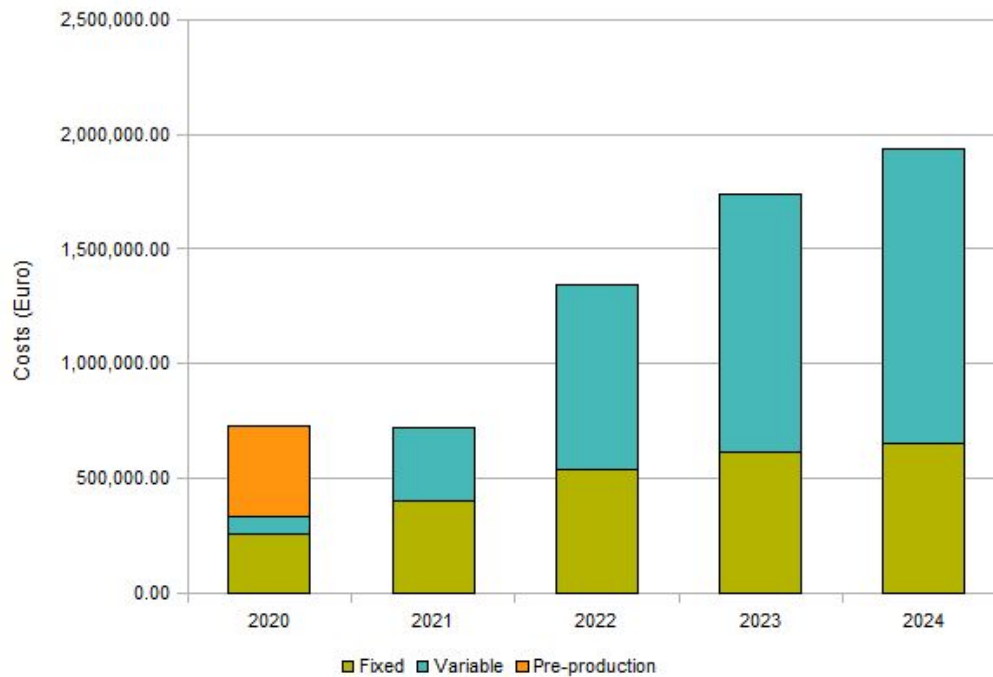


Figure 8.1. Annual total costs.



### 8.3.8. Operating Income

Table 8.10 presents the operating income (before taxes). The results are also presented graphically in Figures 8.2 and 8.3.

	2020	2021	2022	2023	2024
Total Costs	729,695.25	721,344.15	1,340,876.10	1,735,954.37	1,934,399.45
Gross Sales	250,000.00	1,000,000.00	2,500,000.00	3,500,000.00	4,000,000.00
<b>Operating Income</b>	<b>-479,695.25</b>	<b>278,655.85</b>	<b>1,159,123.90</b>	<b>1,764,045.63</b>	<b>2,065,600.55</b>
<b>Cumulative Results</b>	<b>-479,695.25</b>	<b>-201,039.40</b>	<b>958,084.50</b>	<b>2,722,130.13</b>	<b>4,787,730.68</b>

Table 8.10. Operating income.

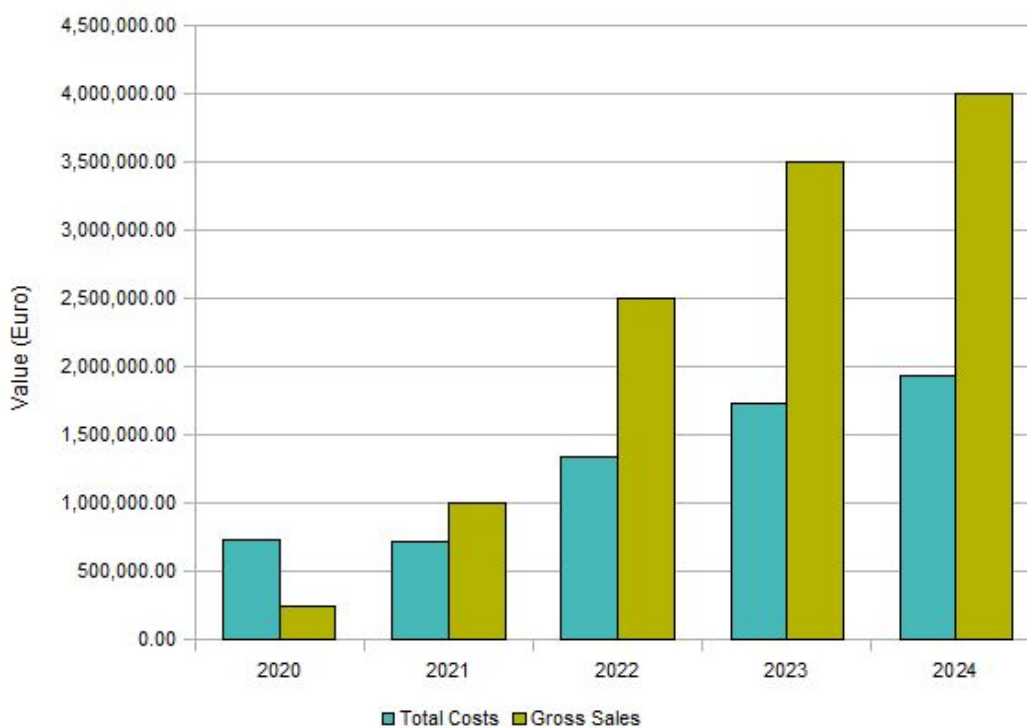


Figure 8.2. Annual total costs and gross sales evolution.

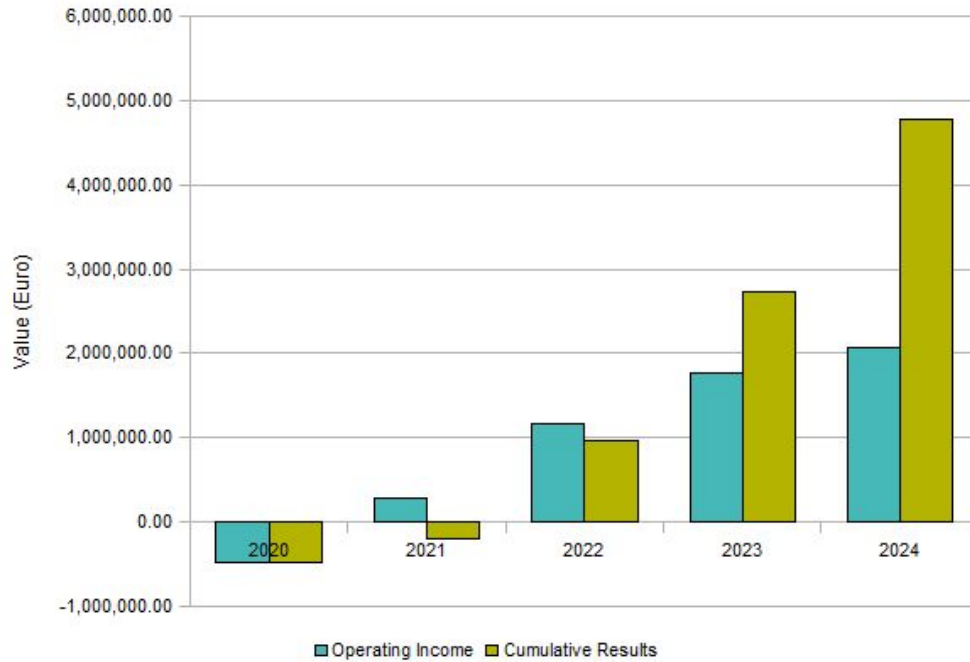


Figure 8.3. Operating income and cumulative results evolution.

It is predicted that during its 3rd year of commercialization (within 3.5 years after project completion) the SIAR business exploitation will reach its break-even with the return of the development investment (self-funding along with all public funding) and also the income of significant revenues as well. This performance is depicted in Figure 8.4.

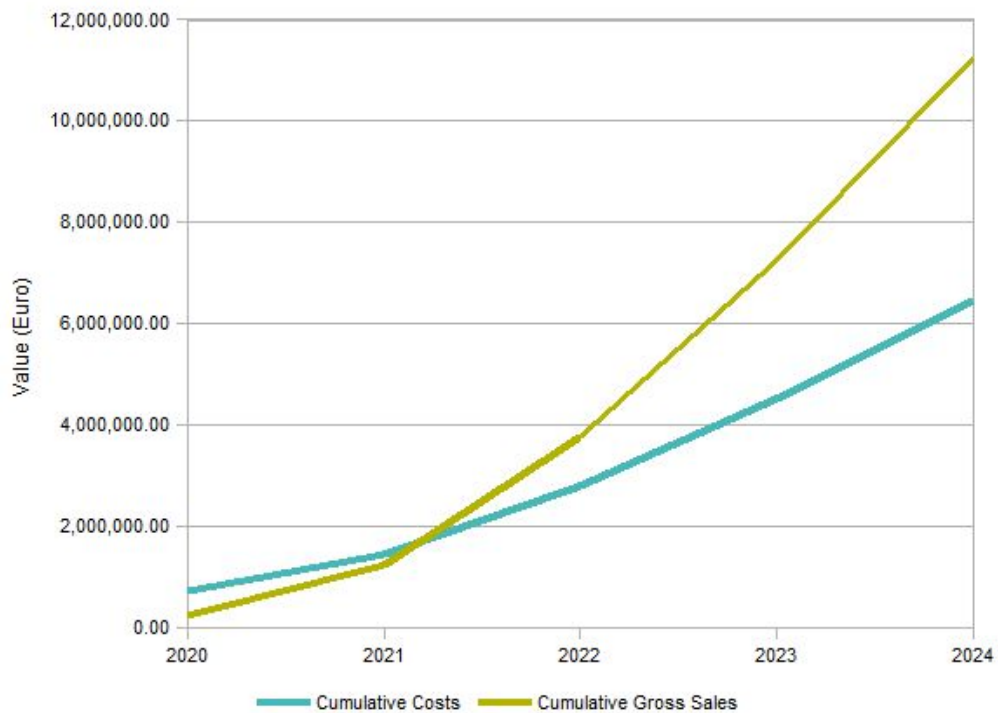


Figure 8.4. Cumulative costs vs Cumulative sales. Break-even during the third year of commercialization.

5 years after its introduction in the market, IDM expects a total turnover close to 11M€ from this business area, with a margin of 40% and ROI of 72%.

The operating income shows the need for an investment of a total of approximately 480k€ for the pre-production phase and the 1st year of commercialization. This investment will be covered according with the following:

- 210k€ will be funded by the EU through the ECHORD++ PDTI initiative
- 100k€ will covered by IDM through its robotics commercial activity (other applications)
- 170k€ will come from seed funding (angel investors, venture capitalists, accredited investors, etc)

## 8.4. Implementation and Control

The execution of the Business Plan will be made more effective by monitoring the activities associated with marketing, i.e., control of the inherent characteristics of the product, its price, distribution and promotion.

In a first phase the development of the prototype will be controlled, optimizing it for production and marketing scale. After the development of the prototype is intended to start production and marketing of pilot units. In addition to the immediate return of investment, these initial sales will also accelerate customer membership curve.

Articulating the marketing of pilot applications and a better knowledge of the market in real time, there will be contacts with potential investors in order to boost the production and marketing of the product on a large scale.

This first phase includes also the control of the product promotion processes and the establishment of partnerships to ease the product entry.

While the product is being placed on the market, the mechanisms that enable an effective customer support will be created. In order to monitor the rate of satisfaction with the products and rapidly introduce any corrective measures, special attention will be given to customer feedback.

The management team will regularly meet to compare the actual results with the expected execution times and the implementation of the budget by introducing any adjustments in the planned activities. They will be metrics to measure progress of short, medium and long term, including:

- Sales volume (monthly analysis by type of customer)
- Results and costs (monthly analysis by type of customer)
- Responsiveness to orders (monthly analysis by type of customer)
- Satisfaction rate with the product (monthly analysis by type of customer)
- Introduction into new markets (quarterly analysis)
- Public perception of the product and attitude toward the brand (half-yearly analysis)
- Annual review of performance of the product in the market

## 8.5. Sewer Inspection Economical Impact

The focus of the Consortium is to develop a reliable solution, that can be easily used by current work forces of sewer inspection services and, last but not the least, will contribute for an effective reduction of costs related with the sewer network inspection and maintenance.

An analysis of the principal cost data for the visitable sewer inspection service in Barcelona (in the challenge call document), mentions that currently:

- An inspection brigade is composed by 2 skilled officers, 1 pawn and a driver equipped with a van (leasing) and costs 110 €/h.
- Nowadays there are 4 brigades available that cost a total of 753.280 €/year.
- These 4 brigades inspect the 1.000.000 m of visitable sewers at least once a year.
- A brigade can approximately inspect 1168 lineal meters per day.
- The unitary cost is 0,75 €/m

Based on the previous experience of SIAR's partners on the development of field robots and sensing acquisition algorithms, it is expected that the SIAR solution can execute its mission at a **medium velocity between 20 to 30 cm per second**. The Consortium is also considering a **power autonomy of 5 hours** (without charging). This means that the SIAR solution, at a 20 cm/s, will be able to cover a **distance of 3600 m** (during the 5 hours). This means that in normal operating conditions the robot will be able to substantially improve the inspected range per day. Presently the inspection teams work 8 hours per day, and in case of need it will be possible to increase the time of operation of the robot by changing its batteries. This is not being considered because in the 8 hour period we still have to consider the time spent for the logistics: transportation of the inspection brigade (including the robot) to the place; setting up the robot; placing the robot for the inspection mission; collecting the robot after the mission; and cleaning the robot.

On the other hand, with an autonomous robot, the composition of a brigade can be redefined. Only one skilled operator and a pawn should be enough for a mission. This will reduce significantly the hourly cost of the brigade. A reduction of at least one third should be expected.

The exact market price for this type of robot is still difficult to define, it should only be possible after an industrialization and advanced market planning, but as discussed in section 3.2, IDM estimates a target price of about 50,000.00€ for the complete SIAR solution at the beginning of its commercialization.

Assuming a lifespan of 5 years for the equipment, and an annual maintenance cost of 15% of the initial value, the total value for the 5 year lifespan raises to 87.500€.

- In a year period, a brigade with an hourly rate of 65€ and a robot will cost:  $65 \cdot 8 \cdot 214 + 87.500/5 = 128.780\text{€}$ .
- 4 brigades should cost 515.120€
- Neglecting the expected increase on the covered distance (see above), and that each team is inspecting the same distance as before, this leads to a unitary cost of **0,51 €/m**.

- Nevertheless, as mentioned before, the SIAR partners expect a big increase in the inspected distance per mission, the robot is expected to inspect at least 3600 m per day (currently 1168 m per day). A conservative comparison of these values allows to define a reachable goal of a unitary cost of **0,20 €/m** for the SIAR inspection.
- Based on preliminary experiments with the perception system (see section 6), the Consortium believes in the possibility of having a real-time system for the **sewer serviceability and structural defect inspection**, and therefore the previous value of **0,20€/m** is still valid for these services. Please notice that the 3D information that will be used for both, sewer serviceability and structural defect inspection, can be gathered online and with enough resolution in the current envisaged solution, and we expect to be able to provide the information without requiring the robot to reduce its velocity, so both services can be offered at the same cost. Moreover, the **sampling system** is already being considered in the platform payload and therefore, the sampling collection should not have an impact on the calculated value.

## References

[Calonder et al, 2012] M. Calonder, V. Lepetit, M. Ozuysal, T. Trzcinski, C. Strecha, and P. Fua, "BRIEF: Computing a Local Binary Descriptor Very Fast," *IEEE Transactions on Pattern Analysis and Machine Intelligence*, vol. 34, no. 7, pp. 1281–1298, 2012.

[ECHORD++, 2014] ECHORD++. "Utility infrastructures and condition monitoring for sewer network. Robots for the inspection and the clearance of the sewer network in cities", Internal Report, 2014

[Hornung et al, 2013] A. Hornung, K.M. Wurm, M. Bennewitz, C. Stachniss, and W. Burgard, "OctoMap: An Efficient Probabilistic 3D Mapping Framework Based on Octrees" in *Autonomous Robots*, 2013; DOI: 10.1007/s10514-012-9321-0.

[Karaman and Frazzoli, 2010] S. Karaman and E. Frazzoli. Optimal kinodynamic motion planning using incremental sampling-based methods. In *IEEE Conf. on Decision and Control*, 2010.

[Lepetit et al, 2008] V. Lepetit, F. Moreno-Noguer, and P. Fua, "EPnP: An Accurate  $O(n)$  Solution to the PnP Problem," *International Journal of Computer Vision*, vol. 81, no. 2, pp. 155–166, 2008.

[Pérez-Lara et al, 2015] J. Pérez-Lara, F. Caballero and L. Merino. "Enhanced Monte Carlo Localization with Visual Place Recognition for Robust Robot Localization". *Journal of Intelligent & Robotic Systems*, 1-16, 2015

[Rosten and Drummond, 2006] E. Rosten and T. Drummond, "Machine Learning for High-speed Corner Detection," in *Proceedings of the 9th European Conference on Computer Vision - Volume Part I, ECCV'06*, (Berlin, Heidelberg), pp. 430–443, 2006.

[Teniente and Andrade-Cetto, 2013] E.H. Teniente and J. Andrade-Cetto. HRA\*: Hybrid randomized path planning for complex 3D environments. In *Proceedings of the IEEE/RSJ International Conference on Intelligent Robots and Systems*, pages 1766-1771, Tokyo, November 2013.